NTNU – Trondheim
Norwegian University of
Science and Technology

Renormalised Intrinsic and Extrinsic Impurity Induced Spin-orbit Scattering in Graphene

Halvor Gislesen
Hans Skarsvåg

Master of Science in Physics and Mathematics
Submission date: June 2012
Supervisor: Arne Brataas, IFY

Norwegian University of Science and Technology
Department of Physics

Abstract

We study the effect of an impurity potential on spin-memory loss in graphene. Various general methods for finding the spin-orbit related effect of a slowly varying impurity potential on a semiconductor have been examined. We have also revisited problems concerning electronic properties and spin relaxation in graphene. To this end, the bandstructure for graphene has been calculated through analytical and computational methods. The following results have been reproduced: Low energy excitations behave like massless relativistic particles with an effective speed of light at roughly 10^6 m/s. Intrinsic spin-orbit coupling splits the bands at the Fermi level. The importance of the d orbitals for this effect is also shown. Extrinsic spin-orbit coupling induced by a perpendicular electric field give rise to a Rashba type Hamiltonian. Our novel results are related to extrinsic effects from an impurity. We have calculated the renormalised impurity induced spin-orbit coupling due to mixing of the conduction bands and the other bands. This renormalisation is at most comparable to the vacuum term, and thus cannot explain the experimental results on spin relaxation.

Sammendrag

Vi ser på effekten av et urenhetspotensial på spinnlevetid i grafen. Ulike generelle metoder for å finne den effektive spinn-bane-relaterte virkningen av et langsomt varierende urenhetspotensial på en halvleder er blitt undersøkt. Vi har også sett på løste problemer angående elektroniske egenskaper og spinnlevetid i grafen. Med dette for øye har vi funnet båndstrukturen til grafen ved analytiske og numeriske metoder. De følgende resultatene har blitt reprodusert: Lavenergi eksitasjoner oppfører seg som masseløse fermioner med en effektiv fart på 10^6 m/s. Den intrinsiske spinn-bane-koblingen splitter båndene ved ferminivået. Betydningen *d*-orbitalene har på denne effekten har blitt vist. Den ekstrinsiske spinn-bane-koblingen indusert av et ortogonalt elektrisk felt gir en Rashba-type Hamilton-operator. Våre nye resultater er relatert til de ekstrinsiske effektene av en urenhet. Vi har regnet ut den renormaliserte urenhetsinduserte spinn-bane-koblingen på grunn av miksing av ledningsbåndene og de andre båndene. Denne renormaliseringen er høyst sammelignbar med vakuumleddet, og kan dermed ikke forklare de eksperimentelle resultatene på spinnlevetid.

Preface

This master thesis concludes our five year degree in applied physics and mathematics with a specialisation in applied physics. The thesis was done over one semester (30ECTS) and is a continuation of a project half this size we did the previous semester on the spin-orbit interaction in graphene. We have included a small part of this work in the thesis, most of which is improved a great deal to make it more understandable to the reader.

We both feel very appreciative to have been able to study something we enjoy and love. One of the best decisions we have made as students is by no doubt choosing Professor Arne Brataas as our supervisor. He has been more than generous with his time, giving us invaluable advice and going into the details of our derivations and problems. Though he has a lot on his plate, we have always felt welcome whenever we have needed his help. For this we are very grateful.

A small thanks also has to go to our fellow student Øyvind Persvik for help with some of the finer points of LaTeX.

Contents

1 Introduction

Carbon is the building block of life on earth. It is the fourth most abundant element in the universe. Carbon is a nonmetal with four valence electrons available to form covalent bonds. This opens up a world of chemical compounds and allotropes, with a wide range of properties. Diamond, a cubic structure of carbon, is the hardest material found in nature and it does not conduct electricity. Graphite on the other hand is one of the worlds softest materials, and it conducts electricity. Synthetically made allotropes, such as spherical fullerenes or buckyballs [1] and carbon nanotubes [2] have been a hot topic in physics and chemistry for more than twenty years. In 2004, a breakthrough in the field of nanomaterials was made. Graphene, the world's first free-standing 2D material, was discovered by mechanical exfoliation of graphite [3][4]. It has since been the subject of intense research activity. Geim and Novoselov, graphene's discoverers, were awarded the 2010 Nobel Prize in Physics "for groundbreaking experiments regarding the two-dimensional material graphene" [5].

Graphene can be imagined as a single layer of graphite and in that capacity it has been known as a theoretical construct for calculating the bandstructure of graphite since Wallace first investigated so called "monolayer graphite" in 1947 [6]. It was long held as an absolute that a free-standing two-dimensional material was a physical impossibility; Peierls and Landau argued that such a material would be thermodynamically unstable and would collapse into a three-dimensional structure [7][8]. The impossiblity of two-dimensional crystalline long-range order was further reinforced by Mermin [9]. So it caused no small amount of commotion when Geim and Novoselov announced the discovery of graphene, the experimental realisation of Wallace's model two-dimensional system. Other early theoretical work was done by McClure [10] and Slonczewski and Weiss [11]. The spin-orbit coupling in graphite was examined by Slonczewski [12] in 1955, McClure and Yafet [13] in 1960 and Dresselhaus and Dresselhaus [14] in 1965, while the relativistic behaviour at the Dirac points was described by DiVincenzo and Mele [15] and Semenoff [16] in 1984.

Bilayer graphene has its own exotic properties, but this is outside the scope of our investigation and thus bilayer graphene will not be treated in this thesis.

As mentioned, graphene was first isolated using mechanical exfoliation of graphite, in what has been dubbed the "scotch tape" method. An adhesive tape was used to split the graphite crystal and remove layer after layer until a single layer was left [4]. This technique can be automated by using ultrasonic cleavage [17][18]. This is however not the only way to make graphene; graphene can also be produced by a variety of methods, including epitaxial growth on silicon carbide by thermal decomposition, where silicon carbide is heated to evaporate Si [19], sonification and reduction of graphite oxide [20], and chemical vapor deposition on metal substrates [21]. In 2010, a method for producing arbitrarily large graphene sheets was discovered [22]. In this roll-to-roll "printing press" method, chemical vapor deposition on copper was preformed and if done at very low pressure the growth automatically stops after a single layer.

A wide variety of extraordinary properties have been reported for graphene. Graphene is the thinnest known material in the universe, one atom thick [17]. It is the strongest material in terms of the Young's modulus ever measured [23] [17]. At the same time, it is one of the softest materials [24]. The optical transmittance is independent of the frequency and is very high with a value of $\approx 1 - \pi\alpha \approx 97.7\%$, where α is the fine structure constant [25]. The heat conductance surpasses that of any other material [17]. It has the highest measured carrier mobility at room temperature [26]. A graphene oxide membrane is impermable to gasses even as elementary as He, H_2, N_2 and Ar, however, surprisingly water evaporates through the membrane unimpeded as if it was an open container [27]. Following this experiment, Geim *et al.* sealed a bottle of vodka with a graphene membrane and returned later to find the solution stronger than they had left it, hinting at possible room-temperature distillation or filtration applications for graphene in the future [28]. Graphene exhibit phenomena associated with quantum electrodynamics, such as the Klein tunneling [29]. An anamalous half-integer quantum Hall effect has been observed at room

temperature [30][31]. In addition, the fractional quantum Hall effect has been observed at low temperatures [32][33]. Spin injection has been demonstrated at room temperature [34].

Graphene display promising electronic properties. A 100GHz graphene transistor was produced by IBM in 2010 [35], a performance much higher than that of a silicon transistor [36]. In 2011, the first graphene integrated circuit was made by IBM, a broadband radio-frequency mixer unaffected by temperatures up to 400 K [37]. Graphene's optical transmittance also means that it can be used for transparent electrodes in for instance LCD screens or solar cells.

Spintronics

The electron spin is an intrinsic form of angular momentum [38]. In 1924, Pauli postulated a new two-valued degree of freedom for the electron without a classical analogy and used it to formulate the Pauli exclusion principle [39]. The following year, seeking to explain the anomalous Zeeman effect, Kronig proposed to Pauli the idea of a spinning electron, who outright rejected it on the grounds that the electron would have to rotate many times faster than the speed of light to produce the necessary angular momentum. Kronig then abandoned his idea, and it would be Uhlenbeck and Goudsmit under the supervision of Ehrenfest later that year who first published a theory of the electron spin [40][41]. They correctly proposed that this could explain both the anomalous Zeeman effect and deviations from Sommerfeld's theory of the atomic fine structure observed in emission spectra at the time. While the theory of spin did qualitatively explain these deviations, Heisenberg was quick to point out there was a discrepancy of a factor of two from the experimental result [42]. The following year, Thomas showed [43] that this was due to the use of an incorrect rest frame for the electron, the rest frame should be rotating relative to the laboratory frame of reference, and introduced what is now called Thomas precession. Convinced by this breakthrough, Pauli then developed a quantum mechanical theory of the spin with the spin matrices that bear his name, and Dirac later showed

that this can also be seen as a direct result of his relativistic description of quantum mechanics. The first direct experimental evidence of the electron spin oddly enough happened before the events described above. This was the famous Stern-Gerlach experiment in 1922 [44], where silver atoms were passed through a magnetic field, resulting in a splitting of the beam into two. At the time, it was thought that this was due to the orbital angular momentum of the silver atoms, an incorrect assumption. After the discovery of the electron spin, these results could be explained.

Spintronics is the detection and manipulation of the spin degree of freedom [45][46]. While the term spintronics is a recent invention, it was coined in 1996 by Wolf as a portmanteau of *spin transport* and *electronics* [47][46], the theory behind it is much older. Lord Kelvin first discovered what is now called anisotropic magnetoresistance (AMR) in 1857 [48][49], namely that the resistance increased when the current was flowing in the same direction as the magnetic field and decreased when it was perpendicular to the magnetic field. However, that this was due to the spin-orbit interaction was of course not realised until much later by Bloch and Gentile [50], after the discovery of the electron spin. Another effect, tunneling magnetoresistance (TMR), was discovered by Julière in 1975 [51], where a tunneling barrier was inserted between two ferromagnetic conductors. By individually controlling the magnetisation of the ferromagnetic conductors to be parallel or antiparallel of each other, this allows switching the device between two states of different electrical resistance. The big breakthrough, however, came with the discovery of the giant magnetoresistance (GMR) in 1988 by Grünberg *et al.* [52] and Fert *et al.* [53], for which Grünberg and Fert recieved the 2007 Nobel Prize in Physics. In GMR, the ferromagnetic layers are seperated by a non-ferromagnetic metal. It was soon realised that GMR could be used to improve read heads in modern hard disk drives for the personal computer [54] ; the first GMR read heads were developed by Parkin at IBM and reached the market in 1997 [55]. This caused a manyfold increase in the area density of storage media. The last decade TMR based read heads have begun replacing read heads based on GMR [38].

Magnetoresistive random-access memory (MRAM) is a new spintronics-based non-volatile type of memory, non-volatile meaning it retains its information even when the power is turned off. It is predicted to be a candidate for a "universal memory", that is, a replacement for the multiple different memory technologies currently in use [56]. Commercially available MRAM are made from magnetic tunneling junctions using TMR, however using this method for writing to the memory suffers greatly when the size of the device is reduced [57]. A possible solution to this problem is using spin-transfer torques (STT) where a spin current transfers a torque on the magnetisation of the ferromagnetic material that stores the information. STT was first discussed by Slonczewski [58] and Berger [59].

A parallel line of inquiry for spintronic devices came with the experimental demonstration of spin injection by Johnson and Silsbee in 1985 [60]. In 1976, Aronov and Pikus proposed [61] spin injection into semiconductors, which was not achieved until 1999 by groups lead by Molenkamp [62] and Awschalom [63]. Spin injection is the injection of a nonequilibrium spin ensemble into a nonmagnetic material, e.g. a paramagnet or semiconductor [64]. By using spin injection in combination with spin detection and spin manipulation in the form of a gate-controlled spin-orbit coupling, it is possible to envision a spin field-effect transistor (SFET). This was first proposed by Datta and Das in 1989 [65] and has motivated a huge interest in the field, but still has not seen experimental realisation [46].

The lifetimes of the spin accumulations are important for many spintronic devices. Spin relaxation is a process that reduces the spin accumulation. There are four major mechanisms of spin relaxation: Elliot-Yafet, D'yakonov-Perel', Bir-Aronov-Pikus and the hyperfine interaction [46] [38].

Elliot-Yafet: As we shall later see, Bloch states, i.e. solutions of the Schrödinger equation for a periodic potential, are not necessarily spin eigenstates [38]. Instead, the states are a combination of opposite spin states. For each wavevector, there are two mutually orthogonal spin orientations; however, spin orientations

from different wavevector are not necessarily paralell or anti-parallel, but may have any angle between them. This means that a momentum scattering event caused by for instance an impurity, boundary or phonon changes the spin orientation along with the momentum. In other words, the spin relaxation time is proportional to the momentum relaxation time, $\tau_{\mathrm{EY}} \propto \tau_{\mathrm{m}}$.

D'yakonov-Perel': As mentioned, the spin-orbit interaction induces a momentum-dependent effective magnetic field. This effective magnet field causes the spin to precess in an analogy to Larmor precession. This precession does not by itself cause spin relaxation; it changes the direction of the spin polarisation, but not the magnitude of the ensemble averaged spin [38]. However, momentum scattering causes the magnetic field to change direction and magnitude [46]. This again changes the precession of the spin, and the spin phase experiences a random walk. Frequent collisions slows down the electrons, which reduces the effective magnetic field and thereby suppress the D'yakonov-Perel' mechanism. Thus, for the D'yakonov-Perel' mechanism, the spin relaxation time is typically inversely proportional to the momentum relaxation time, $\tau_{\mathrm{DP}} \propto 1/\tau_{\mathrm{m}}$

Bir-Aronov-Pikus: The Bir-Aronov-Pikus mechanism is important when there is a big overlap between the electron and hole wavefunctions. This causes an electron-hole exchange interaction, which means that a spin-flip for the hole induces a spin-flip for the electron. This effect is due to the Pauli exclusion principle [38].

Hyperfine interaction: The hyperfine interaction is a result of the magnetic field created by nuclear spins. This field interacts with the spin of the electrons and may cause spin relaxation [38].

Spintronics offer exciting opportunities for the future, and a full understanding of spin relaxation in materials proposed as a basis for spintronic devices is vital. Graphene is one of the materials proposed since its small intrinsic spin-orbit coupling should generate the long spin lifetimes necessary for practical usage [66]. However, experiments have shown a much shorter lifetime than predicted [67][68]. The reason for this discrepancy is still not fully understood from a

theoretical point of view. With this as motivation, we will investigate the effects of impurites on the spin-orbit coupling in graphene and seek to elucidate the mechanism responsible for spin relaxation in graphene.

Part I

2 Multiple-scale analysis

Multiple-scale analysis [69] is an effective method to find approximate solutions to problems involving large variations in length or time-scales. We will apply this method to find how the electronic states are affected by an impurity, when the impurity potential is assumed to be slowly varying compared to the variation of the periodic potential due to the lattice. We will first consider a one dimensional case and later extend the model to three dimensions and include the spin-orbit coupling.

2.1 One dimension

Let us consider an infinite chain of atoms with a lattice spacing a. This gives rise to a periodic potential $V(x) = V(x + a)$. The Schrödinger equation for an electron on this chain is

$$\left[-\frac{\hbar^2}{2m_0}\frac{\partial^2}{\partial x^2} + V(x)\right]\psi_{nk}(x) = \epsilon_{nk}\psi_{nk}(x), \tag{2.1}$$

where ψ_{nk} are the Bloch functions and n denotes the band. These states form a complete basis with the normalisation

$$\int \mathrm{d}x \psi^*_{nk}\psi_{n'k'} = \delta(k - k')\delta_{nn'}. \tag{2.2}$$

We are now interested in the effect of a slow-varying potential, $U(x)$, caused by an impurity. To solve this we use multiple-scale analysis, following the method presented by Pedersen [70]. The Schrödinger equation is then

$$\left[-\frac{\hbar^2}{2m_0}\frac{\partial^2}{\partial x^2} + V(x) + U(x)\right]\psi(x) = E\psi(x). \tag{2.3}$$

A natural energy scale for the unperturbed Hamiltonian is the typical kinetic energy $E_K = \hbar^2/(2m_0a^2)$, and in the same way the impurity potential will have an energy which is proportional to the inverse square of some length scale $L \gg a$. We use the smallness parameter $\epsilon \equiv a/L$ as a measure of how slowly

the impurity potential varies. Dividing the Schrödinger equation by E_K to get it on a dimensionless form and introducing the dimensionless variable $\xi = x/a$, we have that

$$\frac{U(x)}{E_K} = \epsilon^2 \widetilde{U}(\epsilon\xi), \tag{2.4}$$

and by defining the second length scale, $\eta = \epsilon\xi$, we find

$$-\psi''(\xi,\eta) + [\widetilde{V}(\xi) + \epsilon^2\widetilde{U}(\eta)]\psi(\xi,\eta) = \widetilde{E}\psi(\xi,\eta). \tag{2.5}$$

We now seek to find a perturbative solution to Eq. (2.3) by expanding ψ in terms of ϵ

$$\psi = \psi(\xi,\eta) = \psi^{(0)}(\xi,\eta) + \epsilon\psi^{(1)}(\xi,\eta) + \epsilon^2\psi^{(2)}(\xi,\eta) + \mathcal{O}(\epsilon^3), \tag{2.6}$$

and the same for the energy,

$$\widetilde{E} = \widetilde{E}_0 + \epsilon\widetilde{E}_1 + \epsilon^2\widetilde{E}_2 + \mathcal{O}(\epsilon^3). \tag{2.7}$$

Using the chain rule, we find

$$\psi'' = \frac{\partial^2\psi^{(0)}}{\partial\xi^2} + \epsilon\left(2\frac{\partial^2\psi^{(0)}}{\partial\xi\partial\eta} + \frac{\partial^2\psi^{(1)}}{\partial\xi^2}\right) + \epsilon^2\left(\frac{\partial^2\psi^{(0)}}{\partial\eta^2} + 2\frac{\partial^2\psi^{(1)}}{\partial\xi\partial\eta} + \frac{\partial^2\psi^{(2)}}{\partial\xi^2}\right) + \mathcal{O}(\epsilon^3). \tag{2.8}$$

Neglecting terms of order three and higher in ϵ, Eq. (2.5) becomes

$$\begin{aligned} -\left[\frac{\partial^2\psi^{(0)}}{\partial\xi^2} + \epsilon\left(2\frac{\partial^2\psi^{(0)}}{\partial\xi\partial\eta} + \frac{\partial^2\psi^{(1)}}{\partial\xi^2}\right) + \epsilon^2\left(\frac{\partial^2\psi^{(0)}}{\partial\eta^2} + 2\frac{\partial^2\psi^{(1)}}{\partial\xi\partial\eta} + \frac{\partial^2\psi^{(2)}}{\partial\xi^2}\right)\right] \\ +\widetilde{V}(\xi)\left(\psi^{(0)} + \epsilon\psi^{(1)} + \epsilon^2\psi^{(2)}\right) + \epsilon^2\widetilde{U}(\eta)\psi^{(0)} \\ = \widetilde{E}_0\psi^{(0)} + \epsilon\left(\widetilde{E}_1\psi^{(0)} + \widetilde{E}_0\psi^{(1)}\right) + \epsilon^2\left(\widetilde{E}_0\psi^{(2)} + \widetilde{E}_1\psi^{(1)} + \widetilde{E}_2\psi^{(0)}\right). \end{aligned} \tag{2.9}$$

Separating the terms by order of ϵ, we find

$$(H_0 - \widetilde{E}_0)\psi^{(0)} = 0, \tag{2.10}$$

$$(H_0 - \widetilde{E}_0)\psi^{(1)} = 2\frac{\partial^2\psi^{(0)}}{\partial\xi\partial\eta} + \widetilde{E}_1\psi^{(0)}, \tag{2.11}$$

$$(H_0 - \widetilde{E}_0)\psi^{(2)} = \frac{\partial^2\psi^{(0)}}{\partial\eta^2} + 2\frac{\partial^2\psi^{(1)}}{\partial\xi\partial\eta} + \left(\widetilde{E}_2 - \widetilde{U}(\eta)\right)\psi^{(0)} + \widetilde{E}_1\psi^{(1)}, \tag{2.12}$$

with

$$H_0 = -\frac{\partial^2}{\partial \xi^2} + \widetilde{V}(\xi) \tag{2.13}$$

Eq. (2.10) is the Schrödinger equation without an impurity. It is solved by

$$\psi^{(0)}(\xi, \eta) = \psi_{nk}(\xi) F(\eta), \tag{2.14}$$

where $\psi_{nk}(\xi)$ are the solutions to the unperturbed problem with the corresponding eigenvalues $\widetilde{E}_0 = \epsilon_{nk}$, and $F(\eta)$ is an arbitrary function of η. We now demand that the solutions to Eq. (2.11) do not contain any secular terms, that is, terms growing without bound. This is done by setting the inhomogeneity of Eq. (2.11), the right-hand side, to be orthogonal to the solutions of the homogenous equation (2.10).[69] We assume that $\widetilde{E}_1 = 0$; since the perturbing potential is quadratic in ϵ, any correction to the energy must be at least of the second order in ϵ. Because of the periodicity of the Bloch functions, ψ_{nk}, we integrate only over a unit cell. This leads to the condition

$$p_{nn} = 0, \tag{2.15}$$

where

$$p_{nn'} = 2\pi \int_{\text{cell}} \mathrm{d}\xi \psi^*_{nk_0} \frac{1}{i} \frac{\partial}{\partial \xi} \psi_{n'k_0}, \tag{2.16}$$

is the dimensionless momentum matrix element. This gives us a restriction on which wave vectors we allow, a restriction which is actually equivalent to demanding that ϵ_{nk} has a minimum at $k = k_0$. We will prove this for a system of arbitrary dimensions in Section 3. Expanding the solution about the band minimum is of course the favourable choice, as conduction electrons with energies close to the minimum energy dominate the low temperature electronic properties which is the subject of our investigation. We thus have

$$\psi^{(1)} = 2iF'(\eta) \sum_{l \neq n} \frac{p_{ln}}{\epsilon_{lk_0} - \epsilon_{nk_0}} \psi_{lk_0}(\xi). \tag{2.17}$$

Inserting Eqs. (2.14) and (2.17) into Eq. (2.12) we get

$$\begin{aligned}(H_0 - \widetilde{E}_0)\psi^{(2)} = &\left\{ F''(\eta) + \left[\widetilde{E}_2 - \widetilde{U}(\eta) \right] F(\eta) \right\} \psi_{nk_0}(\xi) \\ &+ 4iF''(\eta) \sum_{l \neq n} \frac{p_{ln}}{\epsilon_{lk_0} - \epsilon_{nk_0}} \frac{\partial}{\partial \xi} \psi_{lk_0}(\xi).\end{aligned} \tag{2.18}$$

Demanding again that the right-hand side is orthogonal to the solutions of the homogeneous equation, ψ_{lk_0}, we get

$$\left(1 - 4\sum_{l\neq n}\frac{|p_{ln}|^2}{\epsilon_{lk_0} - \epsilon_{nk_0}}\right)F''(\eta) + \left[\widetilde{E}_2 - \widetilde{U}(\eta)\right]F(\eta) = 0. \tag{2.19}$$

With dimensions restored and by defining $X = \epsilon x = a\eta$, this may be written as

$$-\frac{\hbar^2}{2m^*}F''(X) + U(X)F(X) = E_2F(X), \tag{2.20}$$

which we can see has the form of a Schrödinger equation for $F(X)$ with an effective mass

$$\frac{1}{m^*} = \frac{1}{m_0} - \frac{2}{m_0^2}\sum_{l\neq n}\frac{|p_{ln}|^2}{\epsilon_{lk_0} - \epsilon_{nk_0}}. \tag{2.21}$$

The effective mass is determined by the matrix element of the momentum operator and the energies at $k = k_0$. This result can easily be generalised to three dimensions so that $x \to \mathbf{x}$.

2.2 Spin-orbit coupling

By introducing the spin-orbit coupling we get an additional term to the Hamiltonian of the form

$$\lambda\boldsymbol{\sigma}\cdot(\nabla V_{\text{tot}}(\mathbf{x}) \times \mathbf{p}), \tag{2.22}$$

where

$$\lambda \equiv \frac{\hbar}{4m_0^2c^2} \tag{2.23}$$

is the spin-orbit coupling constant for vacuum and $V_{\text{tot}}(\mathbf{x}) = V(\mathbf{x}) + U(\mathbf{x})$ is the total potential. As in the preceeding section we rewrite everything in dimensionless form. With $\mathbf{p} = -i(\nabla_{\boldsymbol{\xi}} + \epsilon\nabla_{\boldsymbol{\eta}})$, $\widetilde{V}_{\text{tot}}(\boldsymbol{\xi}, \boldsymbol{\eta}) = \widetilde{V}(\boldsymbol{\xi}) + \epsilon^2\widetilde{U}(\boldsymbol{\eta})$ and $\widetilde{\lambda} = \lambda\hbar/a^2$,

Eq. (2.22) yields

$$\begin{aligned}\widetilde{\lambda}\boldsymbol{\sigma}\cdot(\nabla\widetilde{V}_{\rm tot}(\boldsymbol{\xi},\boldsymbol{\eta})\times\mathbf{p}) =&\widetilde{\lambda}\boldsymbol{\sigma}\cdot\Big[(\nabla_{\boldsymbol{\xi}}\widetilde{V}(\boldsymbol{\xi})\times\mathbf{p}_{\boldsymbol{\xi}})+\epsilon(\nabla_{\boldsymbol{\xi}}\widetilde{V}(\boldsymbol{\xi})\times\mathbf{p}_{\boldsymbol{\eta}})\\ &+\epsilon^3(\nabla_{\boldsymbol{\eta}}\widetilde{U}(\boldsymbol{\eta})\times\mathbf{p}_{\boldsymbol{\xi}})+\epsilon^4(\nabla_{\boldsymbol{\eta}}\widetilde{U}(\boldsymbol{\eta})\times\mathbf{p}_{\boldsymbol{\eta}})\Big] \qquad (2.24)\\ =&\widetilde{\lambda}\boldsymbol{\sigma}\cdot(\nabla_{\boldsymbol{\xi}}\widetilde{V}(\boldsymbol{\xi})\times\mathbf{p}_{\boldsymbol{\xi}})+\epsilon\lambda\boldsymbol{\sigma}\cdot(\nabla_{\boldsymbol{\xi}}\widetilde{V}(\boldsymbol{\xi})\times\mathbf{p}_{\boldsymbol{\eta}})+\mathcal{O}(\epsilon^3). \qquad (2.25)\end{aligned}$$

The Hamiltonian to the second order in ϵ is then

$$H=\mathbf{p}^2+\widetilde{V}_{\rm tot}(\boldsymbol{\xi},\boldsymbol{\eta})+\widetilde{\lambda}\boldsymbol{\sigma}\cdot(\nabla\widetilde{V}_{\rm tot}(\boldsymbol{\xi},\boldsymbol{\eta})\times\mathbf{p})=H_0+\epsilon\widetilde{\boldsymbol{\pi}}\cdot\mathbf{p}_{\boldsymbol{\eta}}+\epsilon^2\mathbf{p}_{\boldsymbol{\eta}}+\epsilon^2\widetilde{U}(\boldsymbol{\eta}), \quad (2.26)$$

where we have introduced the dimensionless velocity operator,

$$\widetilde{\boldsymbol{\pi}}=-2i\nabla_{\boldsymbol{\xi}}+\widetilde{\lambda}\boldsymbol{\sigma}\times\nabla_{\boldsymbol{\xi}}\widetilde{V}(\boldsymbol{\xi}), \quad (2.27)$$

and

$$H_0=\mathbf{p}_{\boldsymbol{\xi}}^2+\widetilde{V}(\boldsymbol{\xi})+\widetilde{\lambda}\boldsymbol{\sigma}\cdot(\nabla_{\boldsymbol{\xi}}\widetilde{V}(\boldsymbol{\xi})\times\mathbf{p}_{\boldsymbol{\xi}}). \quad (2.28)$$

Separating the dimensionless Schrödinger equation by order of ϵ

$$\begin{aligned}(H_0-\widetilde{E}_0)\psi^{(0)} =&0, \qquad (2.29)\\ (H_0-\widetilde{E}_0)\psi^{(1)} =&-\widetilde{\boldsymbol{\pi}}\cdot\mathbf{p}_{\boldsymbol{\eta}}\psi^{(0)}, \qquad (2.30)\\ (H_0-\widetilde{E}_0)\psi^{(2)} =&-\mathbf{p}_{\boldsymbol{\eta}}^2\psi^{(0)}-\widetilde{\boldsymbol{\pi}}\cdot\mathbf{p}_{\boldsymbol{\eta}}\psi^{(1)}+(\widetilde{E}_2-\widetilde{U}(\boldsymbol{\eta}))\psi^{(0)}. \qquad (2.31)\end{aligned}$$

Eq. (2.29) is again the unperturbed Schrödinger equation. It is solved by

$$\psi^{(0)}(\boldsymbol{\xi},\boldsymbol{\eta})=\psi_{n\mathbf{k}}(\boldsymbol{\xi})F(\boldsymbol{\eta}), \quad (2.32)$$

with corresponding eigenvalues ϵ_{nk} and where n now runs over the different spin and orbital states.

Demanding that the right-hand side of Eq. (2.30) should be orthogonal to the solutions of Eq. (2.29) requires that

$$\widetilde{\boldsymbol{\pi}}_{nn}\cdot\mathbf{p}_{\boldsymbol{\eta}}=0, \quad (2.33)$$

where $\widetilde{\boldsymbol{\pi}}_{nn'}$ are the matrix elements of the velocity operator evaluated at $\mathbf{k} = \mathbf{k}_0$,

$$\widetilde{\boldsymbol{\pi}}_{nn'} = (2\pi)^3 \int_{\text{cell}} \mathrm{d}\boldsymbol{\xi} \psi^*_{n\mathbf{k}_0} \boldsymbol{\pi} \psi_{n'\mathbf{k}_0}. \tag{2.34}$$

We then get

$$\psi^{(1)} = -\sum_{l\neq n} \frac{\widetilde{\boldsymbol{\pi}}_{ln} \cdot \mathbf{p}_{\boldsymbol{\eta}} F(\boldsymbol{\eta})}{\epsilon_{l\mathbf{k}} - \epsilon_{n\mathbf{k}}} \psi_{l\mathbf{k}}(\boldsymbol{\xi}). \tag{2.35}$$

Inserting this into Eq. (2.31), we get

$$\begin{aligned}(H_0 - \widetilde{E}_0)\psi^{(2)} = &\left[-\mathbf{p}^2_{\boldsymbol{\eta}} F(\boldsymbol{\eta}) + \left(\widetilde{E}_2 - \widetilde{U}(\boldsymbol{\eta})\right) F(\boldsymbol{\eta})\right] \psi_{n\mathbf{k}}(\boldsymbol{\xi}) \\ &+ \widetilde{\boldsymbol{\pi}} \cdot \mathbf{p}_{\boldsymbol{\eta}} \sum_{l\neq n} \frac{(\widetilde{\boldsymbol{\pi}}_{ln} \cdot \mathbf{p}_{\boldsymbol{\eta}})\, F(\boldsymbol{\eta})}{\epsilon_{l\mathbf{k}} - \epsilon_{n\mathbf{k}}} \psi_{l\mathbf{k}}(\boldsymbol{\xi}).\end{aligned} \tag{2.36}$$

By demanding that the right-hand side is orthogonal to ψ_{nk},

$$0 = -\mathbf{p}^2_{\boldsymbol{\eta}} F(\boldsymbol{\eta}) + \left(\widetilde{E}_2 - \widetilde{U}(\boldsymbol{\eta})\right) F(\boldsymbol{\eta}) + \sum_{l\neq n} \frac{(\widetilde{\boldsymbol{\pi}}_{ln} \cdot \mathbf{p}_{\boldsymbol{\eta}})(\widetilde{\boldsymbol{\pi}}_{nl} \cdot \mathbf{p}_{\boldsymbol{\eta}})}{\epsilon_{l\mathbf{k}} - \epsilon_{n\mathbf{k}}} F(\boldsymbol{\eta}), \tag{2.37}$$

we obtain the following effective Schrödinger equation for $F(\mathbf{X})$ with dimensions restored

$$-\frac{\hbar^2}{2m^*_{\alpha\beta}} \nabla_{\mathbf{X},\alpha} \nabla_{\mathbf{X},\beta} F(\mathbf{X}) + U(\mathbf{X}) F(\mathbf{X}) = E_2 F(\mathbf{X}), \tag{2.38}$$

where we have introduced the effective mass tensor

$$\frac{1}{m^*_{\alpha\beta}} = \frac{1}{m_0}\delta_{\alpha\beta} - 2\sum_{l\neq n} \frac{\pi^\alpha_{ln}\pi^\beta_{nl}}{\epsilon_{l\mathbf{k}} - \epsilon_{n\mathbf{k}}}, \tag{2.39}$$

with $\pi = \widetilde{\pi} E_k \frac{a}{\hbar}$. Thus, the only change we get when introducing the spin-orbit coupling is that the velocity operator takes the place of the momentum operator, $p^\alpha_{ln} \to m_0 \pi^\alpha_{ln}$. Eq. (2.38) is analogous to the result of the one dimensional case, Eq. (2.20), however, by introducing three dimensions, we have to use an effective mass tensor instead of a scalar effective mass, as was to be expected.

When it comes to finding the lowest order correction to the Scrödinger equation, the method we have employed is simple and efficient. As can be seen from Eq. (2.24) the third and fourth order corrections will include a coupling of spin and the impurity potential, a so called extrinsic spin-orbit coupling. Terms like

these could prove interesting, even though we expect them to be small. However, we will let this conclude our treatment using multiple-scale analysis, since we identify that the method becomes increasingly cumbersome when higher order corrections are to be included. For this purpose, the other methods we will include are superior.

3 Luttinger-Kohn

We will now present the Luttinger-Kohn model. The Luttinger-Kohn model is widely used in the study of the electronic properties of semiconductors. Our treatment follows closely the seminal paper *Motion of Electrons and Holes in Perturbed Periodic Fields* by Luttinger and Kohn, published in 1954 [71]. This model will be our main tool for calculating the electronic states in the presence of slowly varying impurity potentials. For the sake of simplicity, we have set $\hbar = 1$.

3.1 Non-degenerate bands

We first consider a semiconductor with a band minimum at the center of the first Brillouin zone, $\mathbf{k} = 0$. The Schrödinger equation for an electron in the periodic potential is

$$H_0\psi_{n\mathbf{k}} = \epsilon_{n\mathbf{k}}\psi_{n\mathbf{k}}, \tag{3.1}$$

where $H_0 = \frac{p^2}{2m_0} + V$, V is the periodic potential due to the crystal, $\epsilon_{n\mathbf{k}}$ is the eigenenergy and $\psi_{n\mathbf{k}}$ are Bloch functions. Our interest is in how an impurity, described by an additional potential U, modifies the electron states. In other words, we want to solve the Schrödinger equation

$$(H_0 + U)\psi = \epsilon\psi. \tag{3.2}$$

Instead of expanding the solution of this equation in the Bloch functions,

$$\psi_{n\mathbf{k}} = e^{i\mathbf{k}\cdot\mathbf{r}}u_{n\mathbf{k}}, \tag{3.3}$$

we choose the Luttinger-Kohn basis,

$$\chi_{n\mathbf{k}} = e^{i\mathbf{k}\cdot\mathbf{r}}u_{n0}. \tag{3.4}$$

Here $u_{n\mathbf{k}}(\mathbf{r})$ is a function with the same periodicity as the crystal potential. Before proceeding we shall show that the Luttinger-Kohn basis is complete. To

this end, we consider an arbitrary function, $f(\mathbf{r})$, which can be expanded in ψ_{nk},

$$\begin{aligned} f(\mathbf{r}) &= \sum_n \int d\mathbf{k} g_n(\mathbf{k}) \psi_{nk} \\ &= \sum_n \int d\mathbf{k} g_n(\mathbf{k}) e^{i\mathbf{k}\cdot\mathbf{r}} u_{nk}. \end{aligned} \tag{3.5}$$

Because u_{n0} is a complete basis with respect to the periodic functions we can expand any of the u_{nk} functions in this basis,

$$u_{nk} = \sum_{n'} b_{nn'}(\mathbf{k}) u_{n'0}. \tag{3.6}$$

Combining this with Eqs. (3.5) and (3.4), we get

$$f(\mathbf{r}) = \sum_{n'} \int d\mathbf{k} \tilde{g}_{n'}(\mathbf{k}) \chi_{n'k}, \tag{3.7}$$

with

$$\tilde{g}_{n'}(\mathbf{k}) = \sum_n g_n(\mathbf{k}) b_{n'n}(\mathbf{k}). \tag{3.8}$$

Eq. (3.7) implies we can expand an arbitrary function in terms of the Luttinger-Kohn basis. The Bloch functions form an orhonormal basis,

$$\langle \psi_{n\mathbf{k}} | \psi_{n'\mathbf{k}'} \rangle = \delta_{nn'} \delta(\mathbf{k} - \mathbf{k}'). \tag{3.9}$$

We shall now see that this is also the case for the Luttinger-Kohn basis.

$$\langle \chi_{n\mathbf{k}} | \chi_{n'\mathbf{k}'} \rangle = \int e^{i(\mathbf{k}'-\mathbf{k})\cdot\mathbf{r}} u^*_{n0} u_{n'0} \mathrm{d}\mathbf{r}. \tag{3.10}$$

First, we note that the product $u^*_{n0} u_{n'0}$ has the same periodicity as the lattice potential, which means we can Fourier-expand it using only the reciprocal lattice vectors, $\mathbf{K}_m$,

$$u^*_{n0} u_{n'0} = \sum_m B_m^{nn'} e^{-i\mathbf{K}_m\cdot\mathbf{r}}, \tag{3.11}$$

where $B_m^{nn'}$ are coefficients that depend on the indices n and n' as well as the reciprocal lattice vector $\mathbf{K}_m$. We then get

$$\begin{aligned} \langle \chi_{n\mathbf{k}} | \chi_{n'\mathbf{k}'} \rangle &= \int \mathrm{d}\mathbf{r} e^{i(\mathbf{k}'-\mathbf{k})\cdot\mathbf{r}} \sum_m B_m^{nn'} e^{-i\mathbf{K}_m\cdot\mathbf{r}} \\ &= (2\pi)^3 \sum_m B_m^{nn'} \delta(\mathbf{k}' - \mathbf{k} - \mathbf{K}_m). \end{aligned} \tag{3.12}$$

Here we have used the fact that the δ-function can be expressed as

$$\delta(\mathbf{k}) = \frac{1}{(2\pi)^3}\int e^{i\mathbf{k}\cdot\mathbf{r}}\mathrm{d}\mathbf{r}. \tag{3.13}$$

In the sum appearing in Eq. (3.12), only the term with $m = 0$ is non-zero, since $\mathbf{k}$ and $\mathbf{k}'$ both are in the first Brillouin zone. This implies that $\mathbf{k}'-\mathbf{k}-\mathbf{K}_m = 0$ is only fulfilled when $\mathbf{K}_m = 0$. Multiplying Eq. (3.11) with $e^{i\mathbf{K}_m\cdot\mathbf{r}}$ and integrating over the unit cell with a volume Ω we get

$$B_m^{nn'} = \frac{1}{\Omega}\int_{\text{cell}} \mathrm{d}\mathbf{r} e^{i\mathbf{K}_m\cdot\mathbf{r}} u_{n0}^* u_{n'0}, \tag{3.14}$$

so that we may insert

$$B_0^{nn'} = \frac{1}{\Omega}\int_{\text{cell}} u_{n0}^* u_{n'0}\mathrm{d}\mathbf{r} = \frac{1}{(2\pi)^3}\delta_{nn'}, \tag{3.15}$$

into Eq. (3.12). This means

$$\langle\chi_{n\mathbf{k}}|\chi_{n'\mathbf{k}'}\rangle = \delta(\mathbf{k}'-\mathbf{k})\delta_{nn'}. \tag{3.16}$$

We have now shown that the Luttinger-Kohn basis is complete and orthonormal. These properties are important for what follows.

Now, expanding ψ in the Luttinger-Kohn basis, we get

$$\psi = \sum_n \int \mathrm{d}\mathbf{k}' A_n(\mathbf{k}')\chi_{n\mathbf{k}'}. \tag{3.17}$$

This expansion inserted into the Schrödinger equation (3.2) results in the following equation for $A_n(\mathbf{k})$

$$\sum_{n'}\int \mathrm{d}\mathbf{k}'\langle n\mathbf{k}|H_0 + U|n'\mathbf{k}'\rangle A_{n'}(\mathbf{k}') = \epsilon A_n(\mathbf{k}). \tag{3.18}$$

Note that

$$\begin{aligned} H_0\chi_{n\mathbf{k}} &= e^{i\mathbf{k}\cdot\mathbf{r}}(H_0 + \frac{\mathbf{k}\cdot\mathbf{p}}{m} + \frac{k^2}{2m})u_{n0} \\ &= e^{i\mathbf{k}\cdot\mathbf{r}}(\epsilon_n + \frac{\mathbf{k}\cdot\mathbf{p}}{m} + \frac{k^2}{2m})u_{n0}, \end{aligned} \tag{3.19}$$

where $\epsilon_n \equiv \epsilon_n(\mathbf{k}=0)$ is the energy at $\mathbf{k}=0$. Therefore, the matrix elements of H_0 are

$$\langle n\mathbf{k}|H_0|n'\mathbf{k}'\rangle = \int e^{i(\mathbf{k}'-\mathbf{k})\cdot\mathbf{r}} u^*_{n0}\left(\epsilon_n + \frac{\mathbf{k}'\cdot\mathbf{p}}{m_0} + \frac{k'^2}{2m_0}\right) u_{n'0}\mathrm{d}\mathbf{r}. \tag{3.20}$$

Since $u^*_{n0}\left(\epsilon_n + \frac{\mathbf{k}\cdot\mathbf{p}}{m_0} + \frac{k^2}{2m_0}\right) u_{n'0}$ has the lattice periodicity, we may expand in terms of the reciprocal lattice vectors in the same way as before. We then find that

$$\begin{aligned}\langle n\mathbf{k}|H_0|n'\mathbf{k}'\rangle &= \frac{(2\pi)^3}{\Omega}\delta(\mathbf{k}-\mathbf{k}')\int_{\text{cell}} u^*_{n0}(\epsilon_{n'} + \frac{\mathbf{k}'\cdot\mathbf{p}}{m_0} + \frac{k'^2}{2m_0})u_{n'0}\mathrm{d}\mathbf{r} \\ &= \delta(\mathbf{k}-\mathbf{k}')\left[\left(\epsilon_n + \frac{k^2}{2m_0}\right)\delta_{nn'} + \frac{\mathbf{k}\cdot\mathbf{p}_{nn'}}{m_0}\right],\end{aligned} \tag{3.21}$$

where we have used Eq. (3.15) so that $\frac{(2\pi)^3}{\Omega}\int_{cell} u^*_{n0}u_{n'0} = 1$ and we have introduced the momentum matrix elements

$$\mathbf{p}_{nn'} = \frac{(2\pi)^3}{\Omega}\int_{\text{cell}} u^*_{n0}\mathbf{p}u_{n'0}\mathrm{d}\mathbf{r}. \tag{3.22}$$

We will now derive an expression for the expectation value of the velocity operator and use this to find the intraband momentum matrix elements, $p_{nn'}$. By a canonical transformation, we introduce

$$\widetilde{H}_0 = e^{-i\mathbf{k}\cdot\mathbf{r}}H_0e^{i\mathbf{k}\cdot\mathbf{r}} = \frac{(\mathbf{k}+\mathbf{p})^2}{2m_0} + V, \tag{3.23}$$

so that

$$\widetilde{H}_0u_{nk} = \epsilon_n(\mathbf{k})u_{nk}. \tag{3.24}$$

Multiplying by $u^*_{nk}\nabla_{\mathbf{k}}$ and integrating, we get

$$\int \mathrm{d}\mathbf{r}u^*_{nk}\nabla_{\mathbf{k}}\left[\widetilde{H}_0u_{n'k}\right] = \int \mathrm{d}\mathbf{r}u^*_{nk}\nabla_{\mathbf{k}}\left[\epsilon_{n'}(\mathbf{k})u_{n'k}\right]. \tag{3.25}$$

The left hand side is then

$$\begin{aligned}&\int \mathrm{d}\mathbf{r}u^*_{nk}(\nabla_{\mathbf{k}}\widetilde{H}_0)u_{n'k} + \int \mathrm{d}\mathbf{r}u^*_{nk}\widetilde{H}_0(\nabla_{\mathbf{k}}u_{n'k}) = \\ &\int \mathrm{d}\mathbf{r}u^*_{nk}(\nabla_{\mathbf{k}}\widetilde{H}_0)u_{n'k} + \int \mathrm{d}\mathbf{r}u^*_{nk}\epsilon_n(\mathbf{k})(\nabla_{\mathbf{k}}u_{n'k}),\end{aligned} \tag{3.26}$$

where we have used that $\widetilde{H}_0$ is Hermitian. The right hand side is

$$\int \mathrm{d}\mathbf{r} u^*_{nk} \nabla_{\mathbf{k}} \left[\epsilon_{n'}(\mathbf{k}) u_{n'k}\right] = \delta_{nn'} \nabla_{\mathbf{k}} \epsilon_{n'}(\mathbf{k}) + \int \mathrm{d}\mathbf{r} u^*_{nk} \epsilon_{n'}(\mathbf{k}) (\nabla_{\mathbf{k}} u_{n'k}), \tag{3.27}$$

so

$$\begin{aligned} \delta_{nn'} \nabla_{\mathbf{k}} \epsilon_n(\mathbf{k}) + [\epsilon_{n'}(\mathbf{k}) - \epsilon_n(\mathbf{k})] \int \mathrm{d}\mathbf{r} u^*_{nk} (\nabla_{\mathbf{k}} u_{n'k}) &= \int \mathrm{d}\mathbf{r} u^*_{nk} (\nabla_{\mathbf{k}} \widetilde{H}_0) u_{n'k} \\ &= \int \mathrm{d}\mathbf{r} u^*_{nk} (\frac{\mathbf{k}+\mathbf{p}}{m_0}) u_{n'k} \\ &= \int \mathrm{d}\mathbf{r} \psi^*_{nk} \frac{\mathbf{p}}{m_0} \psi_{n'k}, \end{aligned} \tag{3.28}$$

which means that we may express the intraband momentum matrix elements as

$$\mathbf{p}_{nn'}(\mathbf{k}) = m_0 \nabla_{\mathbf{k}} \epsilon_n(\mathbf{k}) + m_0 [\epsilon_{n'}(\mathbf{k}) - \epsilon_n(\mathbf{k})] \int \mathrm{d}\mathbf{r} u^*_{nk} (\nabla_{\mathbf{k}} u_{n'k}), \tag{3.29}$$

which is zero at the bottom of a band, i.e. $\mathbf{p}_{nn} = 0$. The matrix elements of U might be found in a similar fashion, with the use of the representation of Eq. (3.11),

$$\begin{aligned} \langle n\mathbf{k}|U|n'\mathbf{k}'\rangle &= \int \mathrm{d}\mathbf{r} e^{i(\mathbf{k}'-\mathbf{k})\cdot\mathbf{r}} U u^*_{n0} u_{n'0} \\ &= \sum_m \int \mathrm{d}\mathbf{r} e^{i(\mathbf{k}'-\mathbf{k})\cdot\mathbf{r}} U B^{nn'}_m e^{-i\mathbf{K}_m\cdot\mathbf{r}}. \end{aligned} \tag{3.30}$$

With the use of the Fourier transform of U,

$$\mathcal{U}(\mathbf{k}) \equiv \frac{1}{(2\pi)^3} \int \mathrm{d}\mathbf{r} e^{-i\mathbf{k}\cdot\mathbf{r}} U(\mathbf{r}), \tag{3.31}$$

we may write this as

$$\langle n\mathbf{k}|U|n'\mathbf{k}'\rangle = (2\pi)^3 \sum_m B^{nn'}_m \mathcal{U}(\mathbf{k} - \mathbf{k}' + \mathbf{K}_m). \tag{3.32}$$

By assumption, the impurity potential U is slowly varying in space. It is then a good approximation to keep only the terms with $m = 0$. Any term with $m \neq 0$

would lead to high frequency components in the Fourier transform, which would be small. This approximates the matrix element to

$$\begin{aligned}\langle n\mathbf{k}|U|n'\mathbf{k}'\rangle &= (2\pi)^3 B_0^{nn'}\mathcal{U}(\mathbf{k}-\mathbf{k}') \\ &= \delta_{nn'}\mathcal{U}(\mathbf{k}-\mathbf{k}'). \end{aligned} \tag{3.33}$$

With this approximation of the impurity potential, Eq. (3.18) may then be written as

$$\left(\epsilon_n + \frac{k^2}{2m_0}\right) A_n(\mathbf{k}) + \sum_{n'\neq n} \frac{\mathbf{k}\cdot\mathbf{p}_{nn'}}{m_0} A_{n'}(\mathbf{k}) + \int \mathrm{d}\mathbf{k}'\mathcal{U}(\mathbf{k}-\mathbf{k}')A_n(\mathbf{k}') = \epsilon A_n(\mathbf{k}). \tag{3.34}$$

This is a set of coupled equations for the expansion coefficients $A_n(\mathbf{k})$. The only approximation in deriving this equation is that $\mathcal{U}(\mathbf{k})$ varies slowly.

We can now get rid of the terms linear in $\mathbf{k}$ by carrying out a canonical transformation. We may view Eq. (3.34) as a matrix equation, of the form

$$HA = \epsilon A. \tag{3.35}$$

By letting

$$B = e^{-S}A, \tag{3.36}$$

we can transform the equation to

$$e^{-S}He^{S}B = \epsilon B \equiv \widetilde{H}B. \tag{3.37}$$

We are interested in the eigenstate to the second order in the wave-vector $\mathbf{k}$. It will become clear that S is linear in wave-vector $\mathbf{k}$ to the lowest order. Expanding $\widetilde{H}$ to second order in S, we get

$$\widetilde{H} = H + [H,S] + \frac{1}{2}[[H,S],S] + \cdots . \tag{3.38}$$

With

$$H = H^{(0)} + H^{(1)} + U, \tag{3.39}$$

where

$$\langle n\mathbf{k}|H^{(0)}|n'\mathbf{k}\rangle = \left(\epsilon_n + \frac{k^2}{2m_0}\right)\delta_{nn'}\delta(\mathbf{k}-\mathbf{k}'), \tag{3.40a}$$

$$\langle n\mathbf{k}|H^{(1)}|n'\mathbf{k}\rangle = \frac{\mathbf{k}\cdot\mathbf{p}_{nn'}}{m_0}\delta(\mathbf{k}-\mathbf{k}'), \tag{3.40b}$$

$$\langle n\mathbf{k}|U|n'\mathbf{k}\rangle = \mathcal{U}(\mathbf{k}-\mathbf{k}')\delta_{nn'}, \tag{3.40c}$$

we get

$$\widetilde{H} = H^{(0)}+U+H^{(1)}+[H^{(0)},S]+[H^{(1)},S]+\frac{1}{2}[[H^{(0)},S],S]+[U,S]+\frac{1}{2}[[U,S],S]+\cdots. \tag{3.41}$$

We now choose S so that

$$H^{(1)} + [H^{(0)}, S] = 0, \tag{3.42}$$

and thus all first order terms in $\mathbf{k}$ are eliminated. This is equivalent to choosing the matrix elements of S to be

$$\langle n\mathbf{k}|S|n'\mathbf{k}'\rangle = \begin{cases} -\frac{\mathbf{k}\cdot\mathbf{p}_{nn'}}{m_0\omega_{nn'}}\delta(\mathbf{k}-\mathbf{k}'), & n \neq n', \\ 0, & n = n', \end{cases} \tag{3.43}$$

where $\omega_{nn'} = \epsilon_n - \epsilon_{n'}$. With this choice, we also get that

$$[H^{(1)}, S] + \frac{1}{2}[[H^{(0)}, S], S] = \frac{1}{2}[H^{(1)}, S]. \tag{3.44}$$

Expressing the identity in our basis, $\mathbb{I} = \int d\mathbf{k} \sum_n |n\mathbf{k}\rangle\langle n\mathbf{k}|$, we find

$$\frac{1}{2}\langle n\mathbf{k}|[H^{(1)},S]|n'\mathbf{k}'\rangle = \frac{k_\alpha k_\beta}{2m_0^2}\left[\sum_{n''\neq n,n'} p^\alpha_{nn''}p^\beta_{n''n'}\left(\frac{1}{\omega_{nn''}}+\frac{1}{\omega_{n'n''}}\right)\right]\delta(\mathbf{k}-\mathbf{k}'), \tag{3.45}$$

where there is an implicit sum over the spatial coordinates $\alpha, \beta \in (x, y, z)$. Similarly we find that

$$\langle n\mathbf{k}|[U,S]|n'\mathbf{k}'\rangle = \begin{cases} \mathcal{U}(\mathbf{k}-\mathbf{k}')\frac{(\mathbf{k}-\mathbf{k}')\cdot\mathbf{p}_{nn'}}{m_0\omega_{nn'}}, & n \neq n', \\ 0, & n = n. \end{cases} \tag{3.46}$$

Admittedly these elements arising from the impurity potential are of first order in $\mathbf{k}$. However, omitting them is a good approximation; the ratio between a typical Fourier component of U and the typical interband separation is very small. Also the off-diagonal matrix elements of $\widetilde{H}$ which are of second order can be neglected, as they would only give higher order contributions when projected onto the lowest energy bands. The result is a diagonal matrix equation for $B_n(\mathbf{k})$,

$$\left(\epsilon_n + \frac{k^2}{2m_0} + \frac{k_\alpha k_\beta}{m_0^2} \sum_{n'' \neq n} \frac{p^\alpha_{nn''} p^\beta_{n''n}}{\omega_{nn''}}\right) B_n(\mathbf{k}) + \int \mathrm{d}\mathbf{k}' \mathcal{U}(\mathbf{k}-\mathbf{k}') B_n(\mathbf{k}') = \epsilon B(\mathbf{k}). \tag{3.47}$$

By using the f-sum rule from Appendix A, we see that the expression in the bracket on the left hand side is the second order expansion of $\epsilon_n(\mathbf{k})$, so that

$$\epsilon_n(\mathbf{k}) B_n(\mathbf{k}) + \int \mathrm{d}\mathbf{k}' \mathcal{U}(\mathbf{k}-\mathbf{k}') B_n(\mathbf{k}') = \epsilon B_n(\mathbf{k}), \tag{3.48}$$

where $\epsilon_n(\mathbf{k})$ is to be expanded to second order in wave-vector $\mathbf{k}$. We can now do a Fourier transformation to real space coordinates. We therefore introduce a function

$$F_n(\mathbf{r}) \equiv \int \mathrm{d}\mathbf{k} e^{i\mathbf{k}\cdot\mathbf{r}} B_n(\mathbf{k}), \tag{3.49}$$

or equivalently

$$B_n(\mathbf{k}) = \frac{\Omega}{(2\pi)^3} \sum_m e^{-i\mathbf{k}\cdot\mathbf{R}_m} F_n(\mathbf{R}_m). \tag{3.50}$$

We then get

$$\left[\epsilon_n(-i\nabla) + U(\mathbf{r})\right] F_n(\mathbf{r}) = \epsilon F_n(\mathbf{r}). \tag{3.51}$$

Note that as a zeroth order approximation we have $B_n(\mathbf{k}) \approx A_n(\mathbf{k})$ so

$$\begin{aligned} \psi &\approx \sum_n \int \mathrm{d}\mathbf{k} B_n(\mathbf{k}) e^{i\mathbf{k}\cdot\mathbf{r}} u_{n0}(\mathbf{r}) \\ &= \sum_n F_n(\mathbf{r}) u_{n0}(\mathbf{r}). \end{aligned} \tag{3.52}$$

Because there is no coupling between the states $F_n(\mathbf{r})$ we can now choose to look at a single band, for example the conduction band, which takes the form

$$\psi = F(\mathbf{r}) \psi_c(\mathbf{r}), \tag{3.53}$$

where $\psi_c(\mathbf{r})$ is the Bloch function at the band minimum, and $F(\mathbf{r})$ is an envelope function centered at the impurity.

3.2 Degenerate bands

If the bands are degenerate we will have to modify the procedure slightly. For reasons of simplicity we consider a crystal which has inversion symmetry about some point. Let us assume an r-fold degeneracy at the band minimum, which is assumed to be located at $\mathbf{k} = 0$. We denote the degenerate states ϕ_j, where $j \in [1, r]$.

$$H_0\phi_j = \epsilon_0\phi_j. \tag{3.54}$$

All the other bands are denoted by ϕ_i where $i \notin [1, r]$. For a crystal with a center of symmetry, the parity operator, $\mathcal{P}$, commutes with the Hamiltonian, which means that unless there is some accidental degeneracy the degenerate states, ϕ_j, have the same parity. The momentum matrix elements between states of same parity are zero [71],

$$p^{\alpha}_{jj'} = 0, \tag{3.55}$$

where α denotes the spatial coordinate. Again we expand the solution of the Schrödinger equation in the Luttinger-Kohn basis of Eq. (3.17), which leads to the same equation for the expansion functions $A_n(\mathbf{k})$ as Eq. (3.18):

$$\sum_{n'} \int \mathrm{d}\mathbf{k}' \langle n\mathbf{k}|H_0 + U|n'\mathbf{k}'\rangle A_{n'}(\mathbf{k}') = \epsilon A_n(\mathbf{k}). \tag{3.56}$$

We then follow the same steps as in the case of non-degenerate bands, and with n set to one of the degenerate bands j, we get

$$\left(\epsilon_0 + \frac{k^2}{2m_0}\right) A_j(\mathbf{k}) + \sum_i \frac{k_\alpha p^{\alpha}_{ji}}{m_0} A_i(\mathbf{k}) + \int \mathrm{d}\mathbf{k}' \mathcal{U}(\mathbf{k} - \mathbf{k}') A_j(\mathbf{k}') = \epsilon A_j(\mathbf{k}). \tag{3.57}$$

The canonical transformation we use is then slightly modified and becomes

$$\langle n\mathbf{k}|S|n'\mathbf{k}'\rangle = \begin{cases} -\frac{\mathbf{k}\cdot\mathbf{p}_{nn'}}{m_0\omega_{nn'}}\delta(\mathbf{k} - \mathbf{k}'), & \omega_{nn'} \neq 0, \\ 0, & \omega_{nn'} = 0, \end{cases} \tag{3.58}$$

which means the matrix elements of S are zero for two states in the degenerate bands. For $n = j$, this yields to second order in k

$$\sum_{j'}\left(\epsilon_0\delta_{jj'} + \frac{k^2}{2m_0}\delta_{jj'} + \frac{k_\alpha k_\beta}{m_0^2}\sum_i \frac{p_{ji}^\alpha p_{ij'}^\beta}{\epsilon_0 - \epsilon_i}\right) B_{j'}(\mathbf{k}) + \int \mathcal{U}(\mathbf{k}-\mathbf{k}')B_j(\mathbf{k}')d\mathbf{k}' = \epsilon B_j(\mathbf{k}). \tag{3.59}$$

Note that all off-diagonal terms represent coupling between j and j' states, coupling between j and i states are neglected as they would lead to higher order terms when eliminated. We let ϵ be the energy measured from the bandedge by setting the energy to be zero at ϵ_0,

$$\sum_{j'=1}^{r}(D_{jj'}^{\alpha\beta}k_\alpha k_\beta)B_{j'}(\mathbf{k}) + \int \mathcal{U}(\mathbf{k}-\mathbf{k}')B_j(\mathbf{k}')d\mathbf{k}' = \epsilon B_j(\mathbf{k}), \tag{3.60}$$

with

$$D_{jj'}^{\alpha\beta} = \frac{1}{2m_0}\delta_{jj'}\delta_{\alpha\beta} + \frac{1}{m_0^2}\sum_i \frac{p_{ji}^\alpha p_{ij'}^\beta}{\epsilon_0 - \epsilon_i}. \tag{3.61}$$

Again, introducing the Fourier transformation of $B_j(\mathbf{k})$

$$F_j(\mathbf{r}) = \int e^{i\mathbf{k}\cdot\mathbf{r}}B_j(\mathbf{k})d\mathbf{k}, \tag{3.62}$$

we arrive at the effective equation for the degenerate case

$$\sum_{j'=1}^{r}\left[D_{jj'}^{\alpha\beta}\left(\frac{1}{i}\nabla_\alpha\right)\left(\frac{1}{i}\nabla_\beta\right) + U(\mathbf{r})\delta_{jj'}\right]F_j'(\mathbf{r}) = \epsilon F_j(\mathbf{r}). \tag{3.63}$$

This set of equations are completly analogous to Eq. (3.51), but as we can see the fact that the bands of interest are degenerate greatly increases the complexity of the problem.

3.3 Spin-orbit interaction

We now include the spin-orbit coupling to the Hamiltonian

$$H_{\mathrm{SO}} = \frac{1}{4m_0^2c^2}(\boldsymbol{\sigma}\times\nabla V)\cdot\mathbf{p}, \tag{3.64}$$

where $\boldsymbol{\sigma} = (\sigma_x, \sigma_y, \sigma_z)$, and V is the periodic potential. The modified Hamiltonian,

$$\bar{H}_0 = H_0 + H_{\mathrm{SO}}, \tag{3.65}$$

still has Bloch waves as eigenfunctions. We denote these spin-dependent Bloch waves as $\bar{\psi}_{n\mathbf{k}} = e^{i\mathbf{k}\cdot\mathbf{r}}\bar{u}_{n\mathbf{k}}$, and the corresponding energy $\bar{\epsilon}_{n\mathbf{k}}$. We note that $\bar{u}_{n\mathbf{k}}$ now is a two-component spinor. In the same way as before we choose to expand the solutions in the basis given by

$$\bar{\chi}_{n\mathbf{k}} = e^{i\mathbf{k}\cdot\mathbf{r}}\bar{u}_{n0}, \tag{3.66}$$

so that

$$\psi = \sum_n \int \mathrm{d}\mathbf{k} A_n(\mathbf{k})\bar{\chi}_{n\mathbf{k}}. \tag{3.67}$$

We now proceed in the same way as in the previous sections, the only difference being that the matrix elements $\mathbf{p}_{nn'}$ are replaced by a spin-dependent velocity operator $\boldsymbol{\pi}_{nn'}$ given by

$$\boldsymbol{\pi}_{nn'} = \frac{(2\pi)^3}{\Omega}\int_{\mathrm{cell}} \mathrm{d}\mathbf{r}\bar{u}^*_{n0}\left(\frac{1}{im_0}\nabla + \frac{1}{4m_0^2c^2}(\boldsymbol{\sigma}\times\nabla V)\right)\bar{u}_{n'0}. \tag{3.68}$$

Following the same steps as in Section 3.1 we may easily show that

$$\boldsymbol{\pi}_{nn} = \nabla_{\mathbf{k}}\epsilon(\mathbf{k})|_{\mathbf{k}=0}, \tag{3.69}$$

which is zero at the band minimum. The effective mass equation then takes the same form as Eq. (3.63) with $\mathbf{p}_{nn'} \to m_0\boldsymbol{\pi}_{nn'}$.

3.4 Renormalised impurity induced spin-orbit coupling

We need to carry out a more careful inspection of the effect of the canonical transformation on the impurity potential. It is this term which gives rise to a renormalisation of the extrinsic spin-orbit coupling at impurities. To this end, we re-consider the term

$$\frac{1}{2}[[U,S],S] = \frac{1}{2}(USS + SSU - 2SUS), \tag{3.70}$$

which is a result of the canonical transformation. This term was neglected by Luttinger and Kohn [71]. Let us consider the first term on the right hand side of Eq. (3.70)

$$\begin{aligned}
\langle n\mathbf{k}|USS|n'\mathbf{k}'\rangle &= \int \mathrm{d}\mathbf{q} \int \mathrm{d}\mathbf{q}' \sum_{m,m'} \langle n\mathbf{k}|U|m\mathbf{q}\rangle\langle m\mathbf{q}|S|m'\mathbf{q}'\rangle\langle m'\mathbf{q}'|S|n'\mathbf{k}'\rangle \\
&= \int \mathrm{d}\mathbf{q} \int \mathrm{d}\mathbf{q}' \sum_{m,m'} \mathcal{U}(\mathbf{k}-\mathbf{q})\delta_{nm} \frac{q_\alpha \pi^\alpha_{mm'}\delta(\mathbf{q}-\mathbf{q}')}{\omega_{mm'}} \frac{q'_\beta \pi^\beta_{m'n'}\delta(\mathbf{q}'-\mathbf{k}')}{\omega_{m'n'}} \\
&= \int \mathrm{d}\mathbf{q} \sum_{m'} \mathcal{U}(\mathbf{k}-\mathbf{q}) \frac{q_\alpha \pi^\alpha_{nm'}\delta(\mathbf{q}-\mathbf{k}')}{\omega_{nm'}} \frac{k'_\beta \pi^\beta_{m'n'}}{\omega_{m'n'}} \\
&= \sum_m \mathcal{U}(\mathbf{k}-\mathbf{k}') \frac{k'_\alpha k'_\beta \pi^\alpha_{nm}\pi^\beta_{mn'}}{\omega_{nm}\omega_{mn'}}. \qquad (3.71)
\end{aligned}$$

We can now use that S is anti-Hermitian and that U is Hermitian, so that with $(\pi^\alpha_{nm})^* = \pi^\alpha_{mn}$ we have

$$\begin{aligned}
\langle n\mathbf{k}|SSU|n'\mathbf{k}'\rangle &= \langle n'\mathbf{k}'|USS|n\mathbf{k}\rangle^\dagger \\
&= \sum_m \mathcal{U}(\mathbf{k}-\mathbf{k}') \frac{k_\alpha k_\beta \pi^\alpha_{nm}\pi^\beta_{mn'}}{\omega_{nm}\omega_{mn'}}. \qquad (3.72)
\end{aligned}$$

Finally, the last term on the right hand side of Eq. (3.70) is

$$\begin{aligned}
\langle n\mathbf{k}|SUS|n'\mathbf{k}'\rangle &= \int \mathrm{d}\mathbf{q} \int \mathrm{d}\mathbf{q}' \sum_{m,m'} \langle n\mathbf{k}|S|m\mathbf{q}\rangle\langle m\mathbf{q}|U|m'\mathbf{q}'\rangle\langle m'\mathbf{q}'|S|n'\mathbf{k}'\rangle \\
&= \int \mathrm{d}\mathbf{q} \int \mathrm{d}\mathbf{q}' \sum_{m,m'} \frac{k_\alpha \pi^\alpha_{nm}\delta(\mathbf{k}-\mathbf{q})}{\omega_{nm}} \mathcal{U}(\mathbf{q}-\mathbf{q}')\delta_{mm'} \frac{q'_\beta \pi^\beta_{m'n'}\delta(\mathbf{q}'-\mathbf{k}')}{\omega_{m'n'}} \\
&= \int \mathrm{d}\mathbf{q} \sum_m \frac{k_\alpha \pi^\alpha_{nm}\delta(\mathbf{k}-\mathbf{q})}{\omega_{nm}} \mathcal{U}(\mathbf{q}-\mathbf{k}') \frac{k'_\beta \pi^\beta_{mn'}}{\omega_{mn'}} \\
&= \sum_m \frac{k_\alpha \pi^\alpha_{nm}}{\omega_{nm}} \mathcal{U}(\mathbf{k}-\mathbf{k}') \frac{k'_\beta \pi^\beta_{mn'}}{\omega_{mn'}} \\
&= \sum_m \mathcal{U}(\mathbf{k}-\mathbf{k}') \frac{k_\alpha k'_\beta \pi^\alpha_{nm}\pi^\beta_{mn'}}{\omega_{nm}\omega_{mn'}}. \qquad (3.73)
\end{aligned}$$

Let us now look at the contribution to the effective Schrödinger equation of Eq. (3.51) from these terms. We again keep only terms which correspond to

intraband coupling. The total contribution is

$$\int \mathrm{d}\mathbf{k} \int \mathrm{d}\mathbf{k}' \sum_{j'} \langle j\mathbf{k}| \frac{1}{2}[[U,S],S]|j'\mathbf{k}'\rangle B_j(\mathbf{k}') e^{i\mathbf{k}\cdot\mathbf{r}}. \tag{3.74}$$

To simplify the calculations we look only at the $\mathbf{k}, \mathbf{k}'$ dependent part of the terms, starting with the matrix element of SSU.

$$\begin{aligned} &\int \mathrm{d}\mathbf{k} \int \mathrm{d}\mathbf{k}' \mathcal{U}(\mathbf{k}-\mathbf{k}') k_\alpha k_\beta B(\mathbf{k}') e^{i\mathbf{k}\cdot\mathbf{r}} \\ &= - \int \mathrm{d}\mathbf{k} \int \mathrm{d}\mathbf{k}' \mathcal{U}(\mathbf{k}-\mathbf{k}') B(\mathbf{k}') \nabla_\alpha \nabla_\beta e^{i\mathbf{k}\cdot\mathbf{r}} \\ &= - \nabla_\alpha \nabla_\beta \left[U(\mathbf{r}) F(\mathbf{r}) \right]. \end{aligned} \tag{3.75}$$

We continue in the same way for SUS,

$$\begin{aligned} &\int \mathrm{d}\mathbf{k} \int \mathrm{d}\mathbf{k}' \mathcal{U}(\mathbf{k}-\mathbf{k}') k_\alpha k'_\beta B(\mathbf{k}') e^{i\mathbf{k}\cdot\mathbf{r}} \\ &= - i\nabla_\alpha \left[\int \mathrm{d}\mathbf{k}' k'_\beta \int \mathrm{d}\mathbf{k} \mathcal{U}(\mathbf{k}-\mathbf{k}') e^{i\mathbf{k}\cdot\mathbf{r}} B(\mathbf{k}') \right] \\ &= - i\nabla_\alpha \left[U(\mathbf{r}) \int \mathrm{d}\mathbf{k}' k_\beta e^{i\mathbf{k}'\cdot\mathbf{r}} B(\mathbf{k}') \right] \\ &= - \nabla_\alpha \left[U(\mathbf{r}) \nabla_\beta F(\mathbf{r}) \right], \end{aligned} \tag{3.76}$$

and finally for SSU,

$$\begin{aligned} &\int \mathrm{d}\mathbf{k} \int \mathrm{d}\mathbf{k}' \mathcal{U}(\mathbf{k}-\mathbf{k}') k'_\alpha k'_\beta B(\mathbf{k}') e^{i\mathbf{k}\cdot\mathbf{r}} \\ &= U(\mathbf{r}) \int \mathrm{d}\mathbf{k}' k'_\alpha k'_\beta e^{i\mathbf{k}'\cdot\mathbf{r}} B(\mathbf{k}') \\ &= - U(\mathbf{r}) \nabla_\alpha \nabla_\beta F(\mathbf{r}). \end{aligned} \tag{3.77}$$

We may then write down the total contribution from the term in question to Eq. (3.51).

$$\begin{aligned}
&\int \mathrm{d}\mathbf{k} \int \mathrm{d}\mathbf{k}' \sum_{j'} \langle j\mathbf{k}| \frac{1}{2}[[U,S],S]|j'\mathbf{k}'\rangle B_{j'}(\mathbf{k}') e^{i\mathbf{k}\cdot\mathbf{r}} \\
&= \sum_{j'} \frac{1}{2} \big\{ -U(\mathbf{r})\nabla_\alpha\nabla_\beta F_{j'}(\mathbf{r}) - \nabla_\alpha\nabla_\beta \left[U(\mathbf{r})F_{j'}(\mathbf{r})\right] \\
&\quad + 2\nabla_\alpha \left[U(\mathbf{r})\nabla_\beta F_{j'}(\mathbf{r})\right] \big\} \sum_m \frac{\pi^\alpha_{jm}\pi^\beta_{mj'}}{\omega_{jm}\omega_{mj'}} \\
&= \sum_{j'} \frac{1}{2} \big\{ -\left[\nabla_\alpha\nabla_\beta U(\mathbf{r})\right] F_{j'}(\mathbf{r}) \\
&\quad + \left[\nabla_\alpha U(\mathbf{r})\right] \nabla_\beta F_{j'}(\mathbf{r}) - \left[\nabla_\beta U(\mathbf{r})\right] \nabla_\alpha F_{j'}(\mathbf{r}) \big\} \sum_m \frac{\pi^\alpha_{jm}\pi^\beta_{mj'}}{\omega_{jm}\omega_{mj'}}.
\end{aligned} \tag{3.78}$$

Because $\nabla_\alpha\nabla_\beta = \nabla_\beta\nabla_\alpha$ the first term is symmetric with respect to exchange to α and β, and with

$$\begin{aligned}
&\left[\nabla_\alpha U(\mathbf{r})\right] \nabla_\beta F_{j'}(\mathbf{r}) - \left[\nabla_\beta U(\mathbf{r})\right] \nabla_\alpha F_{j'}(\mathbf{r}) = \\
&- \left\{\left[\nabla_\beta U(\mathbf{r})\right] \nabla_\alpha F_{j'}(\mathbf{r}) - \left[\nabla_\alpha U(\mathbf{r})\right] \nabla_\beta F_{j'}(\mathbf{r})\right\},
\end{aligned} \tag{3.79}$$

we see that the two other terms form an anti-symmetry part. The contribution will no doubt be very small, but depending on the momentum matrix elements it could be qualitatively important in that it renormalises the spin-orbit coupling at extrinsic impurities.

3.5 Germanium

The germanium crystal has a diamond structure. The choice of coordinate axes are shown in Figure 1. If we neglect the effect of the spin-orbit coupling, germanium has a three-fold degeneracy in the highest valence bands at $\mathbf{k} = 0$. Because of the diamond structure symmetry, the eigenfunctions corresponding to these bands contain only p orbitals, and the conduction band only s orbitals. We will first show how the effect from a single impurity in absence of spin-orbit coupling on the valence band can be calculated using the method presented.

Secondly, we will show how the splitting of the valence bands due to the spin-orbit coupling affects the conduction band (see Figure 2).

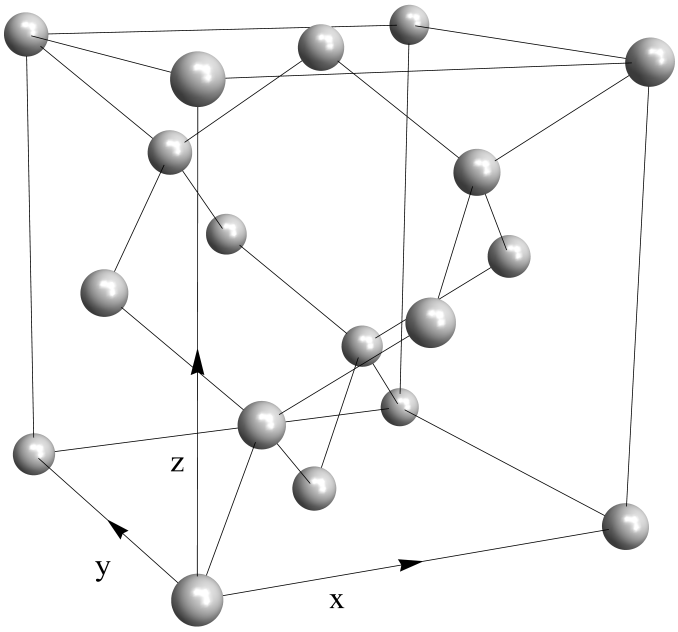

Figure 1. Unit cell of germanium lattice with coordinate axes. It has a diamond structure, or equivalently a face centered cubic lattice with a basis $(0, 0, 0)$ and $\frac{1}{4}(1, 1, 1)$.

Valence bands in the absence of the spin-orbit coupling

First we now will look at the form of the equations of the valence bands, thus giving a coupled set of equations to describe the holes, disregarding the effect of the spin-orbit coupling. We also here follow the method outlined by Luttinger and Kohn [71]. The three degenerate valence states are denoted by the index j and the conduction band s state by i. Finding the equations for the three valence bands is now just a matter of finding the matrix D, defined by

$$D_{jj'} = k_\alpha k_\beta D^{\alpha\beta}_{jj'}. \tag{3.80}$$

We choose our basis to be (X, Y, Z) where X contains only p_x orbitals and so on. Let us first look at the (X, X) element.

$$D_{XX} = k_\alpha k_\beta (\frac{1}{2m_0}\delta_{XX}\delta_{\alpha\beta} + \frac{1}{m_0^2}\sum_i \frac{p^\alpha_{Xi}p^\beta_{iX}}{\epsilon_0 - \epsilon_i}). \tag{3.81}$$

Because of cubic symmetry

$$\sum_i \frac{p^y_{Xi}p^y_{iX}}{\epsilon_0 - \epsilon_i} = \sum_i \frac{p^z_{Xi}p^z_{iX}}{\epsilon_0 - \epsilon_i}. \tag{3.82}$$

$p^\beta_{\alpha i}$ will only be non zero if state i is anti symmetric in both α and β, and symmetric in $\gamma \neq \alpha, \beta$, from this it follows that

$$p^y_{Xi}p^z_{iX} = 0. \tag{3.83}$$

We can then write down a simple expression for the matrix element of Eq. (3.81),

$$D_{XX} = Ak_x^2 + B(k_y^2 + k_z^2), \tag{3.84}$$

where

$$A = \frac{1}{2m_0} + \frac{1}{m_0^2}\sum_i \frac{p^x_{Xi}p^x_{iX}}{\epsilon_0 - \epsilon_i}, \tag{3.85a}$$

$$B = \frac{1}{2m_0} + \frac{1}{m_0^2}\sum_i \frac{p^y_{Xi}p^y_{iX}}{\epsilon_0 - \epsilon_i}. \tag{3.85b}$$

And for the (X, Y) component by using the same arguments we find that

$$D_{XY} = Ck_xk_y, \tag{3.86}$$

where

$$C = \frac{1}{m_0^2}\sum_i \frac{p^x_{Xi}p^y_{iY} + p^y_{Xi}p^x_{iY}}{\epsilon_0 - \epsilon_i}. \tag{3.87}$$

The other matrix elements now easily follow from cyclic change of coordinates, and we get

$$D = \begin{pmatrix} Ak_x^2 + B(k_y^2 + k_z^2) & Ck_xk_y & Ck_xk_z \\ Ck_xk_y & Ak_y^2 + B(k_x^2 + k_z^2) & Ck_yk_z \\ Ck_xk_z & Ck_yk_z & Ak_z^2 + B(k_x^2 + k_y^2) \end{pmatrix}, \tag{3.88}$$

which determines the equation for the functions F_n.

Effect of an impurity on conduction band with the spin-orbit coupling

We will now look at how the valence band affects the conduction band when the spin-orbit coupling is included, neglecting the effect of the other bands as in the Kane model [72][73], and also how the term presented in Section 3.4 give rise to an impurity-induced effective spin-orbit coupling.

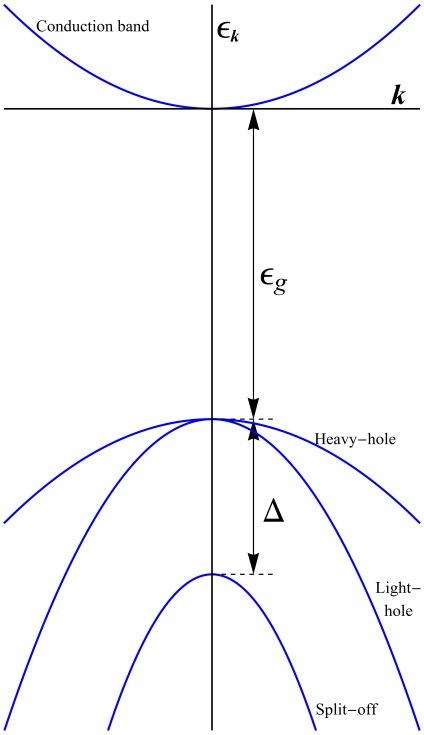

Figure 2. Illustration of the effective bandstructure of germanium. The spin-orbit coupling splits the valence bands.ϵ_g is the bandgap and Δ is the spin-orbit splitting. The two valence bands named heavy-hole and light-hole due to the curvature give a fourfold degeneracy at $\mathbf{k} = 0$.

The spin-orbit Hamiltonian in a basis $(|p_x\uparrow\rangle, |p_y\uparrow\rangle, |p_z\uparrow\rangle, |p_x\downarrow\rangle, |p_y\downarrow\rangle, |p_z\downarrow\rangle)$

is

$$H_{\mathrm{SO}} = \frac{\Delta}{3}\begin{pmatrix} 0 & -i & 0 & 0 & 0 & 1 \\ i & 0 & 0 & 0 & 0 & i \\ 0 & 0 & 0 & -1 & i & 0 \\ 0 & 0 & -1 & 0 & i & 0 \\ 0 & 0 & -i & -i & 0 & 0 \\ 1 & i & 0 & 0 & 0 & 0 \end{pmatrix}, \tag{3.89}$$

where $\frac{\Delta}{3}$ is the spin-orbit coupling constant. Because the p states are degenerate in the absence of spin-orbit coupling at $\mathbf{k} = 0$, we simply need to diagonalise H_{SO} to diagonalise the entire Hamiltonian of the previously degenerate states. This is done by a unitary transformation, so that

$$\widetilde{H}_{\mathrm{SO}} = U^{\dagger} H_{\mathrm{SO}} U \tag{3.90}$$

is a diagonal matrix. We find

$$U = \begin{pmatrix} \frac{1}{\sqrt{3}} & 0 & -\frac{1}{\sqrt{2}} & 0 & 0 & \frac{i}{\sqrt{6}} \\ \frac{i}{\sqrt{3}} & 0 & 0 & 0 & 0 & \sqrt{\frac{2}{3}} \\ 0 & -\frac{i}{\sqrt{3}} & 0 & \frac{i}{\sqrt{2}} & \frac{1}{\sqrt{6}} & 0 \\ 0 & \frac{i}{\sqrt{3}} & 0 & 0 & \sqrt{\frac{2}{3}} & 0 \\ 0 & \frac{1}{\sqrt{3}} & 0 & \frac{1}{\sqrt{2}} & \frac{i}{\sqrt{6}} & 0 \\ \frac{1}{\sqrt{3}} & 0 & \frac{1}{\sqrt{2}} & 0 & 0 & \frac{i}{\sqrt{6}} \end{pmatrix}, \tag{3.91}$$

and

$$\widetilde{H}_{\mathrm{SO}} = \begin{pmatrix} \frac{\Delta}{3} & 0 & 0 & 0 & 0 & 0 \\ 0 & \frac{\Delta}{3} & 0 & 0 & 0 & 0 \\ 0 & 0 & \frac{\Delta}{3} & 0 & 0 & 0 \\ 0 & 0 & 0 & \frac{\Delta}{3} & 0 & 0 \\ 0 & 0 & 0 & 0 & -\frac{2\Delta}{3} & 0 \\ 0 & 0 & 0 & 0 & 0 & -\frac{2\Delta}{3} \end{pmatrix}. \tag{3.92}$$

As can be seen from Eq. (3.92), we now have a quadruplet and a doublet, where the doublet has an energy Δ lower than the quadruplet, see Figure 2. The conduction band is of course not affected by the spin-orbit coupling since

it only contain s orbitals, and remains a doublet, $|s\uparrow\rangle$, $|s\downarrow\rangle$. We proceed to discuss the electronic properties at finite wave-vectors. We will now look at the contribution from the valence band to the sum. Let the energy difference between the conduction band and the quadruplet be denoted ϵ_g. We may then write

$$\frac{p^{\alpha}_{cv}p^{\beta}_{vc'}}{m_0^2\omega_{cv}\omega_{vc'}} = \begin{cases} -\frac{p^{\alpha}_{cv}p^{\beta}_{vc'}}{m_0^2\epsilon_g^2}, & \text{if the } v \text{ state is in the quadruplet,} \\ -\frac{p^{\alpha}_{cv}p^{\beta}_{vc'}}{m_0^2(\epsilon_g+\Delta)^2} \ , & \text{if the } v \text{ state is in the doublet,} \end{cases} \tag{3.93}$$

where the subscript c, c' denotes states of the conduction band, and v, v' the valence band. We now insert the eigenfunctions defined by the transformation matrix given in Eq. (3.91) and define the matrix element of the momentum operator between a state containing only p_x orbitals, $|x\rangle$, and a state containing only s orbitals, $|s\rangle$, to be

$$P \equiv \langle x|\frac{p_x}{m_0}|s\rangle. \tag{3.94}$$

Using a computational tool like Mathematica we get the explicit form of Eq. (3.93),

$$\begin{aligned} &\sum_v \frac{p^{\alpha}_{cv}p^{\beta}_{vc'}}{m_0^2\omega_{cv}\omega_{vc'}} = \\ &-\frac{|P|^2}{3}\left[\delta_{\alpha\beta}\left(\frac{2}{\epsilon_g^2}+\frac{1}{(\epsilon_g+\Delta)^2}\right) + 2i\epsilon_{\alpha\beta\gamma}\langle c|S_\gamma|c'\rangle\left(\frac{1}{(\epsilon_g+\Delta)^2}-\frac{1}{\epsilon_g^2}\right)\right], \end{aligned} \tag{3.95}$$

where S_γ is the γ component of the spin operator $\mathbf{S}$. We may then write the term

$$\int \mathrm{d}\mathbf{k}\int \mathrm{d}\mathbf{k}'\sum_{j'}\langle j\mathbf{k}|\frac{1}{2}[[U,S],S]|j'\mathbf{k}'\rangle B_{j'}(\mathbf{k}')e^{i\mathbf{k}\cdot\mathbf{r}} \tag{3.96}$$

in matrix form,

$$
\begin{aligned}
&-\frac{|P|^2}{3}\left[\delta_{\alpha\beta}\left(\frac{2}{\epsilon_g^2}+\frac{1}{(\epsilon_g+\Delta)^2}\right)+2i\epsilon_{\alpha\beta\gamma}S_\gamma\left(\frac{1}{(\epsilon_g+\Delta)^2}-\frac{1}{\epsilon_g^2}\right)\right]\\
&\times\frac{1}{2}\Big\{-\Big[\nabla_\alpha\nabla_\beta U(\mathbf{r})\Big]F(\mathbf{r})-\Big[\nabla_\beta U(\mathbf{r})\Big]\nabla_\alpha F(\mathbf{r})+\Big[\nabla_\alpha U(\mathbf{r})\Big]\nabla_\beta F(\mathbf{r})\Big\}\\
=&\frac{|P|^2}{6}\Big[\nabla^2 U(\mathbf{r})\Big]F(\mathbf{r})\left(\frac{2}{\epsilon_g^2}+\frac{1}{(\epsilon_g+\Delta)^2}\right)\\
&-\frac{i2|P|^2}{3}\Big[\mathbf{S}\times\nabla U(\mathbf{r})\Big]\cdot\nabla F(\mathbf{r})\left(\frac{1}{(\epsilon_g+\Delta)^2}-\frac{1}{\epsilon_g^2}\right)\\
=&\left\{\frac{\nabla^2 U(\mathbf{r})}{4m^*E_1}+\frac{g^*}{2m_0E_2}\Big[\mathbf{S}\times\nabla U(\mathbf{r})\Big]\cdot(-i\nabla)\right\}F(\mathbf{r}),
\end{aligned}
\tag{3.97}
$$

where

$$E_1=\frac{\epsilon_g(\epsilon_g+\Delta)(3\epsilon_g+2\Delta)}{3\epsilon_g^2+4\epsilon_g\Delta+2\Delta^2}, \tag{3.98a}$$

$$E_2=\frac{\epsilon_g(\epsilon_g+\Delta)}{2\epsilon_g+\Delta}, \tag{3.98b}$$

$$\frac{1}{m^*}=\frac{1}{m_0}+\frac{2|P|^2}{3}\left\{\frac{3\epsilon_g+\Delta}{\epsilon_g(\epsilon_g+\Delta)}\right\}, \tag{3.98c}$$

$$g^*=g_0-\frac{4m_0|P|^2}{3}\left\{\frac{\Delta}{\epsilon_g(\epsilon_g+\Delta)}\right\}, \tag{3.98d}$$

and $F(\mathbf{r})$ is a spinor. The definitions of E_1, E_2, the effective mass and the effective g-factor is the same as in Ref. [74], detailed in the next section. The first term is not that interesting, as it will only give some overall change to the potential. The second term is on the other hand very interesting as it renormalises the spin-orbit coupling at the extrinsic impurity, so that the coupling constant for vacuum is replaced, $1/4m_0^2c^2 \to g^*/2m_0E_2$. In germanium this renormalised coupling constant is much stronger than that of vacuum.

4 The method of Nozières and Lewiner

To get a different notion of how the Luttinger-Kohn method works, and also how time dependence may be introduced, we will work out the theory in an alternate way. To this end, we follow a method first presented by Nozières and Lewiner [74].

4.1 General approach

We still consider a semiconductor, and we are interested in the behaviour of electrons in the conduction band near the band minimum at $\mathbf{k} = \mathbf{k}_0$. An arbitrary state, $\Psi = \psi_1 + \psi_2$, has components of both the conduction band wavefunction

$$\psi_1 = \sum_{j \in c} \int \mathrm{d}\mathbf{k} A_j(\mathbf{k}) \bar{\chi}_{j\mathbf{k}}(\mathbf{r}) \tag{4.1}$$

and the other bands

$$\psi_2 = \sum_{i \in v} \int \mathrm{d}\mathbf{k} A_i(\mathbf{k}) \bar{\chi}_{i\mathbf{k}}(\mathbf{r}). \tag{4.2}$$

Ψ satisfies the time dependent Schrödinger equation,

$$i\dot{\Psi} = H\Psi. \tag{4.3}$$

Before employing the Luttinger-Kohn model we will look at how we may acquire an effective equation for the conduction bands. The Schrödinger equation may be written as two coupled equations, where $h, h^\dagger$ is the coupling between the conduction band states and the other band states,

$$i\dot{\psi}_1 = H_1\psi_1 + h\psi_2, \tag{4.4a}$$

$$i\dot{\psi}_2 = h^\dagger\psi_1 + H_2\psi_2. \tag{4.4b}$$

H_2 is a sum of two components, one which gives us the energy gap measured from the conduction band at the band minimum, H_g, and one which describes any coupling between the other bands, H_2', resembling H_1,

$$H_2 = H_g + H_2'. \tag{4.5}$$

H_g is considered to be large compared to the other components of H. To eliminate ψ_2 from Eq. (4.4a), we solve Eq. (4.4b) for ψ_2 by using an iteration scheme up to second order in $1/H_2$,

$$\begin{aligned}\psi_2 &= -\frac{1}{H_2}h^\dagger\psi_1 + \frac{i}{H_2}\dot{\psi}_2 \\ &= -\frac{1}{H_2}h^\dagger\psi_1 - \frac{i}{H_2^2}\left(\dot{h}^\dagger\psi_1 + h^\dagger\dot{\psi}_1\right) + \mathcal{O}(\frac{1}{H_2^3}).\end{aligned} \tag{4.6}$$

Expanding Eq. (4.6) in the inverse of the bandgap, $1/H_g$, up to second order

$$\psi_2 = \left[-\frac{1}{H_g}h^\dagger + \frac{1}{H_g}H_2'\frac{1}{H_g}h^\dagger - \frac{i}{H_g^2}\dot{h}^\dagger\right]\psi_1 - \frac{i}{H_g^2}h^\dagger\dot{\psi}_1 + \mathcal{O}(\frac{1}{H_g^3}). \tag{4.7}$$

We can now eliminate ψ_2 by inserting the expression for ψ_2 from Eq. (4.7) into Eq. (4.4a) and get

$$i(1+\Lambda)\dot{\psi}_1 = \bar{H}\psi_1, \tag{4.8}$$

with

$$\Lambda = h\frac{1}{H_g^2}h^\dagger, \tag{4.9}$$

and

$$\bar{H} = H_1 - h\frac{1}{H_g}h^\dagger + h\frac{1}{H_g}H_2'\frac{1}{H_g}h^\dagger - ih\frac{1}{H_g^2}\dot{h}^\dagger. \tag{4.10}$$

We thus have a Schrödinger-like equation for ψ_1. Due to normaliasation of Ψ and the orthogonality of ψ_1 and ψ_2, we have to the second order in $1/H_g$ that

$$\begin{aligned}1 &= \langle\psi_1|\psi_1\rangle + \langle\psi_2|\psi_2\rangle \\ &= \langle\psi_1|(1+\Lambda)|\psi_1\rangle.\end{aligned} \tag{4.11}$$

We now introduce an effective wave function for the conduction band

$$\psi_{\text{eff}} = (1+\frac{\Lambda}{2})\psi_1, \tag{4.12}$$

which as we can see from Eq. (4.11) is normalised.

Taking the time derivative and using Eq. (4.8) to second order in $1/H_g$

$$\begin{aligned}
\dot{\psi}_{\text{eff}} &= \left(1+\frac{\Lambda}{2}\right)\dot{\psi}_1 + \frac{\dot{\Lambda}}{2}\psi_1 \\
&= -\left(1+\frac{\Lambda}{2}\right) i(1-\Lambda)\bar{H}\psi_1 + \frac{\dot{\Lambda}}{2}\psi_1 \\
&= -i\left(1-\frac{\Lambda}{2}\right)\bar{H}\psi_1 + \frac{1}{2}\left(\dot{h}\frac{1}{H_g^2}h^\dagger + h\frac{1}{H_g^2}\dot{h}^\dagger\right)\psi_1 \\
&= -i\left(1-\frac{\Lambda}{2}\right)\bar{H}\left(1-\frac{\Lambda}{2}\right)\psi_{\text{eff}} + \frac{1}{2}\left(\dot{h}\frac{1}{H_g^2}h^\dagger + h\frac{1}{H_g^2}\dot{h}^\dagger\right)\left(1-\frac{\Lambda}{2}\right)\psi_{\text{eff}} \\
&= -i\left(\bar{H} - \frac{\Lambda}{2}\bar{H} - \bar{H}\frac{\Lambda}{2} + \frac{i}{2}\dot{h}\frac{1}{H_g^2}h^\dagger + \frac{i}{2}h\frac{1}{H_g^2}\dot{h}^\dagger\right)\psi_{\text{eff}}. \qquad (4.13)
\end{aligned}$$

This gives us the following effective Schrödinger equation

$$i\dot{\psi}_{\text{eff}} = H_{\text{eff}}\psi_{\text{eff}}, \qquad (4.14)$$

with

$$H_{\text{eff}} = H_0 + \delta H, \qquad (4.15)$$

where

$$H_0 = H_1 - h\frac{1}{H_g}h^\dagger, \qquad (4.16)$$

and

$$\delta H = -\frac{\Lambda H_0 + H_0\Lambda}{2} + h\frac{1}{H_g}H_2'\frac{1}{H_g}h^\dagger + \frac{i}{2}\left[\dot{h}\frac{1}{H_g^2}h^\dagger - h\frac{1}{H_g^2}\dot{h}^\dagger\right]. \qquad (4.17)$$

Now that we have found the desired effective equation for the conduction bands, we again look to the Luttinger-Kohn model. Introducing the functions

$$G_n(\mathbf{r}) = \int \mathrm{d}\mathbf{k} A_n(\mathbf{k}) e^{i\mathbf{k}\cdot\mathbf{r}}, \qquad (4.18)$$

Eqs. (4.1) and (4.2) takes the form

$$\psi_1 = \sum_{n\in c} G_n(\mathbf{r}) u_{n\mathbf{k}_0}, \qquad (4.19a)$$

$$\psi_2 = \sum_{n\in v} G_n(\mathbf{r}) u_{n\mathbf{k}_0}. \qquad (4.19b)$$

The Hamiltonian for the functions $G_n(\mathbf{r})$ are readily obtained by Fourier transforming Eq. (3.34).

$$H = \mathcal{E} + \frac{\hbar^2 k^2}{2m_0} + \hbar\mathbf{k}\cdot\boldsymbol{\pi}, \tag{4.20}$$

where $\mathbf{k} = -i\nabla$, $\mathcal{E}$ is a diagonal matrix with elements ϵ_n and $\boldsymbol{\pi}$ is a matrix with elements

$$\boldsymbol{\pi}_{nn'} = \langle n\mathbf{k}_0| - \frac{i\hbar}{m_0}\nabla + \frac{\hbar}{2m_0^2c^2}\mathbf{S}\times\nabla V|n'\mathbf{k}_0\rangle, \tag{4.21}$$

where $\mathbf{S} = \boldsymbol{\sigma}/2$ is the spin operator. By letting ϵ_n be the energy measured from the bottom of the conduction band we have that $H_g = \mathcal{E}$. We then have all the components necessary for finding the effective Hamiltonian.

4.2 Germanium with time dependent electric and magnetic field

For a better illustration we again turn to germanium. We now make the system time dependent by turning on a spatially uniform, time dependent E and B field. The Hamiltonian for the envelope functions is

$$H = \mathcal{E} + \frac{\hbar^2 k^2}{2m_0} + g_0\beta\mathbf{S}\cdot\mathbf{B} + \hbar\mathbf{k}\cdot\boldsymbol{\pi}, \tag{4.22}$$

where we get an extra term due to the coupling between the magnetic moment caused by spin and the surrounding magnetic field, with the free space g-factor for an electron $g_0 \approx 2$, and the Bohr magneton $\beta = e\hbar/(2m_0)$. Also the canonical wavevector is modified, and now includes an additional term due to the vector potential $\mathbf{A}(\mathbf{r}, t)$,

$$\mathbf{k} = -i\nabla + \frac{e\mathbf{A}}{\hbar}, \tag{4.23}$$

which means its components no longer commute,

$$[k_\alpha, k_\beta] = -\frac{ie}{\hbar}\epsilon_{\alpha\beta\gamma}B_\gamma. \tag{4.24}$$

The matrix elements of the velocity operator $\boldsymbol{\pi}$ at $\mathbf{k} = 0$ are

$$\boldsymbol{\pi}_{nn'} = \langle n0| - \frac{i\hbar}{m_0}\nabla + \frac{\hbar}{2m_0^2c^2}\mathbf{S}\times\nabla V|n'0\rangle, \tag{4.25}$$

but we disregard the spin-dependent part as this is a very good approximation for germanium [74], and write

$$m_0\boldsymbol{\pi}_{nn'} \to \mathbf{p}_{nn'} = \langle n0| - i\hbar\nabla|n'0\rangle. \tag{4.26}$$

Since we are doing an expansion in the inverse of the bandgap, neglecting contributions from other bands than the valence bands is a good approximation. Because

$$\langle v|\frac{1}{H_g^n}|v'\rangle = \begin{cases} \delta_{vv'}\frac{1}{(-\epsilon_g)^n}, & v \text{ is in the quadruplet,} \\ \delta_{vv'}\frac{1}{(-\epsilon_g-\Delta)^n}, & v \text{ is in the doublet,} \end{cases} \tag{4.27}$$

we get the following relation by inserting the identity, $\mathbb{I} = \sum_n |n\rangle\langle n|$, and comparing with Eq. (3.95),

$$\begin{aligned} \frac{1}{m_0^2}\langle c|p_\alpha\frac{1}{H_g^n}p_\beta|c'\rangle =& \frac{|P|^2}{3}\left[\delta_{\alpha\beta}\left\{\frac{2}{(-\epsilon_g)^n}+\frac{1}{(-\epsilon_g-\Delta)^n}\right\}\right. \\ &\left. +2i\epsilon_{\alpha\beta\gamma}\langle c|S_\gamma|c'\rangle\left\{\frac{1}{(-\epsilon_g-\Delta)^n}-\frac{1}{(-\epsilon_g)^n}\right\}\right], \end{aligned} \tag{4.28}$$

where as before $P \equiv \langle x|p_x/m_0|s\rangle$. Since the momentum operator has no elements coupling between the conduction bands or between the valence bands we recognise H_1 and H_2' to be

$$H_1 = H_2' = \frac{\hbar^2k^2}{2m_0} + g_0\beta\mathbf{S}\cdot\mathbf{B}, \tag{4.29}$$

and the coupling

$$h = \frac{\hbar\mathbf{k}\cdot\mathbf{p}}{m_0}. \tag{4.30}$$

Using Eq. (4.28), we may then with ease calculate H_0 defined by Eq. (4.16),

$$\begin{aligned} H_0 =& \frac{\hbar^2k^2}{2m_0} + g_0\beta\mathbf{S}\cdot\mathbf{B} - \frac{\hbar^2}{m_0^2}k_\alpha p_\alpha\frac{1}{H_g}p_\beta k_\beta \\ =& \frac{\hbar^2k^2}{2m_0} + g_0\beta\mathbf{S}\cdot\mathbf{B} - \hbar^2k_\alpha k_\beta\frac{|P|^2}{3}\left[\delta_{\alpha\beta}\left\{\frac{2}{(-\epsilon_g)}+\frac{1}{(-\epsilon_g-\Delta)}\right\}\right. \\ &\left. +2i\epsilon_{\alpha\beta\gamma}S_\gamma\left\{\frac{1}{(-\epsilon_g-\Delta)}-\frac{1}{(-\epsilon_g)}\right\}\right]. \end{aligned} \tag{4.31}$$

Because the Levi-Cevita tensor is anti-symmetric in all indices, $\epsilon_{\alpha\beta\gamma}k_\alpha k_\beta = \epsilon_{\alpha\beta\gamma}(k_\alpha k_\beta - k_\beta k_\alpha)/2$. Using this and the commutation relation Eq. (4.24), we get

$$\begin{aligned} H_0 =& \frac{\hbar^2 k^2}{2m_0} + g_0\beta \mathbf{S}\cdot\mathbf{B} + \hbar^2 k_\alpha k_\beta \delta_{\alpha\beta}\frac{|P|^2}{3}\left\{\frac{2}{\epsilon_g} + \frac{1}{\epsilon_g+\Delta}\right\} \\ &+ \frac{\hbar^2|P|^2}{3} 2i \frac{\epsilon_{\alpha\beta\gamma}(k_\alpha k_\beta - k_\beta k_\alpha)}{2} S_\gamma \left\{\frac{1}{(\epsilon_g+\Delta)} - \frac{1}{\epsilon_g}\right\}. \\ =& \frac{\hbar^2 k^2}{2}\left[\frac{1}{m_0} + \frac{2|P|^2}{3}\left\{\frac{3\epsilon_g+\Delta}{\epsilon_g(\epsilon_g+\Delta)}\right\}\right] \\ &+ \left[g_0\beta\mathbf{S}\cdot\mathbf{B} - \frac{|P|^2}{3} i\epsilon_{\alpha\beta\gamma}\frac{ie}{\hbar}\epsilon_{\alpha\beta\delta}B_\delta S_\gamma \left\{\frac{-\Delta}{\epsilon_g(\epsilon_g+\Delta)}\right\}\right], \end{aligned} \tag{4.32}$$

which, by using the relation $\epsilon_{\alpha\beta\gamma}\epsilon_{\alpha\beta\delta} = 2\delta_{\gamma\delta}$, results in H_0 given in the neat form

$$H_0 = \frac{\hbar^2 k^2}{2m^*} + g^*\beta\mathbf{S}\cdot\mathbf{B}, \tag{4.33}$$

with an effective mass and g-factor given by

$$\frac{1}{m^*} = \frac{1}{m_0} + \frac{2|P|^2}{3}\left\{\frac{3\epsilon_g+\Delta}{\epsilon_g(\epsilon_g+\Delta)}\right\}, \tag{4.34}$$

$$g^* = g_0 - \frac{4m_0|P|^2}{3}\left\{\frac{\Delta}{\epsilon_g(\epsilon_g+\Delta)}\right\}. \tag{4.35}$$

For germanium $|g^*| \gg g_0$ and $m^* \ll m_0$, so we may neglect g_0 and $1/m_0$. Using the same procedure, Eq. (4.9) may then be written as

$$\begin{aligned} \Lambda =& \frac{\hbar^2}{m_0^2} k_\alpha p_\alpha \frac{1}{H_g^2} p_\beta k_\beta \\ =& \hbar^2 k_\alpha k_\beta \frac{|P|^2}{3}\left[\delta_{\alpha\beta}\left\{\frac{2}{(-\epsilon_g)^2} + \frac{1}{(-\epsilon_g-\Delta)^2}\right\}\right. \\ &\left. + 2i\epsilon_{\alpha\beta\gamma}S_\gamma\left\{\frac{1}{(-\epsilon_g-\Delta)^2} - \frac{1}{(-\epsilon_g)^2}\right\}\right] \\ =& \frac{\hbar^2 k^2}{2m^* E_1} + \frac{g^*\beta}{E_2}\mathbf{S}\cdot\mathbf{B}, \end{aligned} \tag{4.36}$$

with as in Section 3.5

$$E_1 = \frac{\epsilon_g(\epsilon_g+\Delta)(3\epsilon_g+2\Delta)}{3\epsilon_g^2+4\epsilon_g\Delta+2\Delta^2}, \tag{4.37a}$$

$$E_2 = \frac{\epsilon_g(\epsilon_g+\Delta)}{2\epsilon_g+\Delta}. \tag{4.37b}$$

We note that Eq. (4.17) contains the time derivative of h. This gives rise to terms that are dependent on the electric field, $\mathbf{E} = -\partial\mathbf{A}/\partial t$:

$$\dot{h} = \frac{\hbar}{m_0}\frac{\partial \mathbf{k}\cdot\mathbf{p}}{\partial t} = \frac{e}{m_0}\frac{\partial \mathbf{A}}{\partial t}\cdot\mathbf{p} = -\frac{e\mathbf{E}\cdot\mathbf{p}}{m_0}. \tag{4.38}$$

We disregard terms of order k^4 since it is irrelevant for the spin-related effects that are the subject of our investigation. The constant term $(\mathbf{B}\cdot\mathbf{S})^2 = B^2/4$ is also ignored. Since we here only consider spatially uniform E and B fields, k^2 will commute with both $\mathbf{B}$ and $\mathbf{E}$. Eq. (4.17) then becomes

$$\begin{aligned}\delta H =& -\frac{\Lambda H_0 + H_0\Lambda}{2} + \frac{\hbar^2}{m_0^2}k_\alpha p_\alpha \frac{1}{H_g}H_2'\frac{1}{H_g}p_\beta k_\beta \\ &- \frac{ie\hbar}{2m_0^2}\left[E_\alpha p_\alpha \frac{1}{H_g^2}p_\beta \hbar k_\beta - \hbar k_\alpha p_\alpha \frac{1}{H_g^2}p_\beta E_\beta\right] \\ =& -\Lambda H_0 + \Lambda H_2' - \frac{i\hbar^2 e}{2m_0^2}p_\alpha\frac{1}{H_g^2}p_\beta[E_\alpha k_\beta - k_\alpha E_\beta].\end{aligned} \tag{4.39}$$

The second term in Eq. (4.39) will be negligible compared to the first in the limit $m^* \ll m_0$ and $|g^*| \gg g_0$.

$$\begin{aligned}\delta H =& -\left[\frac{\hbar^2k^2}{2m^*E_1} + \frac{g^*\beta}{E_2}\mathbf{S}\cdot\mathbf{B}\right]\left[\frac{\hbar^2k^2}{2m^*} + g^*\beta\mathbf{S}\cdot\mathbf{B}\right] \\ &- \frac{ie\hbar^2|P|^2}{6}\left[\delta_{\alpha\beta}\frac{(3\epsilon_g+2\Delta)}{\epsilon_g(\epsilon_g+\Delta)E_1} - 2i\epsilon_{\alpha\beta\gamma}S_\gamma\frac{\Delta}{\epsilon_g(\epsilon_g+\Delta)E_2}\right][E_\alpha k_\beta - k_\alpha E_\beta] \\ =& -\frac{\hbar^2k^2}{2m^*}\frac{g^*\beta}{E_0}\mathbf{S}\cdot\mathbf{B} - \frac{g^*\beta\hbar}{E_2}(\mathbf{k}\times\mathbf{E})\cdot\mathbf{S},\end{aligned} \tag{4.40}$$

where $1/E_0 = 1/E_1 + 1/E_2$.

As in Section 3 we now introduce the impurity potential $U(\mathbf{r})$, which is assumed to be spin independent and slowly varying in space. To keep track of the origin

of the terms, we distinguish between the potential in H_1 and H_2, even though they are the same,

$$U_1 = U_2 = U(\mathbf{r}). \tag{4.41}$$

The contribution from this impurity to the effective Hamiltonian will according to Eq. (4.15) reduce to

$$\begin{aligned} U_{\text{eff}} =& U_1 - \frac{\Lambda U_1 + U_1 \Lambda}{2} + \frac{\hbar^2}{m_0^2} k_\alpha p_\alpha \frac{1}{H_g} U_2 \frac{1}{H_g} p_\beta k_\beta \\ =& U_1 + \frac{i\hbar^2 (\nabla U_1) \cdot \mathbf{k}}{2m^* E_1} + \frac{\hbar^2 (\nabla^2 U_1)}{4m^* E_1} - U_1 \frac{\hbar^2 k^2}{2m^* E_1} - U_1 \frac{g^* \beta}{E_2} \mathbf{S} \cdot \mathbf{B} \\ &+ k_\alpha U_2 k_\beta \frac{\hbar^2 |P|^2}{3} \left[\delta_{\alpha\beta} \frac{(3\epsilon_g + 2\Delta)}{\epsilon_g (\epsilon_g + \Delta) E_1} - 2i \epsilon_{\alpha\beta\gamma} S_\gamma \frac{\Delta}{\epsilon_g (\epsilon_g + \Delta) E_2} \right]. \end{aligned} \tag{4.42}$$

With $U_1 = U_2$, this reduces to

$$\begin{aligned} U_{\text{eff}} =& U_1 \left(1 - \frac{g^* \beta}{E_2} \mathbf{S} \cdot \mathbf{B} \right) + \frac{\hbar^2 (\nabla^2 U_1)}{4m^* E_1} + \frac{i g^* \beta \hbar}{e E_2} \epsilon_{\alpha\beta\gamma} S_\gamma k_\alpha U_2 k_\beta \\ =& U_1 \left(1 - \frac{g^* \beta}{E_2} \mathbf{S} \cdot \mathbf{B} \right) + \frac{\hbar^2 (\nabla^2 U_1)}{4m^* E_1} - \frac{i g^* \beta}{e E_2} U_2 \epsilon_{\alpha\beta\gamma} S_\gamma \frac{ie}{2} \epsilon_{\alpha\beta\delta} B_\delta \\ &+ \frac{g^* \beta \hbar}{e E_2} \epsilon_{\alpha\beta\gamma} S_\gamma (\nabla U_2)_\alpha k_\beta, \end{aligned} \tag{4.43}$$

where we have commuted k_α with U_2 and again used the relation $\epsilon_{\alpha\beta\gamma} k_\alpha k_\beta = \epsilon_{\alpha\beta\gamma}(k_\alpha k_\beta - k_\beta k_\alpha)/2$ together with the commutation relation from Eq. (4.24). We then get

$$U_{\text{eff}} = U_1 + \frac{\hbar^2 (\nabla^2 U_1)}{4m^* E_1} + \frac{g^* \beta}{E_2} \mathbf{S} \cdot \mathbf{B} \, (U_2 - U_1) + \frac{g^* \beta \hbar}{e E_2} (\nabla U_2) \cdot (\mathbf{k} \times \mathbf{S}). \tag{4.44}$$

Discarding the non-spin-dependent correction and again with $U_1 = U_2$ this reduces to

$$U_{\text{eff}} = U_1 + \frac{g^* \beta \hbar}{e E_2} (\nabla U_2) \cdot (\mathbf{k} \times \mathbf{S}). \tag{4.45}$$

The total effective Hamiltonian becomes

$$H_{\text{eff}} = H_0 - \frac{\hbar^2 k^2}{2m^*} \frac{g^* \beta}{E_0} \mathbf{S} \cdot \mathbf{B} + \frac{g^* \beta \hbar}{E_2} (\mathbf{k} \times \mathbf{S}) \cdot \mathbf{E} + U_1 + \frac{g^* \beta \hbar}{e E_2} (\mathbf{k} \times \mathbf{S}) \cdot \nabla U_2. \tag{4.46}$$

This is the same result as in Section 3.5, but with additional terms due to the electric and magnetic field.

By introducing a scalar electrostatic potential, $\phi = -\mathbf{E}\cdot\mathbf{r}$ and an effective position operator

$$\mathbf{r}_{\text{eff}} = \mathbf{r} + \boldsymbol{\rho}, \tag{4.47}$$

with

$$\boldsymbol{\rho} = \frac{g^*\beta\hbar}{eE_2}\mathbf{k}\times\mathbf{S}, \tag{4.48}$$

we can see that the effective Hamiltonian, Eq. (4.46), reduces to

$$H_{\text{eff}} = H_0 - \frac{\hbar^2k^2}{2m^*}\frac{g^*\beta}{E_0}\mathbf{S}\cdot\mathbf{B} + e\mathbf{E}\cdot\mathbf{r}_{\text{eff}} + U(\mathbf{r}_{\text{eff}}). \tag{4.49}$$

Here $U(\mathbf{r}_{\text{eff}})$ is to be expanded to the first order in $\boldsymbol{\rho}$. The correction to the position operator due to the spin-orbit coupling may then be considered as an electric dipole moment, $\boldsymbol{\mu} = -e\boldsymbol{\rho}$, as can clearly be seen from Eq. (4.46).

Part II

5 Bandstructure of graphene

Graphene is a one-atom-thick two-dimensional layer of carbon atoms arranged in a honeycomb structure. Carbon atoms have four valence electrons. In graphene, three of these, namely the $2s$, $2p_x$, and $2p_y$ orbitals, are used to make chemical bonds to the three nearest neighbours through a sp^2 hybridisation. These are called the σ bands and are responsible for the strong chemical bonds in graphene and the exceptional mechanical properties. The remaining $2p_z$ orbital form the π bands which govern the electronic properties of graphene. We will first concentrate on the π bands and later investigate what effects the σ bands as well as the d orbitals have on the π bands.

5.1 π bands

The honeycomb structure of graphene is equivalent to a system of two interlocking triangular sublattices, which we will label as A and B, respectively. We use the primitive lattice vectors

$$\mathbf{a}_1 = \frac{a}{2}(1, \sqrt{3})\,, \tag{5.1a}$$

$$\mathbf{a}_2 = \frac{a}{2}(-1, \sqrt{3}), \tag{5.1b}$$

where $a = |\mathbf{a}_1| = |\mathbf{a}_2| = 2.46$ Å is the lattice constant of the triangular sublattices, i.e. the next-nearest neighbour distance of graphene.

We find the reciprocal lattice vectors, $\mathbf{G}_i$, by using the well-known relation $\mathbf{a}_i \cdot \mathbf{G}_j = 2\pi\delta_{ij}$,

$$\mathbf{G}_1 = \frac{2\pi}{\sqrt{3}a}(\sqrt{3}, 1)\,, \tag{5.2a}$$

$$\mathbf{G}_2 = \frac{2\pi}{\sqrt{3}a}(-\sqrt{3}, 1). \tag{5.2b}$$

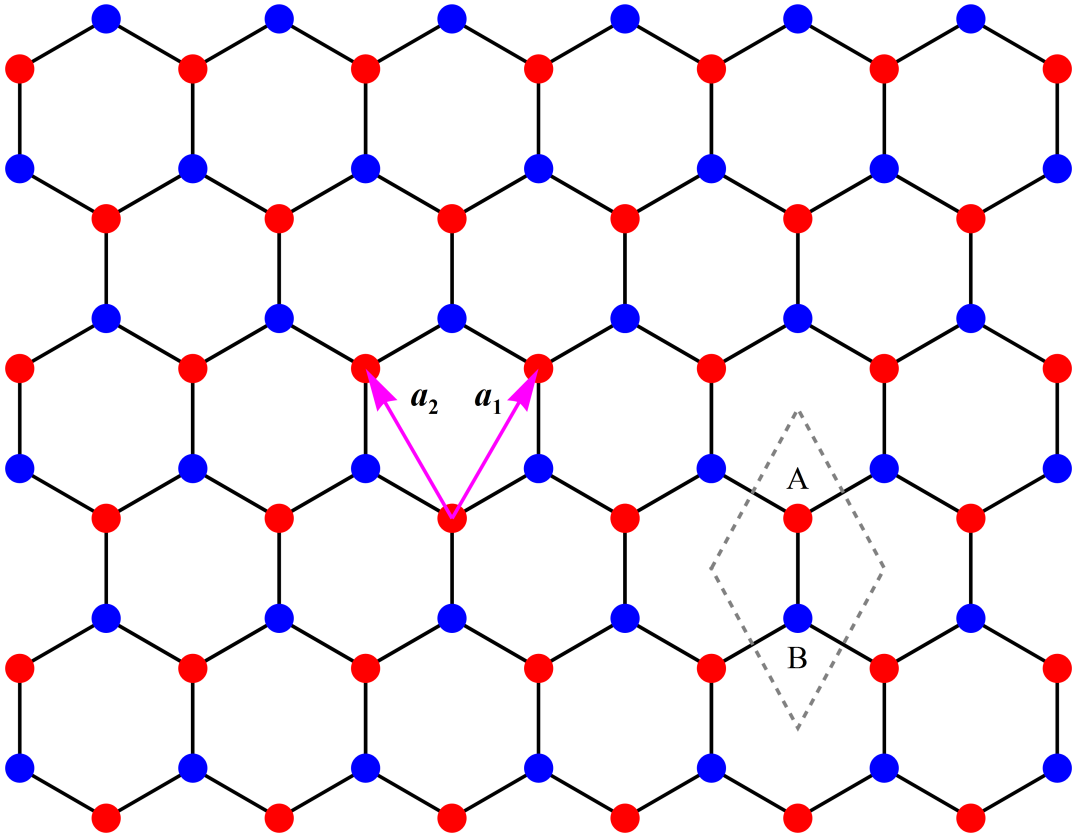

Figure 3. The graphene lattice has a honeycomb structure. The A sites (red) and the B sites (blue) each form a Bravais lattice with the primitive lattice vectors $\mathbf{a_1}$ and $\mathbf{a_2}$. The grey parallelogram is a unit cell with a basis of two carbon atoms.

The nearest neighbour vectors for the A sites in the honeycomb lattice depicted in Figure 4 are

$$\boldsymbol{\delta}_1 = \frac{a}{\sqrt{3}}(0, -1)\,, \tag{5.3a}$$

$$\boldsymbol{\delta}_2 = \frac{a}{\sqrt{3}}(\frac{\sqrt{3}}{2}, \frac{1}{2})\,, \tag{5.3b}$$

$$\boldsymbol{\delta}_3 = \frac{a}{\sqrt{3}}(-\frac{\sqrt{3}}{2}, \frac{1}{2}). \tag{5.3c}$$

The second quantised form of the tight-binding Hamiltonian in the nearest neigh-

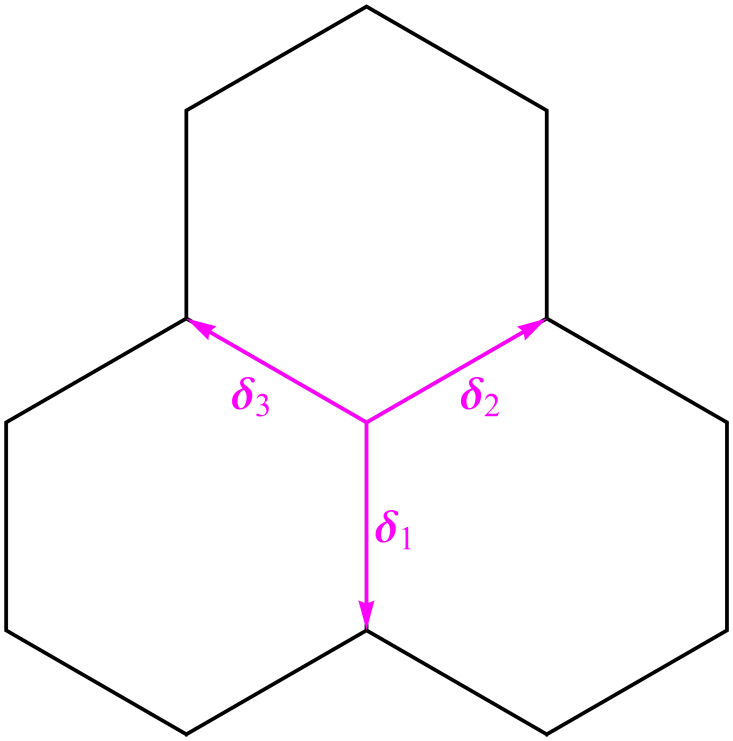

Figure 4. The nearest neighbour vectors in graphene for an A atom, corresponding to Eq. (5.3).

bour approximation for the π bands is

$$H_\pi = -t \sum_{\langle ij \rangle} \left[a_i^\dagger b_j + b_j^\dagger a_i \right], \tag{5.4}$$

where $a_i^\dagger$ (a_i) creates (anihilates) an electron at site i of sublattice A, $b_j^\dagger$ (b_j) creates (anhiliates) an electron at site j of sublattice B and $t = 3.033$ eV is the hopping integral. We use the Fourier transformation

$$a_{\mathbf{k}}^\dagger = \frac{1}{\sqrt{N}} \sum_i e^{i\mathbf{k}\cdot\mathbf{R}_i} a_i^\dagger, \tag{5.5a}$$

$$a_i^\dagger = \frac{1}{\sqrt{N}} \sum_{\mathbf{k}}^{B.Z.} e^{-i\mathbf{k}\cdot\mathbf{R}_i} a_{\mathbf{k}}^\dagger, \tag{5.5b}$$

and similarly for the operators b_j, where $\mathbf{R}_i$ is the position of the ith lattice site and N the number of lattice sites of the sublattices. Since we are consid-

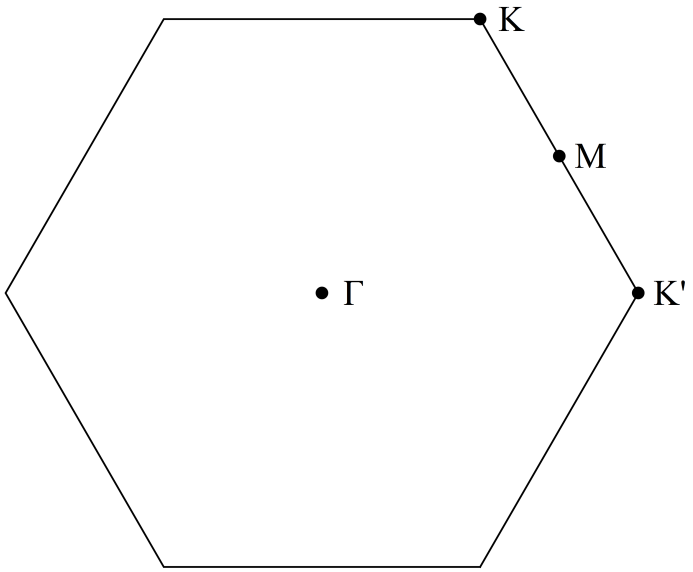

Figure 5. The first Brillouin zone is a hexagon. The points of high symmetry have been marked. In the center of the hexagon (Γ) we have $\mathbf{k} = 0$. The top right corner is the K point, and the left corner is the K' point. In between K and K' we have M.

ering an infinitely large graphene sheet, any expression containing N should be understood in the limit $N \to \infty$. We may express Eq. (5.4) as

$$H_\pi = -\frac{t}{N}\sum_{\langle ij\rangle}\sum_{\mathbf{k},\mathbf{k}'} e^{-i\mathbf{k}\cdot\mathbf{R}_i} a^\dagger_{\mathbf{k}} e^{i\mathbf{k}'\cdot\mathbf{R}_j} b_{\mathbf{k}'} + H.c. \tag{5.6}$$

We now choose there to be no phase difference for hopping to nearest neighbour 1, e.g. for hopping from an A site to the nearest neighbour $\boldsymbol{\delta}_1$ from Eq. (5.3a). This is just a simple unitary transformation and does not change the physics. By introducing $\mathbf{R}_j = \mathbf{R}_i + \boldsymbol{\delta}_j - \boldsymbol{\delta}_1$ and summing over nearest neighbours, j, this

is

$$H_\pi = -\frac{t}{N}\sum_{\langle ij\rangle}\sum_{\mathbf{k},\mathbf{k}'} e^{i\mathbf{R}_i\cdot(\mathbf{k}'-\mathbf{k})}e^{i\mathbf{k}'\cdot(\boldsymbol{\delta}_j-\boldsymbol{\delta}_1)}a^\dagger_{\mathbf{k}}b_{\mathbf{k}'} + H.c. \tag{5.7}$$

$$= -\frac{t}{N}\sum_{i}\sum_{\mathbf{k},\mathbf{k}'} e^{i\mathbf{R}_i\cdot(\mathbf{k}'-\mathbf{k})}(1+e^{i\mathbf{k}'\cdot\mathbf{a}_1}+e^{i\mathbf{k}'\cdot\mathbf{a}_2})a^\dagger_{\mathbf{k}}b_{\mathbf{k}'} + H.c. \tag{5.8}$$

$$\tag{5.9}$$

Using that $\frac{1}{N}\sum_i e^{i\mathbf{R}_i\cdot(\mathbf{k}'-\mathbf{k})} = \delta_{\mathbf{k}\mathbf{k}'}$, we get

$$\begin{aligned} H_\pi &= -t\sum_{\mathbf{k},\mathbf{k}'}\delta_{\mathbf{k}\mathbf{k}'}(1+e^{i\mathbf{k}\cdot\mathbf{a}_1}+e^{i\mathbf{k}\cdot\mathbf{a}_2})a^\dagger_{\mathbf{k}}b_{\mathbf{k}} + H.c. \\ &= -t\sum_{\mathbf{k}}(1+e^{i\mathbf{k}\cdot\mathbf{a}_1}+e^{i\mathbf{k}\cdot\mathbf{a}_2})a^\dagger_{\mathbf{k}}b_{\mathbf{k}} + H.c., \end{aligned} \tag{5.10}$$

or in a matrix form

$$H_\pi = \sum_{\mathbf{k}}\begin{pmatrix} a^\dagger_{\mathbf{k}} & b^\dagger_{\mathbf{k}}\end{pmatrix}\begin{pmatrix} 0 & -tf(\mathbf{k}) \\ -tf^*(\mathbf{k}) & 0\end{pmatrix}\begin{pmatrix} a_{\mathbf{k}} \\ b_{\mathbf{k}}\end{pmatrix}, \tag{5.11}$$

where $f(\mathbf{k}) = 1+e^{i\mathbf{k}\cdot\mathbf{a}_1}+e^{i\mathbf{k}\cdot\mathbf{a}_2} = 1+2e^{i\frac{\sqrt{3}}{2}k_y a}\cos\frac{k_x a}{2}$. Diagonalising, we obtain the eigenenergies

$$\begin{aligned} \epsilon^\pm_{\mathbf{k}} &= \pm t|f(\mathbf{k})| \\ &= \pm t\sqrt{3+2\cos(k_x a)+4\cos\left(\frac{\sqrt{3}}{2}k_y a\right)\cos\left(\frac{1}{2}k_x a\right)}. \end{aligned} \tag{5.12}$$

This has been plotted in Figure 6. The corresponding eigenfunctions are

$$u^\pm = \frac{1}{\sqrt{2}}\begin{pmatrix} 1 \\ \mp\frac{f^*(\mathbf{k})}{|f(\mathbf{k})|}\end{pmatrix}, \tag{5.13}$$

given in a basis of $(|p_z A\rangle, |p_z B\rangle)$.

The two energy bands touch at the so-called Dirac points,

$$\mathbf{K} = (\frac{2\pi}{3a}, \frac{2\pi}{\sqrt{3}a}), \qquad \mathbf{K}' = (\frac{4\pi}{3a}, 0), \tag{5.14}$$

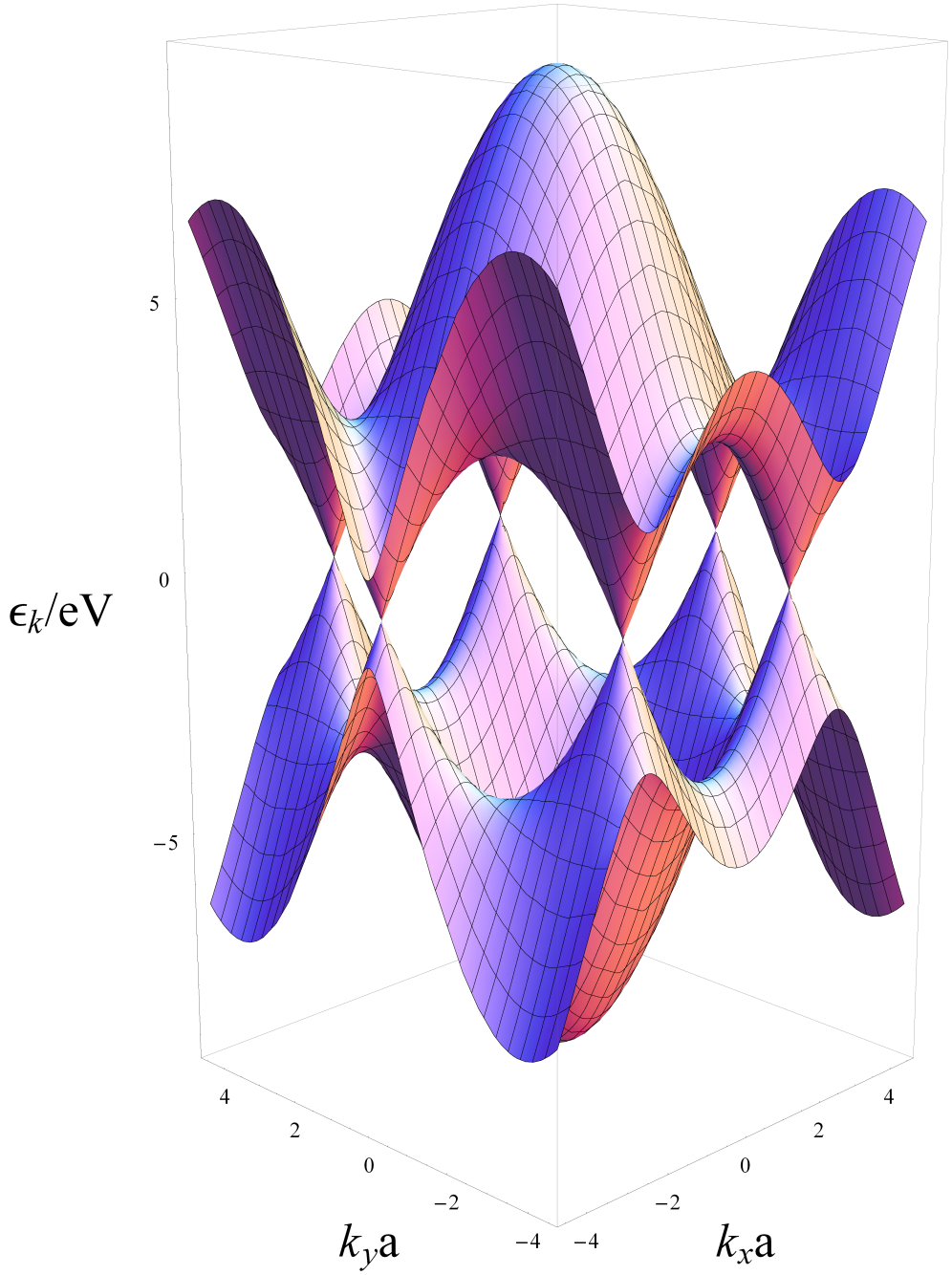

Figure 6. Bandstructure of the π bands in the first Brillouin zone as a function of the momentum $\mathbf{k}$. At the K and K' points where the bands touch they form Dirac cones.

and are characterised by a linear (conical) dispersion relation close to these points. There are actually six points like these in the first Brillouin zone, but only two of them are unique; the remaining are connected to K and K' by the reciprocal lattice vectors $\mathbf{b}_1$ and $\mathbf{b}_2$.

Expanding around the K point, we get for small momenta $\mathbf{q} = \mathbf{k} - \mathbf{K}$

$$\begin{aligned} f(\mathbf{q}) &= 1 - 2e^{i\frac{\sqrt{3}}{2}q_y a}\cos(\frac{\pi}{3} + \frac{q_x a}{2}) \\ &= 1 - 2(1 + i\frac{\sqrt{3}}{2}q_y a + \mathcal{O}(q_y^2))(\frac{1}{2} - \frac{\sqrt{3}}{4}q_x a + \mathcal{O}(q_x^2)) \\ &= \frac{\sqrt{3}a}{2}(q_x - iq_y) + \mathcal{O}(\mathbf{q}^2). \end{aligned} \tag{5.15}$$

In the limit $|a\mathbf{q}| \ll 1$, Eq. (5.11) can then be approximated to linear order in $\mathbf{q}$,

$$\begin{aligned} H_\pi(\mathbf{K}) &= -\frac{\sqrt{3}}{2}ta \sum_{|\mathbf{q}|\ll 1/a} \begin{pmatrix} a^\dagger_{\mathbf{K}+\mathbf{q}} & b^\dagger_{\mathbf{K}+\mathbf{q}} \end{pmatrix} \begin{pmatrix} 0 & q_x - iq_y \\ q_x + iq_y & 0 \end{pmatrix} \begin{pmatrix} a_{\mathbf{K}+\mathbf{q}} \\ b_{\mathbf{K}+\mathbf{q}} \end{pmatrix} \\ &= -\frac{\sqrt{3}}{2}ta \sum_{|\mathbf{q}|\ll 1/a} \Psi^\dagger \boldsymbol{\sigma}\cdot\mathbf{q}\Psi, \end{aligned} \tag{5.16}$$

where $\boldsymbol{\sigma} = (\sigma_x, \sigma_y)$ are Pauli matrices acting on the sublattice A/B pseudospin space and

$$\Psi = \begin{pmatrix} a_{\mathbf{K}+\mathbf{q}} \\ b_{\mathbf{K}+\mathbf{q}} \end{pmatrix}. \tag{5.17}$$

Eq. (5.16) describes a coupling of momentum to the pseudospin degree of freedom. Similarly for small momentum about $\mathbf{k} = \mathbf{K}'$,

$$H_\pi(\mathbf{K}') = \frac{\sqrt{3}}{2}ta \sum_{|\mathbf{q}|\ll 1/a} \Psi^\dagger \boldsymbol{\sigma}^*\cdot\mathbf{q}\Psi. \tag{5.18}$$

We then get the linear dispersion in the vicinity of the Dirac points,

$$\epsilon(\mathbf{q}) = \pm\hbar v_F|\mathbf{q}|\,, \tag{5.19}$$

where we have introduced a Fermi velocity $v_F = \frac{\sqrt{3}}{2}ta/\hbar \approx 10^6\,\mathrm{m/s}$. Thus, the low energy excitations behave as massless fermions described by the Dirac equation.

Table 1. Slater-Koster hopping integrals, $t^{\mu,\nu}$, where $l = x/r = \cos\phi$, $m = y/r = \sin\phi$ and $n = z/r = \cos\theta$. $n = \cos\theta = 0$ since we are only considering flat graphene. [75][76]

$t^{s,s}$	$V_{ss\sigma}$
$t^{s,x}$	$lV_{sp\sigma}$
$t^{x,x}$	$l^2V_{pp\sigma} + (1-l^2)V_{pp\pi}$
$t^{x,y}$	$lmV_{pp\sigma} - lmV_{pp\pi}$
$t^{x,z}$	$lnV_{pp\sigma} - lnV_{pp\pi}$

Table 2. Hopping parameters taken from [77][78].

Parameter	Energy (eV)
ϵ_s	-8.868
ϵ_p	0
$V_{ss\sigma}$	-6.769
$V_{sp\sigma}$	+5.580
$V_{pp\sigma}$	+5.037
$V_{pp\pi}$	-3.033

5.2 σ bands

Up until this point, we have just considered the p_z orbitals that generate the π bands. We will now consider the effect of the s, p_x and p_y orbitals that form the σ bands. We use the same procedure as for the π bands, but we now have to distinguish between the on-site atomic energies of the s orbitals, ϵ_s, and the p orbitals, ϵ_p. Also the hopping integrals depend on the relative angles, see Table 1 and Figure 7.

As can be seen from Table 1, because we are only considering flat graphene, there is no hopping between p_z and s, p_x, or p_y orbitals. The π bands and the

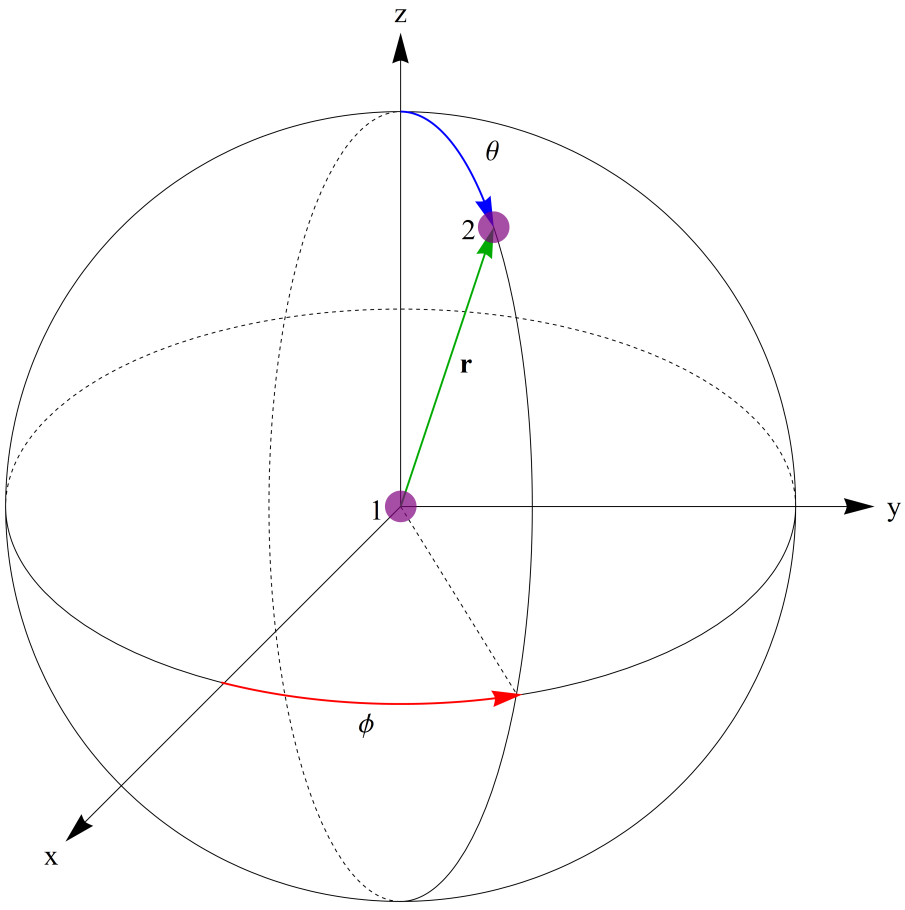

Figure 7. The relative angles which enters into the calculation of the hopping matrix elements for hopping from orbital 1 to orbital 2.

σ bands can then be treated separately,

$$H = H_\pi + H_\sigma. \tag{5.20}$$

The Hamiltonian for the σ bands can be split into an on-site atomic part and a hopping part,

$$H_\sigma = H_{\sigma a} + H_{\sigma h}\,, \tag{5.21}$$

where, using the same convention as before by labelling the states for the A and

B lattices independently,

$$H_{\sigma a} = \sum_{i} \sum_{\mu;\chi=\uparrow,\downarrow} \epsilon_{\mu} \left(a^{\dagger}_{i\mu\chi} a_{i\mu\chi} + b^{\dagger}_{i\mu\chi} b_{i\mu\chi} \right) , \tag{5.22a}$$

$$H_{\sigma h} = \sum_{\langle ij \rangle} \sum_{\mu;\nu;\chi=\uparrow,\downarrow} t^{\mu\nu}_{ij} a^{\dagger}_{i\mu\chi} b_{j\nu\chi} + H.c. , \tag{5.22b}$$

where $\mu, \nu \in (s, p_x, p_y)$ and χ denotes spin. Our Hamiltonian, H, is an 8×8 matrix. $a^{\dagger}_{i\mu\chi}(a_{i\mu\chi})$ denotes the creation (annihilation) operator for a μ orbital with spin χ on the ith atom of sublattice A. $t^{\mu\nu}_{ij}$ is the hopping integral for an electron going from the state ν on site j to the state μ on site i. Eq. (5.22b) has been calculated in Mathematica using the two-center Slater-Koster approximation [76][79], with the general hopping integrals given in Tables 1 and 2. The bandstructure of the π and σ bands has been plotted in Figure 8.

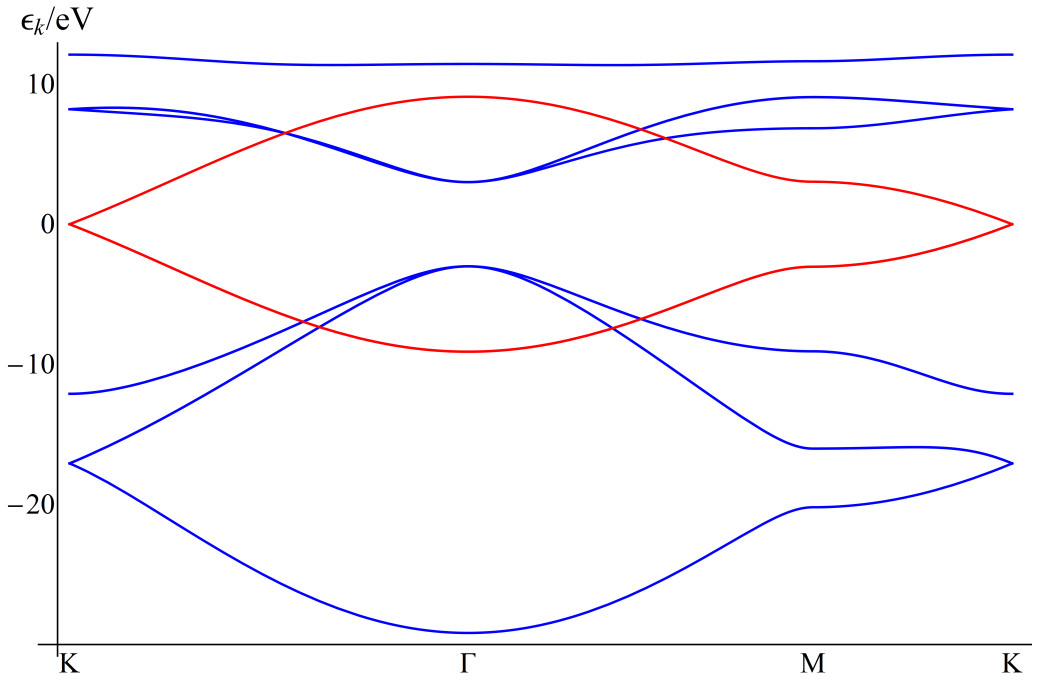

Figure 8. Energy of the σ bands (blue) and the π bands (red) in the nearest neighbour approximation as a function of momentum $\mathbf{k}$ between the high symmetry points K, Γ, M and back to K. See Figure 5.

Evaluated at the K-point, the Hamiltonian for the σ-bands is

$$H_{\sigma K} = \begin{pmatrix} \epsilon_s & 0 & 0 & 0 & \pm i\alpha & \alpha \\ 0 & \epsilon_p & 0 & \mp i\alpha & -\beta & \mp i\beta \\ 0 & 0 & \epsilon_p & -\alpha & \mp i\beta & \beta \\ 0 & \pm i\alpha & -\alpha & \epsilon_s & 0 & 0 \\ \mp i\alpha & -\beta & \pm i\beta & 0 & \epsilon_p & 0 \\ \alpha & \pm i\beta & \beta & 0 & 0 & \epsilon_p \end{pmatrix}, \tag{5.23}$$

where $\alpha = 3/2V_{sp\sigma}$ and $\beta = 3/4(V_{pp\sigma} - V_{pp\pi})$.

As mentioned there is no coupling between the π and σ bands when neglecting the spin-orbit interaction. Thus, the s, p_x and p_y orbitals do not directly contribute to the low-energy electronic properties of graphene. Furthermore, this also means that any effective contribution from the spin-orbit coupling from the σ bands on the π bands will consequently have to be be quadratic in the spin-orbit coupling constant.

5.3 π bands with d orbitals

Since the p_z orbitals do not hybridise with s orbitals or the other p orbitals, one may be inclined to stop here and be satisfied with the result obtained above for the π band. However, it was shown by Slonczewski *et al.* [11] using group theoretical arguments that the p_z orbitals hybridise with orbitals of a higher principal quantum number than 2, most importantly $3d$ orbitals. We will therefore extend our model to include the effect of these orbitals.

We will now consider the π bands to be formed by p_z, as well a small contribution from d_{xz} and d_{yz} to be determined [77].

The Hamiltonian at $\mathbf{k} = \mathbf{K}$ for the π bands with d orbitals has an on-site part and an inter-atomic hopping part,

$$H_\pi = H_{\pi a} + H_{\pi h}\,, \tag{5.24}$$

Table 3. Slater-Koster hopping integrals $t^{\mu,\nu}$ where $l = x/r = \cos\phi$, $m = y/r = \sin\phi$, as before. The terms containing n have been dropped since $n = z/r = \cos\theta = 0$ for flat graphene. [77][76]

$t^{z,z}$	$V_{pp\pi}$
$t^{z,xz}$	$lV_{pd\pi}$
$t^{z,yz}$	$mV_{pd\pi}$
$t^{xz,xz}$	$l^2V_{dd\pi} + m^2V_{dd\delta}$
$t^{xz,xz}$	$m^2V_{dd\pi} + l^2V_{dd\delta}$
$t^{xz,yz}$	$lmV_{dd\pi} - lmV_{dd\delta}$

with

$$H_{\pi a} = \sum_i \sum_{\mu;\chi=\uparrow,\downarrow} \epsilon_\mu \left(a^\dagger_{i\mu\chi} a_{i\mu\chi} + b^\dagger_{i\mu\chi} b_{i\mu\chi} \right) , \tag{5.25a}$$

$$H_{\pi h} = \sum_{\langle ij \rangle} \sum_{\mu,\nu;\chi=\uparrow,\downarrow} t^{\mu\nu}_{ij} a^\dagger_{i\mu\chi} b_{j\nu\chi} + H.c. , \tag{5.25b}$$

where $\mu, \nu \in (p_z, d_{xz}, d_{yz})$. By using the hopping integrals in Table 3, we get the following Hamiltonian for the p_z orbitals and the relevant d orbitals, evaluated at the Dirac points and given in a basis of ($p_{z,A}$, $d_{xz,A}$, $d_{yz,A}$, $p_{z,B}$, $d_{xz,B}$, $d_{yz,B}$):

$$H_{\pi K} = \begin{pmatrix} \epsilon_p & 0 & 0 & 0 & i\tau\gamma & \gamma \\ 0 & \epsilon_d & 0 & -i\tau\gamma & \delta & i\tau\delta \\ 0 & 0 & \epsilon_d & -\gamma & i\tau\delta & -\delta \\ 0 & i\tau\gamma & -\gamma & \epsilon_p & 0 & 0 \\ -i\tau\gamma & \delta & -i\tau\delta & 0 & \epsilon_d & 0 \\ \gamma & -i\tau\delta & -\delta & 0 & 0 & \epsilon_d \end{pmatrix} , \tag{5.26}$$

where $\gamma = \frac{3}{2}V_{pd\pi}$, $\delta = \frac{3}{4}(V_{dd\delta} - V_{dd\pi})$, and $\tau = 1$ for K and -1 for K'. The two lowest eigenvalues of this matrix correspond to two degenerate states which

form the π bands,

$$|1\rangle \approx \frac{1}{\sqrt{N}}\left[|p_{z,A}\rangle + \frac{\gamma}{\epsilon_d - \epsilon_p}\left(i\tau|d_{xz,B}\rangle - |d_{yz,B}\rangle\right)\right], \tag{5.27a}$$

$$|2\rangle \approx \frac{1}{\sqrt{N}}\left[|p_{z,B}\rangle + \frac{\gamma}{\epsilon_d - \epsilon_p}\left(i\tau|d_{xz,A}\rangle + |d_{yz,A}\rangle\right)\right], \tag{5.27b}$$

where we have used that $\gamma \ll (\epsilon_d - \epsilon_p)$. The corresponding eigenvalues are

$$\epsilon_{1,2} \approx \epsilon_p - \frac{2\gamma^2}{\epsilon_d - \epsilon_p}. \tag{5.28}$$

Including hybridisation of p_z and the d orbitals gives a small overall shift of the eigenenergies of the π bands at the Dirac points. We see that the correction to the energies with respect to ϵ_p is quadratic in the p_z-d hopping γ.

The remaining d orbitals, d_{z^2}, d_{xy} and $d_{x^2-y^2}$, hybridise with s, p_x and p_y, but not with p_z in flat graphene. The effect of these three d orbitals will be neglected hereafter. The Slater-Koster tight-binding parameters for s, p_x, p_y, d_{z^2}, d_{xy} and $d_{x^2-y^2}$ are given in Table 4 for reference.

Table 4. Slater-Koster hopping integrals, $t^{\mu,\nu}$ for the σ band with d orbitals where $l = x/r = \cos\phi$, $m = y/r = \sin\phi$, as before. The terms containing n have been dropped since $n = z/r = \cos\theta = 0$ for flat graphene. [76]

t^{s,z^2}	$-\frac{1}{2}(l^2+m^2)V_{sd\sigma}$
$t^{s,xy}$	$\sqrt{3}lmV_{sd\sigma}$
t^{s,x^2-y^2}	$-\frac{1}{2}\sqrt{3}(l^2-m^2)V_{sd\sigma}$
t^{x,z^2}	$-\frac{1}{2}l(l^2+m^2)V_{pd\sigma}$
$t^{x,xy}$	$\sqrt{3}l^2mV_{pd\sigma}+m(1-2l^2)V_{pd\pi}$
t^{x,x^2-y^2}	$\frac{1}{2}\sqrt{3}l(l^2-m^2)V_{pd\sigma}+l(1-l^2+m^2)V_{pd\pi}$
t^{y,z^2}	$-\frac{1}{2}m(l^2+m^2)V_{pd\sigma}$
$t^{y,xy}$	$\sqrt{3}lm^2V_{pd\sigma}+l(1-2m^2)V_{pd\pi}$
t^{y,x^2-y^2}	$\frac{1}{2}\sqrt{3}l(l^2-m^2)V_{pd\sigma}-m(1+l^2-m^2)V_{pd\pi}$
t^{z^2,z^2}	$[-\frac{1}{2}(l^2+m^2)]^2V_{dd\sigma}+\frac{3}{4}(l^2+m^2)^2V_{dd\delta}$
$t^{z^2,xy}$	$-\frac{1}{2}\sqrt{3}lm(l^2+m^2)V_{dd\sigma}-\frac{1}{2}\sqrt{3}lmV_{dd\delta}$
t^{z^2,x^2-y^2}	$-\frac{1}{4}\sqrt{3}(l^2-m^2)(l^2+m^2)V_{dd\sigma}+\frac{1}{4}\sqrt{3}(l^2-m^2)V_{dd\delta}$
$t^{xy,xy}$	$3l^2m^2V_{dd\sigma}+(l^2+m^2-4l^2m^2)V_{dd\pi}+l^2m^2V_{dd\delta}$
t^{xy,x^2-y^2}	$\frac{3}{2}lm(l^2-m^2)V_{dd\sigma}+2lm(m^2-l^2)V_{dd\pi}+\frac{1}{2}\sqrt{3}lm(l^2-m^2)V_{dd\delta}$
$t^{x^2-y^2,x^2-y^2}$	$\frac{3}{4}(l^2-m^2)^2V_{dd\sigma}+[l^2+m^2-(l^2-m^2)^2]V_{dd\pi}+\frac{1}{4}(l^2-m^2)^2V_{dd\delta}$

6 Spin-orbit coupling in graphene

6.1 π-σ spin-orbit coupling

We will now consider the spin-orbit coupling between the π and σ bands, or more specifically between the p orbitals. This gives rise to a new term in the Hamiltonian of the form

$$H_{\mathrm{SO}} = \lambda(\mathbf{s}\times\nabla V)\cdot\mathbf{p}, \tag{6.1}$$

where $\mathbf{s}$ are Pauli matrices acting on the electron spin; $\boldsymbol{\sigma}$ is in this section reserved for pseudospin. Assuming the periodic potential to be spherically symmetric in the vicinity of each atom, and that the electron-atom distance does not vary much, we may approximate this to an on-site effect with

$$H_{\mathrm{SO}} = \Delta \mathbf{L} \cdot \mathbf{S}, \tag{6.2}$$

where Δ is the coupling constant with dimension energy, and $\mathbf{L}$ and $\mathbf{S} = \mathbf{s}/2$ are the dimensionless angular momentum and spin operator respectively.

The spin-orbit coupling leads to a partial splitting of the degenerate π bands at the Dirac points. We expect the new π bands to be doubly degenerate at the Dirac points when considering intrinsic spin-orbit coupling; according to Kramers theorem, inversion symmetry gives $E_{\mathbf{k}\uparrow} = E_{-\mathbf{k}\uparrow}$ and time-reversal symmetry gives $E_{\mathbf{k}\uparrow} = E_{-\mathbf{k}\downarrow}$, which put together yield $E_{\mathbf{k}\uparrow} = E_{\mathbf{k}\downarrow}$.

The s and p orbitals expressed by the orbital and magnetic quantum numbers are

$$|s\rangle = |\ell = 0, m_\ell = 0\rangle, \tag{6.3a}$$

$$|p_x\rangle = \frac{1}{\sqrt{2}} \left(|\ell = 1, m_\ell = -1\rangle - |\ell = 1, m_\ell = 1\rangle \right), \tag{6.3b}$$

$$|p_y\rangle = \frac{i}{\sqrt{2}} \left(|\ell = 1, m_\ell = -1\rangle + |\ell = 1, m_\ell = 1\rangle \right), \tag{6.3c}$$

$$|p_z\rangle = |\ell = 1, m_\ell = 0\rangle . \tag{6.3d}$$

Letting the spin-orbit operator $\Delta \mathbf{L} \cdot \mathbf{S}$ act on the s and p states, Eq. (6.3), we get the following addition to the Hamiltonian

$$H_{\mathrm{SO}} = \Delta \begin{pmatrix} 0 & 0 & -iS_y & iS_x \\ 0 & 0 & 0 & 0 \\ iS_y & 0 & 0 & -iS_z \\ -iS_x & 0 & iS_z & 0 \end{pmatrix}, \tag{6.4}$$

which acts on Ψ,

$$\Psi = \begin{pmatrix} |p_z\rangle \\ |s\rangle \\ |p_x\rangle \\ |p_y\rangle \end{pmatrix}, \tag{6.5}$$

where the elements of Ψ are spinors, e.g.

$$|p_z\rangle = \begin{pmatrix} |p_z \uparrow\rangle \\ |p_z \downarrow\rangle \end{pmatrix}. \tag{6.6}$$

Because Δ is small compared to the typical matrix elements of the tight-binding Hamiltonian, we will treat the spin-orbit part as a perturbation. We then use a canonical transformation to find the effective contribution from the spin-orbit coupling to the π band Hamiltonian. The procedure is then as follows, let H_0 be the diagonalised Hamiltonian and H_1 the perturbation. With a change of basis using the unitary tranformation matrix e^C, where C is anti-Hermitian we get

$$e^C(H_0 + H_1)e^{-C} = H_0 + H_1 + [C, H_0] + [C, H_1] + \frac{1}{2}[C\,[C, H_0]] + \ldots. \tag{6.7}$$

To get rid of the first order term we choose C so that

$$H_1 + [C, H_0] = 0. \tag{6.8}$$

The elements of C are then

$$C_{nn'} = \frac{(H_1)_{nn'}}{\epsilon_n - \epsilon_{n'}}. \tag{6.9}$$

We then arrive at the effective Hamiltonian,

$$H_{\text{eff}} = H_0 + \frac{1}{2}[C, H_1] + \ldots. \tag{6.10}$$

The spin-orbit coupling between the π and σ bands thus gives an effective contribution to the π bands. This can be seen as a result of virtual hopping between the two bands. The first correction to the π band Hamiltonian is then a result

of a virtual process where the electron hops to the σ bands and back again via the spin-orbit coupling. This correction is therefore necessarily quadratic in the spin-orbit coupling constant, and is of the form $\tau\lambda_{\mathrm{SO}}\sigma_z s_z$, where τ is $+1$ and -1 for the K and K' points respectively, $\lambda_{\mathrm{SO}} = \frac{1}{18}\Delta^2\frac{|\epsilon_s-\epsilon_p|}{V_{sp\sigma}^2}$ and σ_i, s_i are the Pauli matrices acting on the pseudo spin and the electron spin respectively.

By applying an external perpendicular electric field, E, the inversion symmetry of graphene is broken and an extrinsic Bychkov-Rashba spin-orbit coupling is induced through the atomic Stark effect. This couples the s and p_z orbitals, giving the following contribution to the total Hamiltonian

$$\langle s|H|p_z\rangle = eEz_{sp}, \quad \langle p_z|H|s\rangle = eEz_{sp}. \tag{6.11}$$

With the spin-orbit coupling this leads to an additional contribution to the effective Hamiltonian,

$$H_{ext} = \begin{pmatrix} 0 & 0 & 0 & eEz_{sp} \\ 0 & 0 & 0 & 0 \\ 0 & 0 & 0 & 0 \\ eEz_{sp} & 0 & 0 & 0 \end{pmatrix}, \tag{6.12}$$

which further splits the bands by $\lambda_R(\tau\sigma_x s_y - \sigma_y s_x)$ where $\lambda_R = \frac{1}{3}\frac{eEz_{sp}\Delta}{V_{sp\sigma}}$ and $z_{sp} = \langle s|\hat{z}|p_z\rangle \sim 0.15$Å [77].

The results we have obtained for the intrinsic and the extrinsic effects agrees with the results of Konschuh *et al.* [77] and Min *et al.* [75] taking different definitions of Δ into account. The form agrees with the results obtained by Kane and Mele [80] and Huertas-Hernando *et al.* [81]. Using the values in Table 2, we find that $\lambda_{\mathrm{SO}} \approx 1\mu$eV and $\lambda_{\mathrm{R}} \approx 5.4\mu$eV for a typical electric field of $E = 1$V/nm.

The effective Hamiltonian in the vicinity of the Dirac points may then be written as

$$H_{\pi\mathrm{eff}} = -\tau\hbar v_F\boldsymbol{\sigma}(\tau)\cdot\mathbf{q} + \lambda_R(\tau\sigma_x s_y - \sigma_y s_x) + \tau\lambda_{\mathrm{SO}}\sigma_z s_z, \tag{6.13}$$

where $\boldsymbol{\sigma}(\tau) = \boldsymbol{\sigma}, \boldsymbol{\sigma}^*$ for K and K' respectively. The eigenvalues evaluated at the Dirac points are

$$\epsilon_{\pi 1} = (1-\tau)\lambda_R + \tau\lambda_{\mathrm{SO}}, \tag{6.14a}$$

$$\epsilon_{\pi 2} = -(1-\tau)\lambda_R + \tau\lambda_{\mathrm{SO}}, \tag{6.14b}$$

$$\epsilon_{\pi 3} = (1+\tau)\lambda_R - \tau\lambda_{\mathrm{SO}}, \tag{6.14c}$$

$$\epsilon_{\pi 4} = -(1+\tau)\lambda_R - \tau\lambda_{\mathrm{SO}}, \tag{6.14d}$$

with the coresponding eigenvectors

$$\psi_{\pi 1} = \frac{1}{\sqrt{2}}(i, 0, 0, 1), \tag{6.15a}$$

$$\psi_{\pi 2} = \frac{1}{\sqrt{2}}(-i, 0, 0, 1), \tag{6.15b}$$

$$\psi_{\pi 3} = \frac{1}{\sqrt{2}}(0, i, 1, 0), \tag{6.15c}$$

$$\psi_{\pi 4} = \frac{1}{\sqrt{2}}(0, -i, 1, 0), \tag{6.15d}$$

in a basis $A\uparrow, A\downarrow, B\uparrow, B\downarrow$. By changing the electric field strength, we can tune λ_R, which in turn means we can directly tune the band gap of graphene through the extrinsic spin-orbit interaction. There are four interesting cases [82]: for $\lambda_R = 0$ we get two doubly degenerate states with a gap of $2\lambda_{\mathrm{SO}}$ as posited initially; for $\lambda_R < \lambda_{\mathrm{SO}}$ the degenaracy of the two lowest bands is lifted, that is, $\epsilon_{\pi 3} \neq \epsilon_{\pi 4}$ for K and $\epsilon_{\pi 1} \neq \epsilon_{\pi 2}$ for K'; for $\lambda_R = \lambda_{\mathrm{SO}}$ three of the bands are degenerate, namely 1, 2 and 3 for K and 1, 3 and 4 for K', and the energy gap to the last band is $4\lambda_{\mathrm{SO}}$; and finally for $\lambda_R > \lambda_{\mathrm{SO}}$ we have the same degeneracy as for $\lambda_R < \lambda_{\mathrm{SO}}$, but now $\epsilon_{\pi 3} > \epsilon_{\pi 1} = \epsilon_{\pi 2} > \epsilon_{\pi 4}$ for K and $\epsilon_{\pi 1} > \epsilon_{\pi 3} = \epsilon_{\pi 4} > \epsilon_{\pi 2}$ for K'. These four cases are plotted in Figure 9.

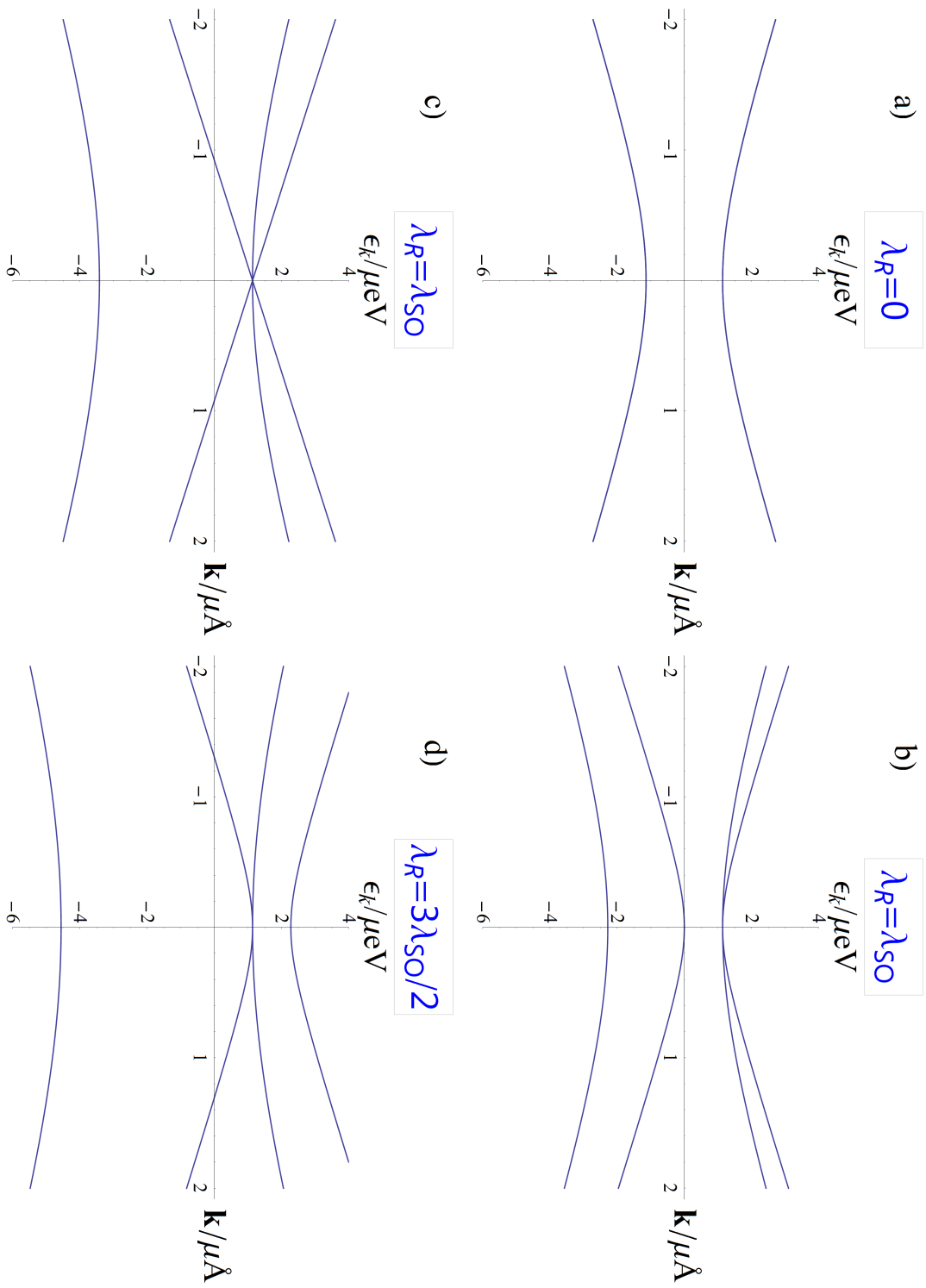

Figure 9. Plot of bandstructure of the π bands in the vicinity of the Dirac points for different values of the electric field strength.

6.2 Spin-orbit coupling with d-orbitals

By including d orbitals the full Hamiltonian takes the form

$$H_K = \begin{pmatrix} H_{\pi K} & 0 \\ 0 & H_{\sigma K} \end{pmatrix} + H_{\mathrm{SO}}, \tag{6.16}$$

where $H_{\pi K}$ is now given in a basis of (p_z, d_{xz}, d_{yz}) and $H_{\sigma K}$ in a basis of $(s, p_x, p_y, d_{z^2}, d_{xy}, d_{x^2-y^2})$.

The d orbitals written in terms of the orbital and magnetic quantum numbers are

$$|d_{z^2}\rangle = |\ell = 2, m_\ell = 0\rangle, \tag{6.17a}$$

$$|d_{yz}\rangle = \frac{i}{\sqrt{2}} \left(|\ell = 2, m_\ell = -1\rangle + |\ell = 2, m_\ell = 1\rangle\right), \tag{6.17b}$$

$$|d_{xz}\rangle = \frac{1}{\sqrt{2}} \left(|\ell = 2, m_\ell = -1\rangle - |\ell = 2, m_\ell = 1\rangle\right), \tag{6.17c}$$

$$|d_{xy}\rangle = \frac{i}{\sqrt{2}} \left(|\ell = 2, m_\ell = -2\rangle - |\ell = 2, m_\ell = 2\rangle\right), \tag{6.17d}$$

$$|d_{x^2-y^2}\rangle = \frac{1}{\sqrt{2}} \left(|\ell = 2, m_\ell = -2\rangle + |\ell = 2, m_\ell = 2\rangle\right). \tag{6.17e}$$

By using Eq. (6.17), we again find the matrix elements for the spin-orbit operator $\mathbf{L} \cdot \mathbf{S}$, this time for the d orbitals. We use a different coupling constant, Δ and Δ_d, for the p and d orbitals respectively. The results are given in Table 5.

As can be seen from Eq. (6.16), even taking d orbitals into account, there is no coupling between the π and σ bands other than the spin-orbit interaction, since all the hopping terms coupling these states are proportional to $n = z/r$ which is zero for flat graphene. This means that any effective contribution to the π bands arising from spin-orbit coupling with the σ bands will still be quadratic in Δ at most and thus comparable to the results already obtained above. However, spin-orbit coupling between the d_{xz} and d_{yz} orbitals in $H_{\pi K}$ may lead to processes that are linear in Δ_d. This would dominate the intrinsic spin-orbit coupling.

Table 5. Matrix elements for the spin-orbit operator $\mathbf{L} \cdot \mathbf{S}$ for the s, p and d orbitals.

Orbital	p_z	p_x	p_y	s
p_z	0	$-iS_y$	iS_x	0
p_x	iS_y	0	$-iS_z$	0
p_y	$-iS_x$	iS_z	0	0
s	0	0	0	0

Orbital	d_{z^2}	d_{yz}	d_{xz}	d_{xy}	$d_{x^2-y^2}$
d_{z^2}	0	$i\sqrt{3}S_x$	$-i\sqrt{3}S_y$	0	0
d_{yz}	$-i\sqrt{3}S_x$	0	iS_z	$-iS_y$	$-iS_x$
d_{xz}	$i\sqrt{3}S_y$	$-iS_z$	0	iS_x	$-iS_y$
d_{xy}	0	iS_y	$-iS_x$	0	$2iS_z$
$d_{x^2-y^2}$	0	iS_x	iS_y	$-2iS_z$	0

Using a Löwdin transformation (see Appendix B for details), we find that the effective Hamiltonian for the π bands is

$$\widetilde{H}_0 \approx \lambda_{\mathrm{SO},d}\sigma_z s_z - \frac{9V_{pd\pi}^2}{2(\epsilon_d - \epsilon_p)}, \tag{6.18}$$

with

$$\lambda_{\mathrm{SO},d} = \frac{9V_{pd\pi}^2}{4(\epsilon_d - \epsilon_p)^2}\Delta_d. \tag{6.19}$$

The spin-independent term in Eq. (6.18) is the correction already found in Eq. (5.28). With $3V_{pd\pi}/2(\epsilon_d - \epsilon_p) \approx 0.0871$ [77], $\lambda_{\mathrm{SO},d} \approx 24\mu$eV. This does indeed dominate the intrinsic spin-orbit coupling.

When applying an extrinsic perpendicular electric field, the d orbitals would give an additional coupling of the π and σ bands, more specifically between the d_{z^2} and p_z orbitals. The effective contribution from this will be linear in the electric field strength and linear in spin-orbit coupling constant for d orbitals at most

and is thus negligible compared to the result obtained for extrinsic spin-orbit coupling for just s and p orbitals.

6.3 Spin relaxation

To get a better insight in spin-relaxation in graphene we have studied articles dealing with both the theoretical [66][68][83][84][85] and experimental [67][86] aspects of this. The in-plane spin relaxation rate for the Elliot-Yafet mechanism due to the intrinsic spin-orbit coupling is [68]

$$\frac{1}{\tau_{\mathrm{EY}\parallel}} \approx \frac{\lambda_{\mathrm{SO}}^2}{\epsilon_F^2}\frac{1}{\tau_{\mathrm{m}}}, \tag{6.20}$$

where $\tau_{\mathrm{EY}\parallel}$ is the in-plane Elliot-Yafet spin relaxation time, ϵ_F is the Fermi energy and τ_m is the momentum relaxation time. The Fermi energy is

$$\epsilon_F = \hbar v_F k_F = \hbar v_F \frac{2\pi}{\lambda_F} = \hbar v_F \sqrt{2\pi n}, \tag{6.21}$$

where k_F is the Fermi wavevector, $\lambda_F = \sqrt{2\pi/n}$ is the Fermi wavelength and n is the carrier density [83]. Using the λ_{SO} we have found (=24 μeV) and a typical value for the carrier density, $n \approx 3.6 \times 10^{16}$ m^{-2} [83] the Elliot-Yafet relaxation time is estimated to be of the order 10^2 ns, comparable to other estimates [68]. Since the effective intrinsic spin-orbit interaction commutes with s_z, the out-of-plane spin should not relax, i.e. $\tau_{\mathrm{EY}\perp} \to \infty$ [68]. Experiments [67][86] have shown that the spin diffusion length is proportional to the elastic mean free path, as is expected for the Elliot-Yafet mechanism, however the same experiments also show a spin lifetime of the order 10^2 ps and that the out-of-plane spins relax much faster than the in-plane spins, contrary to the theoretical estimates.

For the D'yakonov-Perel' mechanism we expect the out-of-plane spins to relax faster than the in-plane spins [83], as experiments show, but the spin relaxation time should be inversely proportional to the momentum relaxation time [83][68]

$$\frac{1}{\tau_{\mathrm{DP}}} \approx \frac{\lambda_{\mathrm{R}}^2}{\hbar^2}\tau_{\mathrm{m}}. \tag{6.22}$$

Thus neither the intrinsic spin-orbit coupling nor a typical Rashba extrinsic spin-orbit coupling can explain the experimental results. This motivates the study of impurity effects.

Furthermore, assuming weak scatterers, the momentum relaxation time scales as $\tau_m \propto \epsilon_F^{-1}$ [83][85]. This means that

$$\frac{1}{\tau_{\mathrm{EY}\parallel}} \propto \frac{\lambda_{\mathrm{SO}}^2}{\epsilon_F}, \tag{6.23}$$

thus the Elliot-Yafet spin relaxation time scales linearly with ϵ_F. Again, assuming weak scatterers, the spin relaxation rate due to the D'yakonov-Perel' mechanism is

$$\frac{1}{\tau_{\mathrm{DP}}} \propto \frac{\lambda_{\mathrm{R}}^2}{\epsilon_F}, \tag{6.24}$$

which means the Elliot-Yafet and D'yakonov-Perel' mechanism scale with $\epsilon_F \propto \sqrt{n}$ in the same way. This might make it difficult to distinguish between the two mechanisms [85].

7 Impurity effect in graphene

We are now interested in how an impurity located above the graphene plane influences both the electronic and spin related properties. We will then use the Luttinger-Kohn $\mathbf{k} \cdot \mathbf{p}$ perturbation theory, as presented in Section 3. First we investigate the impurity problem without any relativistic effects present, and later extend this treatment to include also the spin-orbit interaction.

7.1 Effective Hamiltonian in the absence of relativistic effects

As a first attempt to solve this problem, we use the eigenbasis of the unperturbed Hamiltonian from Eq. (5.13) for the π bands. Our Luttinger-Kohn basis is then

$$\chi_{n\mathbf{k}} = e^{i\mathbf{k}\cdot\mathbf{r}}(e^{i\mathbf{K}\cdot\mathbf{r}}u_{n\mathbf{K}}) = e^{i\mathbf{k}\cdot\mathbf{r}}\psi_{n\mathbf{K}}, \tag{7.1}$$

where $\psi_{n\mathbf{K}}$ is the Bloch function at $\mathbf{k} = \mathbf{K}$. We denote the two eigenstates for the π bands with $n = j \in \{+, -\}$, using the notation from Eq. (5.13), and for the σ bands $n = i \neq j$. With this choice of basis we arrive at the following equation for the π band envelope functions

$$\left[\epsilon_\pi(-i\nabla + \mathbf{K}) + U(\mathbf{r})\right] F_n(\mathbf{r}) = \epsilon F_n(\mathbf{r}), \tag{7.2}$$

where $\epsilon_\pi(-i\nabla + \mathbf{K})$ is to be expanded to the first order in $-i\nabla$, which of course poses a problem since the derivative of ϵ_π is singular at $\mathbf{k} = \mathbf{K}$. A possibility would be to do a change of coordinates to exploit the rotational symmetry of the problem, but also this will yield equations which are difficult to work with.

A more natural choice of basis for the π bands is Bloch functions located at the two sub-lattices, A and B [15]. Because of the degeneracy at the K points also this will be an eigenbasis of the unperturbed Hamiltonian. We denote the two

Bloch waves $\psi^A_{\pi\mathbf{k}}$ and $\psi^B_{\pi\mathbf{k}}$, so that

$$\psi^A_{\pi\mathbf{k}}(\mathbf{r}) = e^{i\mathbf{k}\cdot\mathbf{r}} u^A_{\pi\mathbf{k}}(\mathbf{r}), \tag{7.3}$$

$$\psi^B_{\pi\mathbf{k}}(\mathbf{r}) = e^{i\mathbf{k}\cdot\mathbf{r}} u^B_{\pi\mathbf{k}}(\mathbf{r}). \tag{7.4}$$

The Luttinger-Kohn basis is then the same as before for the σ band, and for the π bands we have

$$\chi^A_{\pi\mathbf{k}} = e^{i\mathbf{k}\cdot\mathbf{r}}(e^{i\mathbf{K}\cdot\mathbf{r}} u^A_{\pi\mathbf{K}}) = e^{i\mathbf{k}\cdot\mathbf{r}}\psi^A_{\pi\mathbf{K}}, \tag{7.5}$$

$$\chi^B_{\pi\mathbf{k}} = e^{i\mathbf{k}\cdot\mathbf{r}}(e^{i\mathbf{K}\cdot\mathbf{r}} u^B_{\pi\mathbf{K}}) = e^{i\mathbf{k}\cdot\mathbf{r}}\psi^B_{\pi\mathbf{K}}. \tag{7.6}$$

In the absence of the spin-orbit coupling there is no coupling between the π and σ bands, which means the momentum operator has no elements connecting these bands. For now, it is therefore sufficient to look at the equation

$$\left[H_\pi + U(\mathbf{r})\right]\psi_\pi = \epsilon\psi_\pi, \tag{7.7}$$

where H_π is the Hamiltonian from Eq. (5.11). Expanding in terms of the Luttinger-Kohn basis we may write the general solution as

$$\psi_\pi(\mathbf{r}) = \int \mathrm{d}\mathbf{k}\left\{g^A(\mathbf{k})\chi^A_{\pi\mathbf{k}}(\mathbf{r}) + g^B(\mathbf{k})\chi^B_{\pi\mathbf{k}}(\mathbf{r})\right\}. \tag{7.8}$$

We then follow the rather straightforward steps as presented in section 3. Projecting Eq. (7.7) on $\chi^A_{\pi\mathbf{k}}$ and $\chi^B_{\pi\mathbf{k}}$, we find the equation for the coefficient functions to the first order in momentum $\mathbf{k}$,

$$\frac{\hbar}{m_0}\mathbf{k}\cdot\begin{pmatrix} \mathbf{p}_{AA} & \mathbf{p}_{AB} \\ \mathbf{p}_{BA} & \mathbf{p}_{BB} \end{pmatrix}\begin{pmatrix} g^A(\mathbf{k}) \\ g^B(\mathbf{k}) \end{pmatrix} + \int \mathrm{d}\mathbf{k}'\,\mathcal{U}(\mathbf{k}-\mathbf{k}')\begin{pmatrix} g^A(\mathbf{k}') \\ g^B(\mathbf{k}') \end{pmatrix} = \epsilon\begin{pmatrix} g^A(\mathbf{k}) \\ g^B(\mathbf{k}) \end{pmatrix}, \tag{7.9}$$

where $\mathbf{p}_{AA} = \frac{(2\pi)^3}{\Omega}\int_{\text{cell}} \psi^{A*}_{\pi\mathbf{K}}(\mathbf{r})\mathbf{p}\psi^A_{\pi\mathbf{K}}(\mathbf{r})\mathrm{d}\mathbf{r}$ and so on for AB, BA and BB. To find the momentum matrix elements we use the fact that, when neglecting relativistic corrections (such as the spin-orbit coupling), we have the relation

$$\mathbf{p} = \frac{m_0}{\hbar}\nabla_{\mathbf{k}} H(\mathbf{k}), \tag{7.10}$$

where $H(\mathbf{k})$ is the Hamiltonian in k space. So in our case we have that

$$\begin{aligned}\begin{pmatrix} \mathbf{p}_{AA} & \mathbf{p}_{AB} \\ \mathbf{p}_{BA} & \mathbf{p}_{BB} \end{pmatrix} &= \frac{m_0}{\hbar}\nabla_{\mathbf{k}} \begin{pmatrix} 0 & -tf(\mathbf{k}) \\ -tf^*(\mathbf{k}) & 0 \end{pmatrix}|_{\mathbf{k}=\mathbf{K}} \\ &= -\frac{m_0}{\hbar}\frac{\sqrt{3}ta}{2} \begin{pmatrix} 0 & \hat{x} - i\hat{y} \\ \hat{x} + i\hat{y} & 0 \end{pmatrix}. \end{aligned} \tag{7.11}$$

Inserting this into Eq. (7.9) we get

$$\begin{aligned} -\frac{\sqrt{3}ta}{2} \begin{pmatrix} 0 & k_x - ik_y \\ k_x + ik_y & 0 \end{pmatrix} \begin{pmatrix} g^A(\mathbf{k}) \\ g^B(\mathbf{k}) \end{pmatrix} \\ + \int \mathrm{d}\mathbf{k}'\, \mathcal{U}(\mathbf{k} - \mathbf{k}') \begin{pmatrix} g^A(\mathbf{k}') \\ g^B(\mathbf{k}') \end{pmatrix} = \epsilon \begin{pmatrix} g^A(\mathbf{k}) \\ g^B(\mathbf{k}) \end{pmatrix}. \end{aligned} \tag{7.12}$$

By Fourier transforming to real space, we get

$$i\frac{\sqrt{3}ta}{2} \begin{pmatrix} 0 & \partial_x - i\partial_y \\ \partial_x + i\partial_y & 0 \end{pmatrix} \begin{pmatrix} G^A(\mathbf{r}) \\ G^B(\mathbf{r}) \end{pmatrix} + U(\mathbf{r}) \begin{pmatrix} G^A(\mathbf{r}) \\ G^B(\mathbf{r}) \end{pmatrix} = \epsilon \begin{pmatrix} G^A(\mathbf{r}) \\ G^B(\mathbf{r}) \end{pmatrix} \tag{7.13}$$

or equivalently

$$\left[i\hbar v_F \nabla \cdot \boldsymbol{\sigma} + U(\mathbf{r})\right] \mathbf{G}(\mathbf{r}) = \epsilon \mathbf{G}(\mathbf{r}), \tag{7.14}$$

where

$$\mathbf{G}(\mathbf{r}) = \begin{pmatrix} G^A(\mathbf{r}) \\ G^B(\mathbf{r}) \end{pmatrix} = \int \mathrm{d}\mathbf{k}\, e^{i\mathbf{k}\cdot\mathbf{r}} \begin{pmatrix} g^A(\mathbf{k}) \\ g^B(\mathbf{k}) \end{pmatrix}. \tag{7.15}$$

The resemblance between Eq. (7.14) and Eq. (5.16) is of course no surprise. If the effect of orbitals of a higher principal quantum number is neglected the higher order corrections are zero. This is due to the fact that the π and σ band do not mix in the absence of relativisic effects.

7.2 Renormalised impurity induced spin-orbit coupling

If we now include the spin-orbit interaction, we replace the momentum operator with the spin-dependent velocity operator, $\mathbf{p} \to m_0\boldsymbol{\pi}$. The equation for the

coefficient functions is then

$$\left(\epsilon_j + \frac{\hbar^2 k^2}{2m_0}\right) g_j(\mathbf{k}) + \sum_n \hbar k_\alpha \pi^\alpha_{jn} g_n(\mathbf{k}) + \int \mathrm{d}\mathbf{k}' \mathcal{U}(\mathbf{k}-\mathbf{k}') g_j(\mathbf{k}') = \epsilon g_j(\mathbf{k}), \quad (7.16)$$

where the sum runs over both the π bands and the σ bands, and $j \in \{|z\uparrow\rangle_A, |z\downarrow\rangle_A, |z\uparrow\rangle_B, |z\downarrow\rangle_B\}$. We may now do the transformation given by Eq. (3.58), to get rid of the coupling to the σ bands. The equation for the transformed coefficient functions, $h_j \equiv e^{-S} g_j$, is then

$$\begin{aligned} &\sum_{j'\in\pi} \left(\epsilon_0 \delta_{jj'} + \hbar k_\alpha \pi^\alpha_{jj'} + \frac{\hbar^2 k^2}{2m_0}\delta_{jj'} + \hbar^2 k_\alpha k_\beta \sum_{i\in\sigma} \frac{\pi^\alpha_{ji}\pi^\beta_{ij'}}{\epsilon_0 - \epsilon_i} \right) h_{j'}(\mathbf{k}) \\ &+ \int d\mathbf{k}' \mathcal{U}(\mathbf{k}-\mathbf{k}') h_j(\mathbf{k}') + \int \mathrm{d}\mathbf{k}' \sum_{j'\in\pi} \langle j\mathbf{k}| \frac{1}{2}[[U,S],S] |j'\mathbf{k}'\rangle h_{j'}(\mathbf{k}') = \epsilon h_j(\mathbf{k}). \end{aligned} \quad (7.17)$$

What we now are interested in is to see if the last term on the left hand side of this equation give rise to any significant impurity induced spin effects. First, we observe that the additional term in Eq. (7.17) due to the coupling to the σ bands is quadratic in momentum $\mathbf{k}$ and quadratic in the interband velocity matrix elements π_{ji}. Looking at Eq. (3.78), we see that we need simply to find the values of the tensor

$$\sum_{i\in\sigma} \frac{\pi^\alpha_{ji}\pi^\beta_{ij'}}{\omega_{ji}\omega_{ij'}}, \quad (7.18)$$

for the different combinations of j, j' and α, β. For graphene the spin-orbit splitting is very small, so assuming the spin-orbit coupling leaves the energy gap between the π bands and any of the σ bands unchanged is a very good approximation. This is different from the case of germanium, where the change in the velocity operator is negligible, but the change in the energy gap is not. Defining a set of 4×4 matrices, $\Pi^{\alpha\beta}$ with elements

$$\left(\Pi^{\alpha\beta}\right)_{jj'} \equiv \sum_{i\in\sigma} \frac{\pi^\alpha_{ji}\pi^\beta_{ij'}}{\omega_{ji}\omega_{ij'}} = \left(S^{\alpha\beta}\right)_{jj'} + \left(A^{\alpha\beta}\right)_{jj'}, \quad (7.19)$$

where S and A denotes the symmetric and antisymmetric part respectively, so that

$$S^{\alpha\beta} = \frac{\Pi^{\alpha\beta} + \Pi^{\beta\alpha}}{2}, \tag{7.20a}$$

$$A^{\alpha\beta} = \frac{\Pi^{\alpha\beta} - \Pi^{\beta\alpha}}{2}. \tag{7.20b}$$

We then need to know the spin-orbit correction to the elements of the velocity operator between the π bands and the σ bands. We will follow the procedure presented by Lew Yan Voon and Ram-Mohan [87]. Using the definition of the velocity operator,

$$\boldsymbol{\pi} \equiv \frac{i}{\hbar}\left[H, \mathbf{r}\right], \tag{7.21}$$

and the relation

$$\langle n\mathbf{k}|\mathbf{r}|m\mathbf{k}\rangle = \frac{i}{\epsilon_{m\mathbf{k}} - \epsilon_{n\mathbf{k}}}\langle n\mathbf{k}|\nabla_{\mathbf{k}} H(\mathbf{k})|m\mathbf{k}\rangle, \tag{7.22}$$

we find that

$$\begin{aligned}\langle n\mathbf{k}|\boldsymbol{\pi}|m\mathbf{k}\rangle =& \frac{1}{\hbar}\langle n\mathbf{k}|\nabla_{\mathbf{k}} H_0|m\mathbf{k}\rangle \\ &- \frac{1}{\hbar}\sum_{n'\neq m}\frac{\langle n\mathbf{k}|H_{\mathrm{SO}}|n'\mathbf{k}\rangle\langle n'\mathbf{k}|\nabla_{\mathbf{k}} H_0|m\mathbf{k}\rangle}{\epsilon_{m\mathbf{k}} - \epsilon_{n'\mathbf{k}}} \\ &- \frac{1}{\hbar}\sum_{n'\neq n}\frac{\langle n\mathbf{k}|\nabla_{\mathbf{k}} H_0|n'\mathbf{k}\rangle\langle n'\mathbf{k}|H_{\mathrm{SO}}|m\mathbf{k}\rangle}{\epsilon_{n\mathbf{k}} - \epsilon_{n'\mathbf{k}}} \\ &+ O((\lambda/\bar{\omega})^2).\end{aligned} \tag{7.23}$$

Here $\bar{\omega}$ is a typical energy gap between the π and σ bands, and $\lambda = \hbar/(4m_0^2c^2)$ is as before the spin-orbit coupling strength for vacuum. The matrix elements of the velocity operator which enters into $\Pi^{\alpha\beta}$ are only between the π and σ states. Since the only coupling between these two bands are through the spin-orbit coupling, the first term of Eq. (7.23) is zero for the matrix elements in question. We calculate $\Pi^{\alpha\beta}$ using Mathematica, for details see Appendix C. We

then arrive at the following result

$$A^{xy} = -ia\sigma_z - ibs_z - ic\sigma_x s_z, \tag{7.24a}$$
$$S^{xy} = -d\sigma_y, \tag{7.24b}$$
$$S^{xx} = -e + f\sigma_x - g\sigma_z s_z, \tag{7.24c}$$
$$S^{yy} = -h - j\sigma_x - k\sigma_z s_z, \tag{7.24d}$$

where σ_i and s_i are Pauli matrices acting on pseudospin and electron spin respectively. By adding the terms from Eq. (6.11) to the correction of the velocity operator of Eq. (7.23) we get also the effect of an extrinsic perpendicular electric field. We then get the additional contribution, $\Pi^{\alpha\beta}_{\text{ext}} = S^{\alpha\beta}_{\text{ext}} + A^{\alpha\beta}_{\text{ext}}$, where we find

$$A^{xy}_{\text{ext}} = i\tilde{a}\sigma_z - ia'\sigma_z s_y, \tag{7.25a}$$
$$S^{xy}_{\text{ext}} = -\tilde{b}\sigma_y - b's_x + c'(\sigma_x s_x - \sigma_y s_y), \tag{7.25b}$$
$$S^{xx}_{\text{ext}} = -\tilde{c} - \tilde{d}\sigma_x - d's_y - e'(\sigma_x s_y + \sigma_y s_x) - f'(\sigma_x s_y - \sigma_y s_x), \tag{7.25c}$$
$$S^{yy}_{\text{ext}} = -\tilde{e} + \tilde{f}\sigma_x + g's_y + h'(\sigma_x s_y + \sigma_y s_x) - j'(\sigma_x s_y - \sigma_y s_x). \tag{7.25d}$$

The coefficents $a, b, c...$ are proportional to Δ^2, the primed coefficients are proportional to $\Delta e E z_{sp}$ and the ones marked with tilde are proportional to $(eEz_{sp})^2$. The signs are chosen so that all these coefficients are positive, see Tables 6, 7 and 8 for numerical values. The asymmetry between the x and y direction is a consequence of our choice of coordinates. We have chosen the coordinate system so that the the matrix elements of the tight-binding Hamiltonian at the K points are either strictly real or strictly imaginary. At the cost of loosing this property, we could make the impurity corrections completely symmetric with respect to x and y; a rotation of 45° makes $S^{xx} = S^{yy}$ and $S^{xx}_{\text{ext}} = S^{yy}_{\text{ext}}$. For the sake of simplicity we refrain from doing this rotation.

Because what we are looking at now is just a correction to the Hamiltonian we neglect any term which is not spin-dependent. These terms are small, and would only give rise to a small overall contribution which treats all spin states in the same way. If we then first look only at the intrinsic part, noting that $g \approx k$ and

$c \gg b$, we may write the contribution to our Hamiltonian as

$$H_{\text{int}} \approx -ic\sigma_x s_z(\nabla U \times \nabla)_z - \frac{g+k}{2}(\nabla^2 U)\sigma_z s_z. \tag{7.26}$$

If we then compare Eq. (7.26) to the vacuum term $\lambda \mathbf{s} \cdot (\nabla U \times \mathbf{p})$, we see that c plays the role of a renormalised λ. With $\Delta = 6\,\text{meV}$ we have that $c/\hbar\lambda \approx 2{\cdot}10^{-2}$, that is to say the effective impurity driven spin-orbit coupling is much smaller than the corresponding vacuum term. The second term in Eq. (7.26) is of the same order of magnitude as the first one, which means also this term is negligible.

Looking at the contribution from the external electric field, there is as expected no terms containing s_z due to the inversion symmetry being broken. The form of this Hamiltonian is very interesting, as the spin flip terms would contribute to the D'yakonov-Perel' and Elliot-Yafet mechanisms. The magnitude of these terms are determined by the coefficients listed in Table 7, note that they are a factor $(eEz_{sp})/\Delta$ larger than that of the intrinsic impurity effect. For a typical electric field of $E = 1\text{V/nm}$, this ratio can be estimated to be $(eEz_{sp})/\Delta \approx 3$ [77]. In conclusion, this is not nearly sufficient to give rise to any significant spin related effects since $c/\hbar\lambda \sim 10^{-2}$. Comparing e.g. the spin-dependent term stemming from the antisymmetric part of $\Pi^{\alpha\beta}_{\text{ext}}$ to the Rashba term from Section 6 we have that $a'\big[\nabla U \times \nabla\big]_z/\lambda_R \sim 10^{-3}(a/L)^2\bar{U}/\text{eV}$, where $\bar{U}$ is the value of the impurity potential at some typical distance from the impurity center.

For the conventional spin-orbit interaction we found the d orbitals to dominate the intrinsic effect. In the same way we expect the d orbitals to give some contribution to $\Pi^{\alpha\beta}$ which will be at most three orders of magnitude larger than that we have found using only the s, p_x, p_y orbitals. The numerical values of the parameters which enters into this calculation are not readily available, and finding them have proven to be difficult. Any analytic calculation is out of the question due to its complexity. This said, we know that even a increase of $\Pi^{\alpha\beta}$ by three orders of magnitude would be far from sufficient to make these terms significant. In the same way as before the d orbitals would not give any

important contribution to the effects due to the applied electric field, so the spin flip terms stay the same.

Table 6. Values of the Δ^2 coefficients.

Coefficient\Units	$a^2\Delta^2 10^{-4}/(\text{eV})^2$
a	2.06
b	0.110
c	3.01
d	1.17
e	5.21
f	1.39
g	1.11
h	7.94
j	1.82
k	1.23

Table 7. Values of the $\Delta(eEz_{sp})$ coefficients.

Coefficient\Units	$a^2\Delta(eEz_{sp})10^{-4}/(\text{eV})^2$
a'	2.40
b'	2.69
c'	4.17
d'	3.37
e'	3.77
f'	2.62
g'	4.72
h'	2.96
j'	5.38

Table 8. Values of the $(eEz_{sp})^2$ coefficients.

Coefficient\Units	$a^2(eEz_{sp})^2 10^{-4}/(\text{eV})^2$
$\tilde{a}$	2.44
$\tilde{b}$	3.49
$\tilde{c}$	9.13
$\tilde{d}$	0.689
$\tilde{e}$	17.3
$\tilde{f}$	9.04

8 Conclusion

In this thesis we have reviewed two models for calculating the effect of a slowly varying impurity potential on a semiconductor. The multiple-scale analysis is an excelent method for finding the lowest order correction to the effective mass theory. However, when higher order corrections are to be included this method becomes increasingly complicated, and defies analytical evaluation. We therefore found it necessary to look to another method, namely the Luttinger-Kohn model. The model is by far more rigorous than the multiple-scale analysis, and it is superior when the aim is to calculate higher order corrections. Applying this method on an impurity problem in germanium gives a good illustration of the dynamics of the model, and we also see how the higher order contributions induce an effective impurity induced spin-orbit coupling. The method of Lewiner and Nozieres is a flavour of the Luttinger-Kohn model. This method is a good aid to illuminate the physics of the problem, and evidently it yields the same results as that of Luttinger and Kohn. It also demonstrates how an external time dependent electro-magnetic field modifies this result.

The bandstructure of graphene has some remarkable properties. In the absence of the spin-orbit coupling it is a zero gap semiconductor. The low energy excitations are governed by the zero mass Dirac equations for two dimensions where the Dirac spinor has been replaced by a pseudospinor. Thus these quasiparticles

behave as massless fermions with an effective speed of light $v_F \approx 10^6$m/s. This makes graphene suitable for experiments on quantum electrodymanical effects, previously only attainable in high energy experiments. When the spin-orbit coupling is included the degeneracy at the Fermi level is lifted. The s and p orbitals contribute to a gap of $2\lambda_{\mathrm{SO}} \approx 1.1\mu$eV. By taking into account the effect of the d orbitals, we find a gap of $2\lambda_{\mathrm{SO},d} \approx 24\mu$eV, which by far dominates the intrinsic spin-orbit coupling. Because the spin-orbit effect in graphene is so small the dependence on the spin-orbit coupling constants is essential. This is the origin of the quantitative difference between λ_{SO} and $\lambda_{\mathrm{SO},d}$: $\lambda_{\mathrm{SO}} \propto \Delta^2$ and $\lambda_{\mathrm{SO},d} \propto \Delta_d$. When an external perpendicular electric field is applied, the inversion symmetry is broken, which together with the spin-orbit coupling between the p orbitals gives rise to a Bychkov-Rashba effect. The magnitude of this effect is proportional to the electric field strength, which means the gap is tunable. Here the effect of the d orbitals is negligible in comparison.

By applying the method of Luttinger and Kohn, we investigated the effect an impurity has on the electronic states of graphene. Here we found the choice of basis to play an important role in the simplification of the equations. Choosing a Luttinger-Kohn basis from Bloch functions located on the A and B sublattice proved to give rather simple equations, avoiding problems due to the singularity of $\nabla_{\mathbf{k}}\epsilon_{\pi\mathbf{k}}$. If relativistic effects are neglected, there is no coupling between the π and σ bands, meaning any higher order correction is zero. By including the spin-orbit correction to the velocity operator, we were able numerically calculate the effective impurity induced spin-orbit coupling due to the coupling to the σ bands. These contributions are roughly 10^{-2} smaller than the impurity vacuum term, making them negligible. We expect that in the same way as for the intrinsic effect the d orbitals would give a contribution at most 10^3 larger. This would at most make it comparable to the vacuum term, which is considered negligible. A perpendicular electric field breaks the inversion symmetry, giving rise to impurity induced spin-flip terms in the effective Hamiltonian. Analogous to the impurity-independent Bychkov-Rashba effect previously mentioned these terms are proportional to the product of the electric field strength and the spin-

orbit coupling constant, and the d orbitals are expected to have a diminutive effect. This effect is a factor $(eEz_{sp})/\Delta$ larger than the calculated impurity induced spin-orbit terms. This makes it too small to give any interesting spin related effects, even for relatively large electric fields. One of the main objectives of this thesis was to try to shed some light on theory of spin realated impurity effects in graphene, and thus help explain the discrepancy between the existing theories and the experimental results. The corrections due to coupling of the impurity potential and the spin-orbit interaction are thus found to play a limited role in this, even when the effect of an perpendicular external electric field is included.

Outlook: Even though we expect that the contribution from the d orbitals to the impurity induced spin-orbit coupling is negligible, it would be interesting to do a DFT calculation to find the relevant hopping parameters, and so find the actual significance of these orbitals. Moreover, there are other effects of impurities which deserve a closer examination. For example we have not discussed the effect of impurity induced curvature, leading to locally non-zero momentum matrix elements between the π and the σ bands. This could result in an impurity induced spin-orbit coupling which is linear in the coupling constant, and it could therefore be several orders of magnitude larger than what we have found.

Appendix A

f-sum rule

Here we derive the f-sum rule as presented in the paper of Luttinger and Kohn [71]. With spin-orbit, the Schrödinger equation, Eq. (3.24) takes the form

$$\left(\bar{H}_0 + \mathbf{k}\cdot\boldsymbol{\pi} + \frac{k^2}{2m_0}\right)\bar{u}_{n\mathbf{k}} = \epsilon_n(\mathbf{k})\bar{u}_{n\mathbf{k}}. \tag{A.1}$$

Using the definition of the velocity operator, we have that the α-component is

$$\boldsymbol{\pi}_\alpha = i[\bar{H}_0, x_\alpha] = \left\{\frac{p_\alpha}{m_0} + \frac{1}{4m_0^2}(\boldsymbol{\sigma}\times\nabla V)_\alpha\right\}, \tag{A.2}$$

where $\bar{H}_0$ is the Hamiltonian from Eq. (3.65). The matrix elements of the commutator are

$$\begin{aligned}\langle n\mathbf{k}|[\bar{H}_0, x_\alpha]|n'\mathbf{k}'\rangle &= \frac{1}{i}\langle n\mathbf{k}|\left\{\frac{p_\alpha}{m_0} + \frac{1}{4m_0^2}(\boldsymbol{\sigma}\times\nabla V)_\alpha\right\}|n'\mathbf{k}'\rangle \\ &= \frac{1}{i}\pi^\alpha_{nn'}\delta(\mathbf{k}-\mathbf{k}').\end{aligned} \tag{A.3}$$

Using the explicit form of the matrix element we may calculate another form of the commutator,

$$\begin{aligned}
&\langle n\mathbf{k}|[\bar{H}_0, x_\alpha]|n'\mathbf{k}'\rangle \\
&= (\epsilon_n(\mathbf{k}) - \epsilon_{n'}(\mathbf{k}'))\langle n\mathbf{k}|x_\alpha|n'\mathbf{k}'\rangle \\
&= (\epsilon_n(\mathbf{k}) - \epsilon_{n'}(\mathbf{k}'))\int \mathrm{d}\mathbf{r} e^{i(\mathbf{k}'-\mathbf{k})\cdot\mathbf{r}}\bar{u}^*_{n\mathbf{k}} x_\alpha \bar{u}_{n'\mathbf{k}'} \\
&= (\epsilon_n(\mathbf{k}) - \epsilon_{n'}(\mathbf{k}'))\int \mathrm{d}\mathbf{r}\left(\frac{1}{i}\frac{\partial e^{i(\mathbf{k}'-\mathbf{k})\cdot\mathbf{r}}}{\partial k'_\alpha}\right)\bar{u}^*_{n\mathbf{k}}\bar{u}_{n'\mathbf{k}'} \\
&= (\epsilon_n(\mathbf{k}) - \epsilon_{n'}(\mathbf{k}'))\left\{\frac{1}{i}\frac{\partial}{\partial k'_\alpha}\delta(\mathbf{k}-\mathbf{k}')\delta_{nn'} - \frac{1}{i}\int \mathrm{d}\mathbf{r} e^{i(\mathbf{k}'-\mathbf{k})\cdot\mathbf{r}}\bar{u}^*_{n\mathbf{k}}\frac{\partial \bar{u}_{n'\mathbf{k}'}}{\partial k'_\alpha}\right\} \\
&= (\epsilon_n(\mathbf{k}) - \epsilon_{n'}(\mathbf{k}'))\left\{\frac{1}{i}\frac{\partial}{\partial k'_\alpha}\delta(\mathbf{k}-\mathbf{k}')\delta_{nn'} + i\delta(\mathbf{k}-\mathbf{k}')\frac{(2\pi)^3}{\Omega}\int_{\text{cell}} \mathrm{d}\mathbf{r}\bar{u}^*_{n\mathbf{k}}\frac{\partial \bar{u}_{n'\mathbf{k}}}{\partial k_\alpha}\right\}.
\end{aligned} \tag{A.4}$$

Thus, combining Eqs. (A.3) and (A.4) for $n \neq n'$, we then have

$$\frac{\pi^\alpha_{nn'}}{\epsilon_n - \epsilon_{n'}} = -\frac{(2\pi)^3}{\Omega}\int_{\text{cell}} \mathrm{d}\mathbf{r}\bar{u}^*_{n\mathbf{k}}\frac{\partial \bar{u}_{n'\mathbf{k}}}{\partial k_\alpha}. \tag{A.5}$$

Multiplying by $\pi^\beta_{n'n}$ and summing over $n' \neq n$ we get

$$\sum_{n'\neq n}\frac{\pi^\alpha_{nn'}\pi^\beta_{n'n}}{\epsilon_{n'} - \epsilon_n} = -\sum_{n'\neq n}\left(\frac{(2\pi)^3}{\Omega}\right)^2\int_{\text{cell}} \mathrm{d}\mathbf{r}'\bar{u}^*_{n\mathbf{k}}\pi_\alpha\bar{u}_{n'\mathbf{k}}\int_{\text{cell}} \mathrm{d}\mathbf{r}\bar{u}^*_{n'\mathbf{k}}\frac{\partial \bar{u}_{n\mathbf{k}}}{\partial k_\beta}. \tag{A.6}$$

For a crystal with a center of symmetry, we have that [71]

$$\int_{\text{cell}} \mathrm{d}\mathbf{r}\bar{u}^*_{n\mathbf{k}}\frac{\partial \bar{u}_{n\mathbf{k}}}{\partial k_\alpha} = 0, \tag{A.7}$$

so the sum on the right hand side of Eq. (A.6) can be extended to include $n' = n$, which allows us to use the completeness of $\bar{u}_{n\mathbf{k}}$,

$$\sum_{n'}\bar{u}_{n'\mathbf{k}}(\mathbf{r}')\bar{u}^*_{n'\mathbf{k}}(\mathbf{r}) = \frac{\Omega}{(2\pi)^3}\delta(\mathbf{r}'-\mathbf{r}), \tag{A.8}$$

where $\mathbf{r}$ and $\mathbf{r}'$ are in the same cell. Eq. (A.6) then becomes

$$\sum_{n'\neq n}\frac{\pi^\alpha_{nn'}\pi^\beta_{n'n}}{\epsilon_{n'} - \epsilon_n} = -\frac{(2\pi)^3}{\Omega}\int_{\text{cell}} \mathrm{d}\mathbf{r}\bar{u}^*_{n\mathbf{k}}\pi_\alpha\frac{\partial \bar{u}_{n\mathbf{k}}}{\partial k_\beta}. \tag{A.9}$$

We now seek to simplify the expression on the right hand side of Eq. (A.9). To that end, it is convinient to note that it is symmetric in α and β for crystals where $\pi^{\alpha}_{nn'} = \pi^{\alpha}_{n'n}$. Eq. (A.9) may then be written as

$$\begin{aligned}\sum_{n' \neq n} \frac{\pi^{\alpha}_{nn'} \pi^{\beta}_{n'n}}{\epsilon_{n'} - \epsilon_n} = &- \frac{1}{2} \frac{(2\pi)^3}{\Omega} \left\{ \int_{\text{cell}} \mathrm{d}\mathbf{r} \bar{u}^*_{n\mathbf{k}} \pi_\alpha \frac{\partial \bar{u}_{n\mathbf{k}}}{\partial k_\beta} \right. \\ &\left. + \int_{\text{cell}} \mathrm{d}\mathbf{r} \bar{u}^*_{n\mathbf{k}} \pi_\beta \frac{\partial \bar{u}_{n\mathbf{k}}}{\partial k_\alpha} \right\}\end{aligned} \tag{A.10}$$

The right hand side can now be simplified by noting its relation to a differentiation of the Schrödinger equation for $\bar{u}_{n\mathbf{k}}$ with respect to k_α and k_β. We have

$$\frac{\partial}{\partial k_\alpha} \frac{\partial}{\partial k_\beta} \left(\left\{ \bar{H}_0 + \mathbf{k} \cdot \boldsymbol{\pi} + \frac{k^2}{2m_0} \right\} \bar{u}_{n\mathbf{k}} \right) = \frac{\partial}{\partial k_\alpha} \frac{\partial}{\partial k_\beta} (\epsilon_n(\mathbf{k}) \bar{u}_{n\mathbf{k}}). \tag{A.11}$$

The left hand side becomes

$$\begin{aligned}\frac{\partial}{\partial k_\alpha} \frac{\partial}{\partial k_\beta} \left(\left\{ \bar{H}_0 + \mathbf{k} \cdot \boldsymbol{\pi} + \frac{k^2}{2m_0} \right\} \bar{u}_{n\mathbf{k}} \right) = &\pi_\alpha \frac{\partial \bar{u}_{n\mathbf{k}}}{\partial k_\beta} + \pi_\beta \frac{\partial \bar{u}_{n\mathbf{k}}}{\partial k_\alpha} + \frac{1}{m_0} \delta_{\alpha\beta} \bar{u}_{n\mathbf{k}} \\ &+ \left\{ \bar{H}_0 + \mathbf{k} \cdot \boldsymbol{\pi} + \frac{k^2}{2m_0} \right\} \frac{\partial^2 \bar{u}_{n\mathbf{k}}}{\partial k_\alpha \partial k_\beta},\end{aligned} \tag{A.12}$$

and the right hand side

$$\frac{\partial}{\partial k_\alpha} \frac{\partial}{\partial k_\beta} (\epsilon_n(\mathbf{k}) \bar{u}_{n\mathbf{k}}) = \frac{\partial^2 \epsilon_n(\mathbf{k})}{\partial k_\alpha \partial k_\beta} \bar{u}_{n\mathbf{k}} + \frac{\partial \epsilon_n(\mathbf{k})}{\partial k_\alpha} \frac{\partial \bar{u}_{n\mathbf{k}}}{\partial k_\beta} + \frac{\partial \epsilon_n(\mathbf{k})}{\partial k_\beta} \frac{\partial \bar{u}_{n\mathbf{k}}}{\partial k_\alpha} + \epsilon_n(\mathbf{k}) \frac{\partial^2 \bar{u}_{n\mathbf{k}}}{\partial k_\alpha \partial k_\beta}. \tag{A.13}$$

Multiplying Eq. (A.11) by $\bar{u}^*_{n\mathbf{k}}$ and integrating over the cell, we obtain

$$\int_{\text{cell}} \mathrm{d}\mathbf{r} \bar{u}^*_{n\mathbf{k}} \left\{ \pi_\alpha \frac{\partial \bar{u}_{n\mathbf{k}}}{\partial k_\beta} + \pi_\beta \frac{\partial \bar{u}_{n\mathbf{k}}}{\partial k_\alpha} \right\} + \frac{\Omega}{(2\pi)^3} \frac{1}{m_0} \delta_{\alpha\beta} = \frac{\Omega}{(2\pi)^3} \frac{\partial^2 \epsilon_n(\mathbf{k})}{\partial k_\alpha \partial k_\beta} \tag{A.14}$$

where we have used Eq. (A.7) and that the Hamiltonian $\bar{H}_0 + \mathbf{k} \cdot \boldsymbol{\pi} + \frac{k^2}{2m_0}$ is Hermitian. We can then readily see that Eq. (A.10) becomes

$$\sum_{n' \neq n} \frac{\pi^{\alpha}_{nn'} \pi^{\beta}_{n'n}}{\epsilon_{n'} - \epsilon_n} = \frac{1}{2m_0} \left(\delta_{\alpha\beta} - m_0 \frac{\partial^2 \epsilon_n(\mathbf{k})}{\partial k_\alpha \partial k_\beta} \right) \tag{A.15}$$

which is the f-sum rule.

Appendix B

Löwdin Transformation

Combining Eq. (5.26) and the spin-orbit coupling given by Table 5, we find the total tight-binding Hamiltonian for the π bands to be

$$H_{\pi K} = \begin{pmatrix} \epsilon_p & 0 & 0 & 0 & i\gamma & \gamma \\ 0 & \epsilon_p & i\gamma & -\gamma & 0 & 0 \\ 0 & -i\gamma & \epsilon_d & -i\Delta_d S_z & \delta & i\delta \\ 0 & -\gamma & i\Delta_d S_z & \epsilon_d & i\delta & -\delta \\ -i\gamma & 0 & \delta & -i\delta & \epsilon_d & -i\Delta_d S_z \\ \gamma & 0 & -i\delta & -\delta & i\Delta_d S_z & \epsilon_d \end{pmatrix}, \tag{B.1}$$

here given in the basis ($p_{z,A}$, $p_{z,B}$, $d_{xz,A}$, $d_{yz,A}$, $d_{xz,B}$, $d_{yz,B}$). We denote the 2×2 p_z part of the matrix $H_{\pi p}$, and the 4×4 d part $H_{\pi d}$, so that

$$H_{\pi K} = \begin{pmatrix} H_{\pi p} & T \\ T^\dagger & H_{\pi d} \end{pmatrix}. \tag{B.2}$$

T and $T^\dagger$ is then the coupling between p_z and d orbitals. Making use of the Löwdin transformation as presented by Konschuh *et al.* [77] with a unitary anti-Hermitian matrix S,

$$\widetilde{H}_{\pi K} = e^{-S} H_{\pi K} e^{S} \tag{B.3}$$

$$\approx H_{\pi K} + [H_{\pi K}, S] + \frac{1}{2}[[H_{\pi K}, S], S], \tag{B.4}$$

where

$$S = \begin{pmatrix} 0 & M \\ -M^\dagger & 0 \end{pmatrix}. \tag{B.5}$$

We then set $H_{\pi p} = 0$ by subtracting ϵ_p from the diagonal and get

$$[H_{\pi K}, S] = \begin{pmatrix} -TM^\dagger - MT^\dagger & -MH_{\pi d} \\ -H_{\pi d}M^\dagger & T^\dagger M + M^\dagger T \end{pmatrix}. \tag{B.6}$$

Setting M so that $H_{\pi K} + [H_{\pi K}, S]$ has a block-diagonal form,

$$T - MH_{\pi d} = 0 \tag{B.7}$$

$$\Rightarrow M = TH_{\pi d}^{-1}, \tag{B.8}$$

the effective Hamiltonian from Eq. (B.4) for the p_z orbitals is

$$\widetilde{H}_{\pi p} \approx H_{\pi p} - TH_{\pi d}^{-1}T^\dagger - \frac{1}{2}\{TH_{\pi d}^{-2}T^\dagger, H_{\pi p}\}, \tag{B.9}$$

where higher-order terms in $H_{\pi d}^{-1}$ are neglected. Inserting $H_{\pi p} = 0$,

$$\widetilde{H}_{\pi p} \approx -TH_{\pi d}^{-1}T^\dagger \tag{B.10}$$

$$\approx \begin{pmatrix} -\frac{2\alpha^2}{\epsilon_d - \epsilon_p + S_z\Delta_d} & 0 \\ 0 & -\frac{2\alpha^2}{\epsilon_d - \epsilon_p - S_z\Delta_d} \end{pmatrix}. \tag{B.11}$$

Assuming $\Delta_d \ll (\epsilon_d - \epsilon_p)$ and expanding,

$$\widetilde{H}_{\pi p} \approx \begin{pmatrix} \frac{2\alpha^2}{\epsilon_d - \epsilon_p}\left(\frac{\Delta_d}{\epsilon_d - \epsilon_p}S_z - 1\right) & 0 \\ 0 & \frac{2\alpha^2}{\epsilon_d - \epsilon_p}\left(-\frac{\Delta_d}{\epsilon_d - \epsilon_p}S_z - 1\right) \end{pmatrix}, \tag{B.12}$$

where we have neglected terms of a higher order in Δ_d.

As $S_z = s_z/2$, this has the form,

$$\widetilde{H}_{\pi p} \approx \lambda_{\mathrm{SO},d}\sigma_z s_z - \frac{2\alpha^2}{\epsilon_d - \epsilon_p}, \tag{B.13}$$

with

$$\lambda_{\mathrm{SO},d} = \frac{\alpha^2}{(\epsilon_d - \epsilon_p)^2}\Delta_d \tag{B.14}$$

$$= \frac{9V_{pd\pi}^2}{4(\epsilon_d - \epsilon_p)^2}\Delta_d. \tag{B.15}$$

Appendix C

Mathematica

The Bandstructure

First we state some assumptions

```
$Assumptions = {x ∈ Reals, y ∈ Reals, z ∈ Reals, V_ssσ ∈ Reals,
   V_spσ ∈ Reals, V_ppσ ∈ Reals, V_ppπ ∈ Reals, ϵ_s ∈ Reals, ϵ_p ∈ Reals, s ∈ Reals};
```

The high symmetry points are

```
K1 := {2 π / 3, 2 π / Sqrt[3]}
K2 := {4 π / 3, 0}
M := (K1 + K2) / 2
Γ := 0
```

where K1 is the K point, and K2 the K' point. The angles between nearest neighbours from an A atom are

```
θ1 := -π / 2
θ2 := π / 6
θ3 := 5 π / 6
```

We will now first find the tight binding Hamiltonian for the σ bands and π bands. We start by defining a 8 x8 matrix, H, with elements $h_{i,j}$, where we will use the basis $(Ap_z\ Bp_z\ As\ Ap_x\ Ap_y\ Bs\ Bp_x\ Bp_y)$, where Ap_z is the p_z state on a A site.

```
H := Table[h_i,j, {i, 8}, {j, 8}]
```

The phases from a B site to an A site, in the direction 1, 2, 3 is

```
ph1 := 1; ph2 := e^(1/2 i (x + Sqrt[3] y)); ph3 := e^(-1/2 i (x - Sqrt[3] y));
```

We already know the elements between the p_z states

```
h1,1 := ϵ_p; h2,2 := ϵ_p; h1,2 := V_ppπ Sum_{i=1}^{3} ph_i; h2,1 := Conjugate[h1,2];
```

And in the absence of the spin-orbit coupling there is no coupling between the σ bands and the π bands

```
For[i = 3, i < 9, i++,
   For[j = 1, j < 3, j++,
      {h_i,j := 0, h_j,i := 0}
      ]
   ]
```

The elements for hopping between s states is similar to that of the p_z states

```
h3,6 := V_ssσ * (ph1 + ph2 + ph3); h6,3 := Conjugate[h3,6];
```

Hopping between s states and p_x or p_y states is a linear combination of $V_{sp\sigma}$ and $V_{sp\pi}$, the latter being zero. Hopping between A and A is of course also zero.

First hopping from B to A, ,

First hopping from B to A, p_x and p_y to s ,

```
h3,7 := Vspσ ∑i=1^3 Cos[θi + π] * phi
h3,8 := Vspσ ∑i=1^3 Sin[θi + π] * phi
```

then A to B

```
h7,3 := Conjugate[h3,7]
h8,3 := Conjugate[h3,8]
```

Hopping from B to A, s to p_x and p_y ,

```
h4,6 := -Vspσ ∑i=1^3 Cos[θi + π] * phi
h5,6 := -Vspσ ∑i=1^3 Sin[θi + π] * phi
```

then A to B

```
h6,4 := Conjugate[h4,6]
h6,5 := Conjugate[h5,6]
```

Hopping from A to A and B to B

```
h6,8 := 0; h8,6 := 0; h3,5 := 0; h5,3 := 0; h6,7 = 0; h7,6 = 0;
```

Hopping from p_x to p_y and and back is a linear combination of $V_{pp\sigma}$ and $V_{pp\pi}$.

The hopping from B to A, p_y to p_x is

```
h4,8 := Vppσ ∑i=1^3 Cos[θi + π] Sin[θi + π] * phi + Vppπ * ∑i=1^3 (-Cos[θi + π] Sin[θi + π] * phi)
```

B to A, p_x to p_y

```
h5,7 := Vppσ ∑i=1^3 Cos[θi + π] Sin[θi + π] * phi + Vppπ * ∑i=1^3 (-Cos[θi + π] Sin[θi + π] * phi)
```

A to B, p_y to p_x

```
h7,5 := Conjugate[h5,7]
```

A to B, p_x to p_y

```
h8,4 := Conjugate[h4,8]
```

Hopping from A to A and B to B is zero in the nearest neighbour approximation,

```
h4,5 := 0; h5,4 := 0; h7,8 := 0; h8,7 := 0; h3,4 = 0; h4,3 = 0;
```

B to A, p_x to p_x

```
h4,7 := Vppσ ∑i=1^3 Cos[θi + π]^2 * phi + Vppπ ∑i=1^3 Sin[θi + π]^2 * phi
```

B to A, p_y to p_y

```
h5,8 := Vppσ ∑i=1^3 Sin[θi + π]^2 * phi + Vppπ ∑i=1^3 Cos[θi + π]^2 * phi
```

A to B, p_x to p_x

```
h7,4 := Conjugate[h4,7]
```

A to B, p_y to p_y

```
h8,5 := Conjugate[h5,8]
```

The diagonal elements are

```
h3,3 := εs; h4,4 := εp; h5,5 := εp; h6,6 := εs; h7,7 := εp; h8,8 := εp;

Hnum := H /. {Vssσ → -6.769, Vspσ → 5.580, Vppσ → 5.037, Vppπ → -3.033, εs → -8.868, εp → 0}
```

We then make a parametrisation from K1 to Γ to M and back to K1, so that we get an informative plot.

```
G[t_] := ((HeavisideTheta[t] - HeavisideTheta[t - 1])
     Eigenvalues[Hnum /. x → (1 - t) * K1[[1]] /. y → (1 - t) * K1[[2]]] +
    (HeavisideTheta[t - 1] - HeavisideTheta[t - 1 - Norm[M] / Norm[K1]])
     Eigenvalues[Hnum /. x → (t - 1) * M[[1]] * Norm[K1] / Norm[M] /.
       y → (t - 1) * M[[2]] * Norm[K1] / Norm[M]] + (HeavisideTheta[t - 1 - Norm[M] / Norm[K1]] -
       HeavisideTheta[t - 1 - Norm[M] / Norm[K1] - Norm[K1 - M] / Norm[K1]]) Eigenvalues[Hnum /.
        x → (M[[1]] + (t - 1 - Norm[M] / Norm[K1]) * (K1[[1]] - M[[1]]) * Norm[K1] / Norm[K1 - M]) /.
       y → (M[[2]] + (t - 1 - Norm[M] / Norm[K1]) (K1[[2]] - M[[2]]) * Norm[K1] / Norm[K1 - M])])
```

```
Plot[Sort[G[u]],
 {u, 0, 1 + Norm[M] / Norm[K1] + Norm[K1 - M] / Norm[K1]}, Ticks → {None, Automatic}]
```

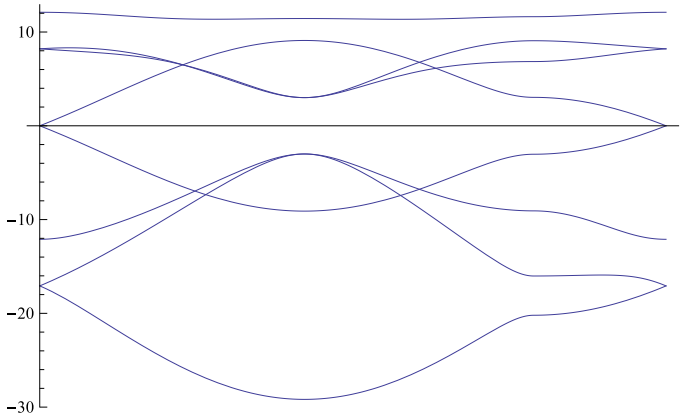


```
MatrixForm[Simplify[H /. {x → K1[[1]], y → K1[[2]]}]]
```

$$\begin{pmatrix}
\epsilon_p & 0 & 0 & 0 & 0 & 0 & 0 & 0 \\
0 & \epsilon_p & 0 & 0 & 0 & 0 & 0 & 0 \\
0 & 0 & \epsilon_s & 0 & 0 & 0 & \frac{3\,i\,V_{sp\sigma}}{2} & \frac{3\,V_{sp\sigma}}{2} \\
0 & 0 & 0 & \epsilon_p & 0 & -\frac{3\,i\,V_{sp\sigma}}{2} & \frac{3}{4}\left(V_{pp\pi}-V_{pp\sigma}\right) & \frac{3}{4}\,i\left(V_{pp\pi}-V_{pp\sigma}\right) \\
0 & 0 & 0 & 0 & \epsilon_p & -\frac{3\,V_{sp\sigma}}{2} & \frac{3}{4}\,i\left(V_{pp\pi}-V_{pp\sigma}\right) & -\frac{3}{4}\left(V_{pp\pi}-V_{pp\sigma}\right) \\
0 & 0 & 0 & \frac{3\,i\,V_{sp\sigma}}{2} & -\frac{3\,V_{sp\sigma}}{2} & \epsilon_s & 0 & 0 \\
0 & 0 & -\frac{3\,i\,V_{sp\sigma}}{2} & \frac{3}{4}\left(V_{pp\pi}-V_{pp\sigma}\right) & -\frac{3}{4}\,i\left(V_{pp\pi}-V_{pp\sigma}\right) & 0 & \epsilon_p & 0 \\
0 & 0 & \frac{3\,V_{sp\sigma}}{2} & -\frac{3}{4}\,i\left(V_{pp\pi}-V_{pp\sigma}\right) & -\frac{3}{4}\left(V_{pp\pi}-V_{pp\sigma}\right) & 0 & 0 & \epsilon_p
\end{pmatrix}$$

Which may be simplified to

$$H_K := \begin{pmatrix}
0 & 0 & 0 & 0 & 0 & 0 & 0 & 0 \\
0 & 0 & 0 & 0 & 0 & 0 & 0 & 0 \\
0 & 0 & s & 0 & 0 & 0 & i\,\alpha & \alpha \\
0 & 0 & 0 & 0 & 0 & -i\,\alpha & -\beta & -i\,\beta \\
0 & 0 & 0 & 0 & 0 & -\alpha & -i\,\beta & \beta \\
0 & 0 & 0 & i\,\alpha & -\alpha & s & 0 & 0 \\
0 & 0 & -i\,\alpha & -\beta & i\,\beta & 0 & 0 & 0 \\
0 & 0 & \alpha & i\,\beta & \beta & 0 & 0 & 0
\end{pmatrix}$$

Where $s = \epsilon_s - \epsilon_p$, $\alpha = \dfrac{3\,V_{sp\sigma}}{4}$, $\beta = \dfrac{3}{4}\left(V_{pp\sigma} - V_{pp\pi}\right)$.

The normalised eigenvectors given as rows are

$$\text{EigenV} := \begin{pmatrix} 1 & 0 & 0 & 0 & 0 & 0 & 0 & 0 \\ 0 & 1 & 0 & 0 & 0 & 0 & 0 & 0 \\ 0 & 0 & -\Phi & 0 & 0 & 0 & -X\,i & X \\ 0 & 0 & 0 & X\,i & X & \Phi & 0 & 0 \\ 0 & 0 & \Psi & 0 & 0 & 0 & -\Omega\,i & \Omega \\ 0 & 0 & 0 & -\Omega\,i & -\Omega & \Psi & 0 & 0 \\ 0 & 0 & 0 & \frac{i}{2} & -\frac{1}{2} & 0 & \frac{i}{2} & \frac{1}{2} \\ 0 & 0 & 0 & -\frac{i}{2} & \frac{1}{2} & 0 & \frac{i}{2} & \frac{1}{2} \end{pmatrix}$$

where $\Phi = 2\sqrt{\frac{1}{8} - \frac{s}{8\sqrt{s^2+8\alpha^2}}}$, $X = \frac{1}{2}\sqrt{1+\frac{s}{\sqrt{s^2+8\alpha^2}}}$,

$\Psi = \frac{2\alpha}{\sqrt{s^2+8\alpha^2 - s\sqrt{s^2+8\alpha^2}}}$, $\Omega = \frac{1}{2}\sqrt{1-\frac{s}{\sqrt{s^2+8\alpha^2}}}$

with the corresponding eigenenergies

$$\epsilon_1 = 0;$$
$$\epsilon_2 = 0;$$
$$\epsilon_3 = \frac{1}{2}\left(s - \sqrt{s^2+8\alpha^2}\right);$$
$$\epsilon_4 = \frac{1}{2}\left(s - \sqrt{s^2+8\alpha^2}\right);$$
$$\epsilon_5 = \frac{1}{2}\left(s + \sqrt{s^2+8\alpha^2}\right);$$
$$\epsilon_6 = \frac{1}{2}\left(s + \sqrt{s^2+8\alpha^2}\right);$$
$$\epsilon_7 = -2\beta;$$
$$\epsilon_8 = 2\beta;$$

The momentum matrices and numerical values for the matrices $\Pi^{\alpha\beta}$

The momentum matrices in the absence of the spin-orbit coupling are

```
Px := Evaluate[FullSimplify[D[FullSimplify[H], x] /. {x → K1[[1]], y → K1[[2]]}]]
Py := Evaluate[FullSimplify[D[FullSimplify[H], y] /. {x → K1[[1]], y → K1[[2]]}]]
```

Defining the Pauli matrices and the eigenvectors,

```
σx := PauliMatrix[1]
σy := PauliMatrix[2]
σz := PauliMatrix[3]
I2 := IdentityMatrix[2]
```

```
For[i = 1, i < 9, i++, {|i⟩ := Evaluate[EigenV[[i]]], ⟨i| := Evaluate[EigenV[[i]]*]}]
```

To simplify the expressions we make a function which gives the numerical values with a decent presicion

```
Presentable[a_] :=
 Return[Chop[SetPrecision[
    Rationalize[Simplify[N[a /. {Φ -> 2 Sqrt[1/8 - s/(8 Sqrt[s^2 + 8 α^2])], X -> 1/2 Sqrt[1 + s/Sqrt[s^2 + 8 α^2]],
      Ψ -> 2 α/Sqrt[s^2 + 8 α^2 - s Sqrt[s^2 + 8 α^2]], Ω -> 1/2 Sqrt[1 - s/Sqrt[s^2 + 8 α^2]]} /. {α -> 3/2 * V_spσ,
      β -> 3/4 (V_ppσ - V_ppπ), γ -> 1/8 Sqrt[3] (V_ppπ + 3 V_ppσ), ξ -> -1/8 Sqrt[3] (3 V_ppπ + V_ppσ)} /.
     {V_ssσ -> -6.769, V_spσ -> 5.580, V_ppσ -> 5.037, V_ppπ -> -3.033,
      ϵ_s -> -8.868, ϵ_p -> 0} /. s -> -8.868]]], 3], 10^-5]]
```

The spin - orbit Hamiltionian with an extrinsic field is

$$HSO := \begin{pmatrix} 0 & 0 & \Lambda & -i\Delta S_y & i\Delta S_x & 0 & 0 & 0 \\ 0 & 0 & 0 & 0 & 0 & \Lambda & -i\Delta S_y & i\Delta S_x \\ \Lambda & 0 & 0 & 0 & 0 & 0 & 0 & 0 \\ i\Delta S_y & 0 & 0 & 0 & -i\Delta S_z & 0 & 0 & 0 \\ -i\Delta S_x & 0 & 0 & i\Delta S_z & 0 & 0 & 0 & 0 \\ 0 & \Lambda & 0 & 0 & 0 & 0 & 0 & 0 \\ 0 & i\Delta S_y & 0 & 0 & 0 & 0 & 0 & -i\Delta S_z \\ 0 & -i\Delta S_x & 0 & 0 & 0 & 0 & i\Delta S_z & 0 \end{pmatrix}$$

where $\Lambda = eEz_{sp}$. We then get the following corrections to the momentum elements,

```
δPx[i_, j_] := (
  -Sum_{l=1}^{8} If[Simplify[ϵ_j == ϵ_l],
      0 * I_2,
      ⟨i|.HSO.|l⟩ ⟨l|.Px.|j⟩ / (ϵ_j - ϵ_l) /. {S_x -> σ_x/2, S_y -> σ_y/2, Λ -> I_2 λ},
      ⟨i|.HSO.|l⟩ ⟨l|.Px.|j⟩ / (ϵ_j - ϵ_l) /. {S_x -> σ_x/2, S_y -> σ_y/2, Λ -> I_2 λ}]
  -Sum_{l=1}^{8} If[Simplify[ϵ_i == ϵ_l],
      0 * I_2,
      ⟨i|.Px.|l⟩ ⟨l|.HSO.|j⟩ / (ϵ_i - ϵ_l) /. {S_x -> σ_x/2, S_y -> σ_y/2, Λ -> I_2 λ},
      ⟨i|.Px.|l⟩ ⟨l|.HSO.|j⟩ / (ϵ_i - ϵ_l) /. {S_x -> σ_x/2, S_y -> σ_y/2, Λ -> I_2 λ}])
```

```
δPy[i_, j_] := (
  -Σ_{l1=1}^{8} If[Simplify[ϵ_j == ϵ_l],
                   0 * I_2,
                   ⟨i|.HSO.|l⟩ ⟨l|.Py.|j⟩ / (ϵ_j - ϵ_l) /. {S_x → σ_x / 2, S_y → σ_y / 2, Λ → I_2 λ},
                   ⟨i|.HSO.|l⟩ ⟨l|.Py.|j⟩ / (ϵ_j - ϵ_l) /. {S_x → σ_x / 2, S_y → σ_y / 2, Λ → I_2 λ}]
  -Σ_{l1=1}^{8} If[Simplify[ϵ_i == ϵ_l],
                   0 * I_2,
                   ⟨i|.Py.|l⟩ ⟨l|.HSO.|j⟩ / (ϵ_i - ϵ_l) /. {S_x → σ_x / 2, S_y → σ_y / 2, Λ → I_2 λ},
                   ⟨i|.Py.|l⟩ ⟨l|.HSO.|j⟩ / (ϵ_i - ϵ_l) /. {S_x → σ_x / 2, S_y → σ_y / 2, Λ → I_2 λ}])
```

And we get the following results for $\Pi^{\alpha\beta} = S^{\alpha\beta} + A^{\alpha\beta}$,

```
Axy := Evaluate[ArrayFlatten[Table[
    Presentable[N[Σ_{r=3}^{8} (δPx[i, r].δPy[r, j] - δPy[i, r].δPx[r, j]) / (2 (ϵ_i - ϵ_r) (ϵ_r - ϵ_j))]], {i, 1, 2}, {j, 1, 2}]]]

Sxy := Evaluate[ArrayFlatten[Table[
    Presentable[N[Σ_{r=3}^{8} (δPx[i, r].δPy[r, j] + δPy[i, r].δPx[r, j]) / (2 (ϵ_i - ϵ_r) (ϵ_r - ϵ_j))]], {i, 1, 2}, {j, 1, 2}]]]

Sxx := Evaluate[
  ArrayFlatten[Table[Presentable[N[Σ_{r=3}^{8} (δPx[i, r].δPx[r, j]) / ((ϵ_i - ϵ_r) (ϵ_r - ϵ_j))]], {i, 1, 2}, {j, 1, 2}]]]

Syy := Evaluate[
  ArrayFlatten[Table[Presentable[N[Σ_{r=3}^{8} (δPy[i, r].δPy[r, j]) / ((ϵ_i - ϵ_r) (ϵ_r - ϵ_j))]], {i, 1, 2}, {j, 1, 2}]]]

Style[MatrixForm[Axy], FontSize → 9]
```

$$\begin{pmatrix} -0.000217\,i\,\Delta^2 + 0.000244\,i\,\lambda^2 & -0.000240\,\Delta\,\lambda & -0.000301\,i\,\Delta^2 & 0 \\ 0.000240\,\Delta\,\lambda & -0.000195\,i\,\Delta^2 + 0.000244\,i\,\lambda^2 & 0 & 0.000301\,i\,\Delta^2 \\ -0.000301\,i\,\Delta^2 & 0 & 0.000195\,i\,\Delta^2 - 0.000244\,i\,\lambda^2 & 0.000240\,\Delta\,\lambda \\ 0 & 0.000301\,i\,\Delta^2 & -0.000240\,\Delta\,\lambda & 0.000217\,i\,\Delta^2 - 0.000244\,i\,\lambda^2 \end{pmatrix}$$

```
Style[MatrixForm[Sxy], FontSize → 9]
```

$$\begin{pmatrix} 0 & -0.000269\,\Delta\,\lambda & 0.0001172\,i\,\Delta^2 + 0.000349\,i\,\lambda^2 & 0.000834\,\Delta\,\lambda \\ -0.000269\,\Delta\,\lambda & 0 & 0 & 0.0001172\,i\,\Delta^2 + 0.000349\,i\,\lambda^2 \\ -0.0001172\,i\,\Delta^2 - 0.000349\,i\,\lambda^2 & 0 & 0 & -0.000269\,\Delta\,\lambda \\ 0.000834\,\Delta\,\lambda & -0.0001172\,i\,\Delta^2 - 0.000349\,i\,\lambda^2 & -0.000269\,\Delta\,\lambda & 0 \end{pmatrix}$$

```
Style[MatrixForm[Sxx], FontSize → 9]
```

$$\begin{pmatrix} -0.000632\,\Delta^2 - 0.000913\,\lambda^2 & 0.000337\,i\,\Delta\,\lambda & 0.000139\,\Delta^2 - 0.0000689\,\lambda^2 & 0.000753\,i\,\Delta\,\lambda \\ -0.000337\,i\,\Delta\,\lambda & -0.000410\,\Delta^2 - 0.000913\,\lambda^2 & -0.000524\,i\,\Delta\,\lambda & 0.000139\,\Delta^2 - 0.0000689\,\lambda^2 \\ 0.000139\,\Delta^2 - 0.0000689\,\lambda^2 & 0.000524\,i\,\Delta\,\lambda & -0.000410\,\Delta^2 - 0.000913\,\lambda^2 & 0.000337\,i\,\Delta\,\lambda \\ -0.000753\,i\,\Delta\,\lambda & 0.000139\,\Delta^2 - 0.0000689\,\lambda^2 & -0.000337\,i\,\Delta\,\lambda & -0.000632\,\Delta^2 - 0.000913\,\lambda^2 \end{pmatrix}$$

```
Style[MatrixForm[Syy], FontSize → 9]
```

$$\begin{pmatrix} -0.000917\,\Delta^2 - 0.00173\,\lambda^2 & -0.000472\,i\,\Delta\,\lambda & -0.000182\,\Delta^2 + 0.000904\,\lambda^2 & -0.000592\,i\,\Delta\,\lambda \\ 0.000472\,i\,\Delta\,\lambda & -0.000670\,\Delta^2 - 0.00173\,\lambda^2 & -0.001076\,i\,\Delta\,\lambda & -0.000182\,\Delta^2 + 0.000904\,\lambda^2 \\ -0.000182\,\Delta^2 + 0.000904\,\lambda^2 & 0.001076\,i\,\Delta\,\lambda & -0.000670\,\Delta^2 - 0.00173\,\lambda^2 & -0.000472\,i\,\Delta\,\lambda \\ 0.000592\,i\,\Delta\,\lambda & -0.000182\,\Delta^2 + 0.000904\,\lambda^2 & 0.000472\,i\,\Delta\,\lambda & -0.000917\,\Delta^2 - 0.00173\,\lambda^2 \end{pmatrix}$$

It is then just a matter of reading off the values. A good trick is to multiply the matrices with $(\sigma_i s_j)/4$ and taking the trace. We then get the coefficient corresponding to the matrix $\sigma_i\, s_j$ (where i and j $\in$ {x,y,z}).

Bibliography

[1] H. W. Kroto, J. R. Heath, S. C. Obrien, R. F. Curl, and R. E. Smalley. C(60): Buckminsterfullerene. *Nature*, 318:162–163, 1985.

[2] S. Iijima. Helical microtubules of graphitic carbon. *Nature*, 354:56–58, 1991.

[3] K. S. Novoselov, A. K. Geim, S. V. Morozov, D. Jiang, Y. Zhang, S. V. Dubonos, I. V. Grigorieva, and A. A. Firsov. Electric Field Effect in Atomically Thin Carbon Films. *Science*, 306:666–669, 2004.

[4] K. S. Novoselov, D. Jiang, F. Schedin, T. J. Booth, V. V. Khotkevich, S. V. Morozov, and A. K. Geim. Two-dimensional atomic crystals. *Proceedings of the National Academy of Sciences of the United States of America*, 102(30):10451–10453, 2005.

[5] Nobelprize.org. The Nobel Prize in Physics 2010. Retrived June 2012 from `http://www.nobelprize.org/nobel_prizes/physics/laureates/2010/`.

[6] P. R. Wallace. The Band Theory of Graphite. *Phys. Rev.*, 71:622–634, 1947.

[7] J. C. Meyer, A. K. Geim, M. I. Katsnelson, K. S. Novoselov, T. J. Booth, and S. Roth. The structure of suspended graphene sheets. *Nature*, 446:60–63, 2007.

[8] A. K. Geim and K. S. Novoselov. The rise of graphene. *Nature Materials*, 6:183–191, 2007.

[9] N. D. Mermin. Crystalline Order in Two Dimensions. *Phys. Rev.*, 176:250–254, 1968.

[10] J. W. McClure. Band Structure of Graphite and de Haas-van Alphen Effect. *Phys. Rev.*, 108:612–618, 1957.

[11] J. C. Slonczewski and P. R. Weiss. Band Structure of Graphite. *Phys. Rev.*, 109:272–279, 1958.

[12] J. C. Slonczewski. Ph.D. thesis, Rutgers University, 1955.

[13] J. W. McClure and Y. Yafet. *Proceedings of the fifth conference on carbon.* Pergamon, 1962.

[14] G. Dresselhaus and M. S. Dresselhaus. Spin-Orbit Interaction in Graphite. *Phys. Rev.*, 140:A401–A412, 1965.

[15] D. P. DiVincenzo and E. J. Mele. Self-consistent effective-mass theory for intralayer screening in graphite intercalation compounds. *Phys. Rev. B*, 29:1685–1694, 1984.

[16] G. W. Semenoff. Condensed-Matter Simulation of a Three-Dimensional Anomaly. *Phys. Rev. Lett.*, 53:2449–2452, 1984.

[17] A. K. Geim. Graphene: Status and Prospects. *Science*, 324:1530–1534, 2009.

[18] Y. Hernandez, V. Nicolosi, M. Lotya, F. M. Blighe, Z. Sun, S. de, I. T. McGovern, B. Holland, M. Byrne, Y. K. Gun'ko, J. J. Boland, P. Niraj, G. Duesberg, S. Krishnamurthy, R. Goodhue, J. Hutchison, V. Scardaci, A. C. Ferrari, and J. N. Coleman. High-yield production of graphene by liquid-phase exfoliation of graphite. *Nature Nanotechnology*, 3:563–568, 2008.

[19] P. Sutter. Epitaxial graphene: How silicon leaves the scene. *Nature Materials*, 8:171–172, 2009.

[20] Y. Zhu, S. Murali, W. Cai, X. Li, J. W. Suk, J. R. Potts, and R. S. Ruoff. Graphene and Graphene Oxide: Synthesis, Properties, and Applications. *Advanced Materials*, 22(35):3906–3924, 2010.

[21] A. Reina, X. Jia, J. Ho, D. Nezich, H. Son, V. Bulovic, M. S. Dresselhaus, and J. Kong. Large Area, Few-Layer Graphene Films on Arbitrary Substrates by Chemical Vapor Deposition. *Nano Letters*, 9(1):30–35, 2009.

[22] S. Bae, H. Kim, Y. Lee, X. Xu, J.-S. Park, Y. Zheng, J. Balakrishnan, T. Lei, H. Ri Kim, Y. I. Song, Y.-J. Kim, K. S. Kim, B. Özyilmaz, J.-H. Ahn, B. H. Hong, and S. Iijima. Roll-to-roll production of 30-inch graphene films for transparent electrodes. *Nature Nanotechnology*, 5:574–578, 2010.

[23] C. Lee, X. Wei, J. W. Kysar, and J. Hone. Measurement of the Elastic Properties and Intrinsic Strength of Monolayer Graphene. *Science*, 321(5887):385–388, 2008.

[24] A. H. Castro Neto. Pauling's dreams for graphene. *Physics*, 2:30, 2009.

[25] A. B. Kuzmenko, E. van Heumen, F. Carbone, and D. van der Marel. Universal Optical Conductance of Graphite. *Phys. Rev. Lett.*, 100:117401, 2008.

[26] S. V. Morozov, K. S. Novoselov, M. I. Katsnelson, F. Schedin, D. C. Elias, J. A. Jaszczak, and A. K. Geim. Giant Intrinsic Carrier Mobilities in Graphene and Its Bilayer. *Phys. Rev. Lett.*, 100:016602, 2008.

[27] R. R. Nair, H. A. Wu, P. N. Jayaram, I. V. Grigorieva, and A. K. Geim. Unimpeded Permeation of Water Through Helium-Leak-Tight Graphene-Based Membranes. *Science*, 335(6067):442–444, 2012.

[28] BBC. Miracle material graphene can distil booze, says study. Retrieved June 2012 from `http://www.bbc.co.uk/news/science-environment-16747208`, 27 January 2012.

[29] M. I. Katsnelson, K. S. Novoselov, and A. K. Geim. Chiral tunnelling and the Klein paradox in graphene. *Nature Physics*, 2:620–625, 2006.

[30] Y. Zhang, Y.-W. Tan, H.L. Stormer, and P. Kim. Experimental observation of the quantum Hall effect and Berry's phase in graphene. *Nature*, 438(7065):201–204, 2005.

[31] K. S. Novoselov, A. K. Geim, S. V. Morozov, D. Jiang, M. I. Katsnelson, I. V. Grigorieva, S. V. Dubonos, and A. A. Firsov. Two-dimensional gas of massless Dirac fermions in graphene. *Nature*, 438:197–200, 2005.

[32] K.I. Bolotin, F. Ghahari, M.D. Shulman, H.L. Stormer, and P. Kim. Observation of the fractional quantum Hall effect in graphene. *Nature*, 462(7270):196–199, 2009.

[33] X. Du, I. Skachko, F. Duerr, A. Luican, and E.Y. Andrei. Fractional quantum Hall effect and insulating phase of Dirac electrons in graphene. *Nature*, 462(7270):192–195, 2009.

[34] M. Ohishi, M. Shiraishi, R. Nouchi, T. Nozaki, T. Shinjo, and Y. Suzuki. Spin Injection into a Graphene Thin Film at Room Temperature. *Japanese Journal of Applied Physics*, 46(25):L605–L607, 2007.

[35] Y.-M. Lin, C. Dimitrakopoulos, K. A. Jenkins, D. B. Farmer, H.-Y. Chiu, A. Grill, and Ph. Avouris. 100-GHz Transistors from Wafer-Scale Epitaxial Graphene. *Science*, 327(5966):662–662, 2010.

[36] F. Schwierz. Graphene transistors. *Nature Nanotechnology*, 5(7):487–496, 2010.

[37] Y.-M. Lin, A. Valdes-Garcia, S.-J. Han, D. B. Farmer, I. Meric, Y. Sun, Y. Wu, C. Dimitrakopoulos, A. Grill, Ph. Avouris, and K. A. Jenkins. Wafer-Scale Graphene Integrated Circuit. *Science*, 332(6035):1294–1297, 2011.

[38] S. Bandyopadhyay. *Introduction to Spintronics*. CRC Press, 2008.

[39] W. Pauli. Über den Einfluß der Geschwindigkeitsabhängigkeit der Elektronenmasse auf den Zeemaneffekt. *Zeitschrift für Physik A Hadrons and Nuclei*, 31:373–385, 1925.

[40] G. E. Uhlenbeck and S. Goudsmit. Ersetzung der Hypothese vom unmechanischen Zwang durch eine Forderung bezüglich des inneren Verhaltens jedes einzelnen Elektrons. *Naturwissenschaften*, 13:953–954, 1925.

[41] G. E. Uhlenbeck and S. Goudsmit. Spinning Electrons and the Structure of Spectra. *Nature*, 117:264–265, 1926.

[42] S. A. Goudsmit, translated by J. H. van der Waals. The discovery of the electron spin. Retrieved June 2012 from `http://www.lorentz.leidenuniv.nl/history/spin/goudsmit.html`.

[43] L. H. Thomas. The Motion of the Spinning Electron. *Nature*, 117:514–514, 1926.

[44] W. Gerlach and O. Stern. Der experimentelle Nachweis der Richtungsquantelung im Magnetfeld. *Zeitschrift für Physik A Hadrons and Nuclei*, 9:349–352, 1922.

[45] A. Brataas. Nanoelectronics: Spin surprise in carbon. *Nature*, 452(7186):419–420, 2008.

[46] I. Žutić, J. Fabian, and S. Das Sarma. Spintronics: Fundamentals and applications. *Rev. Mod. Phys.*, 76:323–410, 2004.

[47] S. A. Wolf and D. Treger. Spintronics: a new paradigm for electronics for the new millennium. *Magnetics, IEEE Transactions on*, 36(5):2748–2751, 2000.

[48] W. Thomson. On the Electro-Dynamic Qualities of Metals:–Effects of Magnetization on the Electric Conductivity of Nickel and of Iron. *Proceedings of the Royal Society of London*, 8:546–550, 1857.

[49] J. A. Støvneng. Lecture notes for TFY4340 Mesoscopic physics, Spring 2012.

[50] F. Bloch and G. Gentile. Zur Anisotropie der Magnetisierung ferromagnetischer Einkristalle. *Zeitschrift für Physik A Hadrons and Nuclei*, 70:395–408, 1931.

[51] M. Jullière. Tunneling between ferromagnetic films. *Physics Letters A*, 54(3):225–226, 1975.

[52] G. Binasch, P. Grünberg, F. Saurenbach, and W. Zinn. Enhanced magnetoresistance in layered magnetic structures with antiferromagnetic interlayer exchange. *Phys. Rev. B*, 39:4828–4830, 1989.

[53] M. N. Baibich, J. M. Broto, A. Fert, F. Nguyen Van Dau, F. Petroff, P. Etienne, G. Creuzet, A. Friederich, and J. Chazelas. Giant Magnetoresistance of (001)Fe/(001)Cr Magnetic Superlattices. *Phys. Rev. Lett.*, 61:2472–2475, 1988.

[54] P. Grünberg. Magnetic field sensor with ferromagnetic thin layers having magnetically antiparallel polarized components, 1990. US Patent 4,949,039.

[55] IBM's 100 Icons of Progress - The Application of Spintronics. Retrieved June 2012 from `http://www-03.ibm.com/ibm/history/ibm100/us/en/icons/spintronics/`.

[56] J. Åkerman. Toward a Universal Memory. *Science*, 308(5721):508–510, 2005.

[57] A. Brataas, A. D. Kent, and H. Ohno. Current-induced torques in magnetic materials. *Nature Materials*, 11(5):372–381, 2012.

[58] J.C. Slonczewski. Current-driven excitation of magnetic multilayers. *Journal of Magnetism and Magnetic Materials*, 159(1-2):L1–L7, 1996.

[59] L. Berger. Emission of spin waves by a magnetic multilayer traversed by a current. *Phys. Rev. B*, 54:9353–9358, 1996.

[60] M. Johnson and R. H. Silsbee. Interfacial charge-spin coupling: Injection and detection of spin magnetization in metals. *Phys. Rev. Lett.*, 55:1790–1793, 1985.

[61] A. G. Aronov and G. E. Pikus. Spin injection into semiconductors. *Sov. Phys. Semicond.*, 10:698–700, 1976.

[62] R. Flederling, M. Kelm, G. Reuscher, W. Ossau, G. Schmidt, A. Waag, and L. W. Molenkamp. Injection and detection of a spin-polarized current in a light-emitting diode. *Nature*, 402(6763):787–790, 1999.

[63] Y. Ohno, D. K. Young, B. Beschoten, F. Matsukura, H. Ohno, and D. D. Awschalom. Electrical spin injection in a ferromagnetic semiconductor heterostructure. *Nature*, 402(6763):790–792, 1999.

[64] J. Fabian and I. Žutić. The standard model of spin injection. *Lecture notes for the 40th IFF Spring School Spintronics–From GMR to Quantum Information*, 2009.

[65] S. Datta and B. Das. Electronic analog of the electro-optic modulator. *Applied Physics Letters*, 56(7):665–667, 1990.

[66] C. Ertler, S. Konschuh, M. Gmitra, and J. Fabian. Electron spin relaxation in graphene: The role of the substrate. *Physical Review B*, 80(4):041405, 2009.

[67] N. Tombros, C. Jozsa, M. Popinciuc, H. T. Jonkman, and B. J. van Wees. Electronic spin transport and spin precession in single graphene layers at room temperature. *Nature*, 448:571–574, 2007.

[68] D. Pesin and A. H. MacDonald. Spintronics and pseudospintronics in graphene and topological insulators. *Nature Materials*, 11(5):409–416, 2012.

[69] C. M. Bender and S. A. Orszag. *Advanced Mathematical Methods for Scientists and Engineers: Asymptotic Methods and Perturbation Theory.* Springer, 1999.

[70] F. B. Pedersen. Simple derivation of the effective-mass equation using a multiple-scale technique. *European Journal of Physics*, 18(1):43–45, 1997.

[71] J. M. Luttinger and W. Kohn. Motion of electrons and holes in perturbed periodic fields. *Phys. Rev.*, 97:869–883, 1955.

[72] E. O. Kane. Band structure of indium antimonide. *Journal of Physics and Chemistry of Solids*, 1(4):249–261, 1957.

[73] C. Lewiner, O. Betbeder-Matibet, and P. Nozières. A field theoretical approach to the anomalous hall effect in semiconductors. *Journal of Physics and Chemistry of Solids*, 34(5):765–777, 1973.

[74] P. Nozières and C. Lewiner. A simple theory of the anomalous hall effect in semiconductors. *Journal de Physique*, 34(10):901–915, 1973.

[75] H. Min, J. E. Hill, N. A. Sinitsyn, B. R. Sahu, L. Kleinman, and A. H. MacDonald. Intrinsic and rashba spin-orbit interactions in graphene sheets. *Phys. Rev. B*, 74:165310, 2006.

[76] J. C. Slater and G. F. Koster. Simplified LCAO Method for the Periodic Potential Problem. *Phys. Rev.*, 94:1498–1524, 1954.

[77] S. Konschuh, M. Gmitra, and J. Fabian. Tight-binding theory of the spin-orbit coupling in graphene. *Phys. Rev. B*, 82:245412, 2010.

[78] R. Saito, G. Dresselhaus, and M.S. Dresselhaus. *Physical properties of carbon nanotubes*. Imperial College Press, 1998.

[79] W. A. Harrison. *Electronic structure and the properties of solids: the physics of the chemical bond*. Dover books on physics. Dover Publications, 1989.

[80] C. L. Kane and E. J. Mele. Quantum Spin Hall Effect in Graphene. *Phys. Rev. Lett.*, 95:226801, 2005.

[81] D. Huertas-Hernando, F. Guinea, and A. Brataas. Spin-orbit coupling in curved graphene, fullerenes, nanotubes, and nanotube caps. *Phys. Rev. B*, 74:155426, 2006.

[82] M. Gmitra, S. Konschuh, C. Ertler, C. Ambrosch-Draxl, and J. Fabian. Band-structure topologies of graphene: Spin-orbit coupling effects from first principles. *Phys. Rev. B*, 80:235431, 2009.

[83] D. Huertas-Hernando, F. Guinea, and A. Brataas. Spin-orbit-mediated spin relaxation in graphene. *Physical review letters*, 103(14):146801, 2009.

[84] A.H. Castro Neto and F. Guinea. Impurity-induced spin-orbit coupling in graphene. *Physical review letters*, 103(2):26804, 2009.

[85] H. Ochoa, A.H. Neto, and F. Guinea. Elliot-Yafet mechanism in graphene. *Arxiv preprint arXiv:1107.3386*, 2011.

[86] N. Tombros, S. Tanabe, A. Veligura, C. Jozsa, M. Popinciuc, HT Jonkman, and BJ Van Wees. Anisotropic spin relaxation in graphene. *Physical Review Letters*, 101(4):46601, 2008.

[87] L. C. Lew Yan Voon and L. R. Ram-Mohan. Tight-binding representation of the optical matrix elements: Theory and applications. *Phys. Rev. B*, 47:15500–15508, 1993.